Omaha Public Power District
Nuclear Analysis
Reload Core Analysis

Neutronics Design Methods and Verification

OPPD-NA-8302-NP

September 1983

ABSTRACT

This document is a Topical Report describing Omaha Public Power District's reload core neutronics design methods for application to Fort Calhoun Station Unit No. 1.

The report addresses the District's neutronics design methodology and its application to the calculation of specific physics parameters for reload cores. In addition, comparisons of results obtained using this methodology to results from experimental measurements and independent calculations are provided.

Proprietary Data Clause

This document is the property of Omaha Public Power District (OPPD) and contains proprietary information, indicated by brackets, developed by Combustion Engineering (CE) and Exxon Nuclear Company, Inc. (ENC). The CE and ENC information was purchased by OPPD under proprietary information agreements.

Table of Contents

Table of Contents (Continued)

Omaha Public Power District
Reload Core Analysis Methodology
Neutronics Design Methods and Verification

1.0 INTRODUCTION

The District's neutronic design calculation methods are described along with results obtained when these methods are compared to experimental measurements and independent calculations. The discussion of calculational methods includes descriptions of the basic computer codes and procedures for applying these codes. Comparison of the calculations to measurements and independent calculations are performed using the same codes and computational methods used in the Fort Calhoun reload core design efforts. The basic physics models, supplied by Combustion Engineering (CE), are described in Section 2.0. Section 3.0 describes the District's application of these models to the Fort Calhoun reactor. Section 4.0 presents the application of these physics models to the reload core analysis. Section 5.0 discusses the comparisons of District calculated data to measured operating data from Fort Calhoun Station and data from independent calculations. Section 6.0 contains the individual references.

2.0 BASIC PHYSICS MODELS

The District's neutronics design analysis for the Fort Calhoun core is based on a combination of multi-group neutron spectrum calculations, which provide cross-sections appropriately averaged over a few broad energy groups and few-group 1-, 2- and 3- dimensional diffusion theory calculations, which result in integral and differential reactivity effects and power distributions. Calculations are performed with the aid of computer programs embodying analytical procedures and fundamental nuclear data consistent with the current State-of-the-Art.

2.1 Neutron Cross-Sections

The data base for both fast and thermal neutron cross-sections is derived from ENDF/B-IV with changes recommended by the

2.1 Neutron Cross-Sections (Continued)

cross-section evaluation working group (Reference 2-1). These recommendations consist of changes to the shielded resonance of U^{238}, and the Watt fission spectrums of U^{235} and Pu^{239}, and changes in λ for U^{235} and Pu^{239}. Few group cross-sections, for subregions of the core that are represented in spatial diffusion calculations, (e.g., fuel pin cells, moderator channels, structural member cells, etc.) are calculated by the DIT latice program. These cross-sections are generated as a function of fuel temperature and moderator temperature to accomodate the temperature feedback routines within the diffusion theory models.

The DIT code performs all the functions of the traditional transport methods which attempt to represent the complexities of the PWR fuel assembly geometry, including neutron energy spectrum interactions in the fuel, control rods, control rod locations (water holes), burnable absorber rods, and incore flux detectors. The essential feature of DIT, which distinguishes it from the traditional methodology is that the spectrum spatial averaging procedures are based on calculations in two-dimensional geometry. Hence few approximations to the geometry representation are necessary. The use of nodal transport theory has made it feasible to retain discrete pin geometry in both the fine and broad energy group calculations. A more complete description of the DIT procedures for generating few-group neutron cross-sections can be found in References 2-2 and 2-3.

Previously, the District utilized the CEPAK program to produce few-group cross-sections. These cross-sections were also generated as functions of fuel and moderator temperature. Comparisons of calculated and measured data reported in Section 5.0 include calculations performed using the CEPAK program.

2.1 Neutron Cross-Sections (Continued)

The CEPAK program is the synthesis of a number of computer codes, many of which were developed at other laboratories, e.g., FORM, THERMOS and CINDER. These programs are interlinked in a consistent way with inputs from differential cross-section data from an extensive library. A description of the CEPAK procedures used to generate few-group neutron cross-sections can be found in Reference 2-4.

2.2 Diffusion Theory Models

The diffusion theory models package used to calculate core physics parameters for Fort Calhoun Station consist of the PDQ-X, ROCS, and QUIX computer codes. The PDQ-X and ROCS codes can be executed in one, two and three dimensions to calculate static and depletion dependent parameters such as reactivities, flux, nuclide and power distributions and CEA worths. The QUIX code is executed in one dimension to calculate axial power distributions and CEA worth [ ].

2.2.1 PDQ-X

The PDQ-X program is an extension of PDQ-7 and HARMONY programs (Reference 2-5) to include the following optional capabilities:

(1) Fuel temperature feedback in the two-dimensional geometry option,

(2) Fuel and moderator feedback in the three-dimensional geometry option,

(3) Poison content criticality searches, and

(4) Spatial feedback on the power distribution with fuel and moderator temperature in the 1-dimensional geometry option.

2.2 Diffusion Theory Model (Continued)

2.2.1 PDQ-X (Continued)

PDQ-X employs macroscopic (static) or microscopic (depletion) cross-section data generated by methods described in Section 2.1.

2.2.2 ROCS

The ROCS program is a course mesh 2-group solution of the neutron diffusion equation based upon a mesh centered higher order finite difference formulation. It incorporates closed channel thermal hydraulic modeling into its evaluation of the interaction of neutron flux effects and the macroscopic physical and thermal properties of distributed materials. Because of its nodal structure and course mesh, ROCS is more efficient than PDQ-X for evaluating a core's static and depletion dependent properties. ROCS also employs macroscopic (static) or microscopic (depletion) cross-sections generated by the methods described in Section 2.1. A more complete description of the ROCS program is found in References 2-3 and 2-6.

2.2.3 QUIX

The QUIX program is a one-dimensional (axial) representation of the core used to determine static and time dependent reactivities and power distributions at selected stages of depletion. This program solves the neutron flux and associated eigenvalue in problems containing up to 140 distinct regions or compositions with variable mesh intervals. The macroscopic cross-section distributions, fission product yields, and

xenon and boron microscopic cross-sections required as input to QUIX are obtained from either a one-dimensional PDQ-X calculation or a three-dimensional ROCS calculation. Local power density (fuel temperature) feedback is included by modifying the point wise macroscopic absorption and removal cross-sections. The change in cross-sections is represented by a function of the difference between the local axial power density and the referenced power density. Moderate density feedback is included by relating changes in the macroscopic absorption and removal cross-sections to the local hydrogen number density which is calculated from enthalpy at each axial segment. These cross-section functions are generated in such a way that the fuel and moderator temperature coefficients calculated by QUIX are equal to or conservative with respect to the fuel and moderator temperature coefficients calculated by ROCS. The axial reflector cross-sections input to QUIX are determined in such a way that the steady state axial power distribution generated by QUIX matches the axial power distribution generated by ROCS. Details of the above treatments are given in Reference 2-7.

In addition to the eigenvalue problem, QUIX will perform four types of searches to obtain a specific eigenvalue, viz., a uniform poison search, buckling search, CEA region boundary search, and a moderator density dependent poison search. The uniform poison search assumes an axially constant macroscopic absorption cross-section whereas the moderator density dependent poison search assumes a distributed macroscop-

2.0 BASIC PHYSICS MODELS (Continued)

2.2 Diffusion Theory Model (Continued)

2.2.3 QUIX (Continued)

ic absorption cross-section dependent upon the axial moderator density. The moderator density dependent search is used to simulate the reactivity effects of the soluable boron in the reactor coolant.

Through the use of rod shadowing factors, shape annealing factors and shape index biases, the QUIX program has the capability of simulating excore detector response expected during normal operation. The procedures used for these simulations are described in Reference 2-8.

3.0 FORT CALHOUN PHYSICS MODELS

The District utilizes the basic CE physics models described in Section 2.0 to model the Fort Calhoun reactor core. The computer codes wh.ch embody these basic physics models are maintained on the CE computer system at Windsor, Connecticutt. The District accesses these computer codes through a time sharing system. CE maintains all documentation and quality assurance programs related to these computer codes. The following paragraphs discuss the specifics of the Fort Calhoun models.

3.1 Neutron Cross-Sections

The two-group neutron cross-sections utilized in the ROCS and PDQ-X models of the Fort Calhoun reactor core are generated using the DIT code. Cross-sections have been generated for unshimmed ENC and CE fuel assemblies and shimmed ENC fuel assemblies. The cross-sections have been generated for the District by CE and are based on information supplied by the District.

3.1 Neutron Cross-Sections (Continued)

The cross-sections utilized to model the Fort Calhoun reactor are in the form of universal table sets. The two-group cross-sections are generated as functions of enrichment, fuel temperature, moderator temperature, burnup and in the case of shimmed fuel assemblies, B4C shim number density. The table sets are applicable over a fuel temperature range from room temperature to 1800°K and a moderator temperature range from room temperature to 800°K. The fine mesh table sets include explicit treatment of the pin cells immediately around the CEA guide tube (water hole) to properly account for the peaking of thermal flux in these water holes. Therefore, no corrections need be applied to the pin powers produced by the fine mesh model.

3.2 Diffusion Theory Models

The District utilizes the PDQ-X, ROCS and QUIX models described in Section 2.0. The PDQ-X model is a fine mesh two-dimensional model. The District utilizes both a two-dimensional and three-dimensional ROCS model. The QUIX model is a one-dimensional model.

3.2.1 PDQ-X

The District's PDQ-X model is a two-group, two-dimensional fine mesh model in which each fuel pin cell and shim pin cell is represented by a single mesh point. The model includes explicit representation of the CEA guide tube (water holes), the CEA's, the interassembly water gaps, the water gap between the outer fuel assembly and the core shroud, the core shroud, the water gap between the core shroud and the core barrel, the core barrel and a portion of the water gap between the core barrel and the thermal shield. The model is representative of the core between 20% and 80% of full core height.

3.0 FORT CALHOUN PHYSICS MODELS (Continued)

3.2 Diffusion Theory Models (Continued)

3.2.1 PDQ-X (Continued)

The PDQ-X model is used to simulate the expected mode of operation in the cycle being analyzed. This calculation results in material distributions and radial peaking factors which are used in the safety analysis and setpoint generation. The mode of operation at the Fort Calhoun reactor is base loaded operation. Base loaded operation consists of reactor operation at or very near rated thermal power throughout the cycle. The lead CEA bank insertion is held to a minimum. Historically the lead CEA bank at Fort Calhoun has been inserted less than 5% of the time whenever the reactor is at a steady state power level. Reference 3-1 dicusses the impact of operation with a time averaged lead bank insertion of [ ]. The model is typically depleted in time steps of 1,000 MWD/MTU.

3.2.2 ROCS

The District utilizes a three-dimensional and a two-dimensional two-group ROCS model. [

] The two-dimensional model is representative of the core between 20% and 80% of full core height. [

] The boundary conditions are derived in accordance with the methodology discussed in Reference 3-2.

3.0 FORT CALHOUN PHYSICS MODELS (Continued)

3.2 Diffusion Theory Models (Continued)

3.2.3 QUIX

The District utilizes a one hundred and twenty-five axial node QUIX model. The data for the QUIX model is obtained from the three-dimensional ROCS calculations.

4.0 APPLICATION OF PHYSICS METHODS

Previous sections have focused on the reactor physics models utilized by the District to model the Fort Calhoun reactor. In this section, calculations of the various core parameters used in the safety analysis are described. The main parameters considered are the radial peaking factors (F_R and F_{xy}), the moderator temperature coefficient, the fuel temperature or Doppler coefficient, the neutron kinetics parameters, CEA drop data, CEA ejection data, CEA scram reactivity, reactivity insertion for the steamline break cooldown, radial peaking data for the asymmetric steam generator event, and axial power distributions.

4.1 Radial Peaking Factors

The radial peaking factors, F_R and F_{xy}, are calculated with the PDQ and 3-D ROCS models. Values of F_{xy} for both unrodded and rodded core configurations are obtained directly from the PDQ power distributions. Since the cross-sections utilized by the PDQ model implicitly account for the peaking of the thermal flux in the CEA guide tubes (water holes) no correction is required to the peaking factors calculated by PDQ. The values of F_R for the unrodded core are obtained by multiplying the integrated assembly powers from ROCS by the pin to box ratio obtained from PDQ. The value of F_R for various rod configurations is derived by multiplying the assembly normalized planar power for each ROCS plane by the pin to box ratio for the rod configuration in that plane and summing these values for all planes and dividing by the number of planes.

4.1 Radial Peaking Factors (Continued)

The uncertainties for the radial peaking factors are given in Reference 4-1.

The physics models are used to calculate the expected values of F_R and F_{xy}. The actual values of F_R and F_{xy} used in the safety analysis are chosen to be conservatively high with respect to those anticipated during the core life.

4.2 Reactivity Coefficients

The ROCS models are used to calculate the moderator temperature coefficient (MTC) and the fuel temperature coefficient (FTC). The MTC is defined as the change in reactivity per degree change in moderator temperature. Calculationally, the MTC at a temperature of T_{mod} is determined by running three calculations; one at T_{mod}, one at T_{mod} + 10°F and one at T_{mod} -10°F. The MTC at a temperature of T_{mod} is the average of the two calculated values. The reactivity change is calculated with the ROCS model by varying the inlet temperature while holding all other parameters such as the fuel temperature and nuclide concentrations constant.

The FTC or Doppler coefficient is defined as a change in reactivity per degree change in the effective fuel temperature. The effect of fuel temperature upon resonance neutron energy absorption is accounted for in the ROCS and PDQ models by means of power feedback options. The representation of the variation in the few group cross-sections with fuel temperature involves two main segments. The first is to represent the variation in cross-section with fuel temperature, the second is to relate fuel temperature to reactor power density. The first portion is included in the basic methods employed to generate the few-group cross-sections. The second portion requires establishment of correlations between fuel temperature (i.e., effective

4.2 Reactivity Coefficients (Continued)

fuel temperature to be used in generation of cross-sections) and the reactor power density. The relationship between fuel temperature and reactor power density employs direct fits to FATES (Reference 4-2) fuel data. This method results in the fuel temperature correlation for each fuel type which is both local, power density and fuel exposure dependent.

The reduction in reactivity resulting from an increase in effective fuel temperature is determined by ROCS. Typically, a temperature interval of 50°F is used to determine this coefficient.

The physics models are used to calculate the expected values of the MTC throughout the cycle. The actual values of the MTC used in the safety analysis are chosen to conservatively bound expected values of the MTC. The measurements of the MTC made during the operation of the reactor include uncertainties to assure that the actual MTC does not exceed the values used in the safety analysis. A fifteen percent uncertainty is applied to the Doppler coefficient when it is used in the safety analysis calculations.

4.3 Neutron Kinetics Parameters

The neutron kinetics parameters β, λ, and the neutron lifetime, ℓ^*, are calculated using Combustion Engineering's BETAF computer code. The technique utilized to calculate the kinetics parameters and the neutron lifetime is based on first order perturbation theory. Details of the perturbation approach are discussed in References 4.3 and 4.4. The computer program, BETAF, uses data from integral files created by direct and adjoint flux solution PDQ calculations. [

]

4.4 Dropped CEA Data

The neutronics data unique to the dropped CEA analysis are the values of F_R and F_{xy} following the drop of a CEA and the reactivity worth of the dropped CEA. The values of F_R and F_{xy} increase due to a large azimuthal tilt caused by the drop of a CEA and occur on the side of the core opposite the dropped CEA. Because the maximum F_R and F_{xy} occur far away from the dropped CEA, the intra-assembly power distribution is not perturbed. Therefore, the "post drop" value of F_R and F_{xy} can be calculated by multiplying the "pre-drop" values of F_R and F_{xy} by the ratio of the assembly power after and before the drop of the CEA. This ratio is the distortion factor. The distortion factor is defined as the ratio of the assembly RPD from a radial power distribution at a given power level and time in core life containing a dropped CEA to assembly RPD from a radial power distribution at the same power level and time in core life without a dropped CEA. [

]

The distortion factor and dropped CEA reactivity worth can be calculated using the 2-D or 3-D ROCS model. The 2-D ROCS calculations yield the F_{xy} distortion factor as a function of CEA bank insertion (i.e., ARO, Bank 4 In, Banks 4+3 In) and power level. [

] The 3-D F_R distortion factor is calculated for a specific CEA insertion and power level. [

4.4 Dropped CEA Data (Continued)

] Sufficient margin exists at the lower power levels [ ] for the F_R dependent DNBR calculations does not adversely effect operating margin. The "post drop" value of F_R using the 3-D F_R distortion factor is calculated by multiplying the "pre-drop" value of F_R for the particular CEA insertion and power level by the 3-D F_R distortion factor.

The 2-D and 3-D ROCS "post drop" power distributions are calculated with fuel temperature and moderator temperature feedback. The calculations assume that the core average Axial Shape Index (ASI) is being controlled within the "constant ASI" limits in accordance with the Fort Calhoun Operating Manual.

Because the [ ] of the dropped CEA during the fuel cycle and because of the [ ] documented in Reference 4-5, [ ] uncertainty is applied to the distortion factor. A [ ] uncertainty is applied to the reactivity worth of the dropped CEA based on the verification contained in Reference 4-5.

4.5 CEA Ejection Data

The neutronics data unique to the CEA ejection analysis are the value of F_{xy} following the ejection of a CEA and the reactivity worth of the ejected CEA. The maximum post ejection value of F_{xy} and maximum ejected CEA reactivity worths are calculated for the maximum CEA insertion allowed by the PDIL at HFP and HZP. The physics parameters are calculated using a HZP 2-D ROCS model or a HZP 2-D PDQ model. The post ejection value of F_{xy} is obtained directly from the PDQ calculation. The post ejection value of F_{xy} is obtained from the 2-D ROCS calculation

4.5 CEA Ejection Data (Continued)

by multiplying the 2-D ROCS post ejection assembly RPD by a conservatively high pin to box ratio. The ROCS methodology is conservative with respect to the more exact PDQ method. The ejected CEA reactivity worth is obtained directly from either calculation. Both the PDQ and ROCS post ejection power distributions are calculated without moderator or fuel temperature feedback.

The post ejection value of F_q is calculated by multiplying the post ejection value of F_{xy} by the maximum value of F_z, the azimuthal tilt allowance, the augmentation factor, the engineering heat flux factor, the fuel densification factor, and the F_q uncertainty documented in Reference 4-1. A [ ] uncertainty is applied to the ejected CEA worth.

4.6 CEA Reactivity

The CEA reactivity calculations done in a reload core safety analysis are the calculation of the total reactivity of CEA's inserted into the core during a reactor trip (CEA scram reactivity), the generation of the scram reactivity curves, and the calculation of required shutdown margin.

The CEA scram reactivity worth at HZP is calculated by obtaining the net worth for all CEA's between the HZP PDIL CEA position and the fully inserted position and subtracting the worth of the highest worth stuck CEA. These calculations are done using the ROCS model. A [ ] uncertainty is applied to the HZP CEA scram reactivity worth. The HZP CEA scram reactivity for the CEA ejection transient is calculated in a similar fashion except that the worth of the ejected and highest stuck worth CEA's are subtracted from the net worth.

The scram CEA worth at HFP is calculated by obtaining the HFP net worth for all CEA's between the HFP PDIL CEA position and

4.6 CEA Reactivity (Continued)

the fully inserted position and subtracting the worth of the highest worth stuck CEA. The thermal hydraulic axial gradient reduction allowance, the moderator void collapse allowance, and the loss of worth between HFP and HZP are alsc subtracted from the HFP net worth for the scram CEA worth to be used in all transients except the four pump loss of flow event and the steam line break incident. These are not applied to the four pump loss of flow scram CEA worth because the closest approach to the SAFDL during the four pump loss of flow event occurs prior to significant CEA insertion. These allowances are not applied to the steam line break (SLB) incident HFP CEA scram worth because the SLB reactivity insertion curves are calculated with the CEA's fully inserted.

The moderator void collapse allowance is 0.0% $\Delta\rho$ at BOC and 0.1% $\Delta\rho$ at EOC. The thermal hydraulic axial gradient reduction allowance is 0.2% $\Delta\rho$ at BOC and 0.4% $\Delta\rho$ at EOC. A [ten percent] uncertainty is applied to the HFP CEA scram reactivity worth. The HFP scram reactivity for the CEA ejection transient is calculated in a similar fashion except that the worth of the ejected and highest stuck worth CEA's are subtracted from the net worth. All CEA worth calculations assume the ASI is being controlled within the "constant ASI" limits in accordance with the Fort Calhoun Operating Manual.

The generation of the scram reactivity curves utilizes the methodology discussed in Reference 4-6.

The calculation of the required shutdown margin is only performed at HZP since the shutdown margin at power is controlled by the PDIL. The available HZP shutdown margin is equivalent to the HZP CEA scram reactivity.

4.7 CEA Withdrawal Data

The reactor core physics data unique to the CEA withdrawal analysis is the maximum differential CEA worth. This is the maximum amount of reactivity at any time in core life that can be added to the core per inch of CEA motion. When the maximum differential CEA worth is combined with the maximum CEA withdrawal rate of 46 inches/minute, a conservative withdrawal rate expressed in $\%\Delta\rho$/sec is obtained and used as input to the CEA withdrawal analysis.

The maximum differential CEA worth is obtained for the sequential withdrawal of the CEA banks from the HZP PDIL to an all rods out condition. The 3-D ROCS model is utilized to calculate this parameter. The calculations are performed assuming that the reactor is being controlled within the "constant ASI" limits in accordance with the Fort Calhoun Operating Manual.

4.8 Reactivity Insertion for Steam Line Break Cooldown

The reactor core physics data unique to the steam line break transient analysis is the reactivity insertion due to the cooldown of the moderator. There are two sources of this reactivity insertion. The first is the positive reactivity insertion due to the increasing density of the moderator as the cooldown progresses. The second is the reactivity insertion due to the Doppler coefficient as the effective fuel temperature changes.

Reactivity insertions due to the moderator density increase and the Doppler coefficient are both calculated using a full core ROCS model. The axial leakage or buckling is adjusted such that the moderator temperature coefficient calculated by the ROCS model corresponds to the most negative Technical Specification limit. The reactivity insertion calculations are performed with all CEA's except the most reactive CEA inserted in the core.

4.8 Reactivity Insertion for Steam Line Break Cooldown (Continued)

The moderator density reactivity insertion curve for the hot zero power steam line break case is calculated by successively lowering the inlet temperature of the ROCS model from 532°F and allowing only moderator temperature feedback in the model. The calculations typically result in a curve of reactivity insertion vs. moderator temperature from a hot zero power temperature of 532°F to 212°F.

The Doppler reactivity insertion curve for the hot zero power case is also calculated by steadily decreasing the inlet temperature of the ROCS model. The fuel temperature feedback in the model allows the production of a curve of Doppler reactivity as a function of fuel temperature. All zero power calculations are performed assuming there is no decay heat and no credit is taken for local voiding in the region of the stuck CEA.

The moderator density reactivity insertion curve for the full power case is calculated by decreasing the power level and core average coolant temperature from full power to the hot zero power inlet temperature and then successively lowering the inlet temperature as in the hot zero power case. Only moderator temperature feedback is utilized in the ROCS model. The Doppler reactivity insertion curve is calculated by a similar procedure utilizing the fuel temperature feedback in the model.

Since the moderator reactivity insertion curve corresponds to an MTC which is at the Technical Specification limit, no additional uncertainty is added to this curve. A fifteen percent uncertainty is applied to the Doppler reactivity insertion curve.

4.9 Asymmetric Steam Generator Event Data

The reactor core physics data unique to the asymmetric steam generator event [

4.9 Asymmetric Steam Generator Event Data (Continued)

] For the range of temperatures considered, the intra-assembly peaking does not vary as the inlet temperature is changed. [

]

[

]

4.10 QUIX Calculations

The District utilizes the QUIX model to perform various axial shape analyses related to the generation of the reactor protective system setpoints. The QUIX calculations are carried out in accordance with the methodology discussed in Reference 4-6.

5.0 VERIFICATION OF NEUTRONICS MODELS FOR FORT CALHOUN STATION

The District has performed extensive verification of the neutronics models used in the reload core analyses. The results of the previous District verification efforts were reported in Reference 5-1. This effort utilized cross-sections produced by CEPAK. The methodology discussed in this report utilizes cross-sections produced by DIT. In order to demonstrate the District's ability to utilize the models with the DIT cross-sections, additional verification was undertaken.

This verification is in addition to the extensive verification of these methods done by Combustion Engineering (CE) and reported in Reference 5-2. It is not the District's intent to repeat CE's extensive verification effort which includes a statistical assessment of the adequacy of the uncertainties used by both CE and the District. Rather, it is the District's intent to demonstrate that the District can adequately model the Fort Calhoun core and that the results of the District's verification effort are consistent with those reported in Reference 5-2.

The District's verification using DIT cross-sections utilizes data recorded for Cycles 6, 7 and 8. Benchmarking was performed for the prediction of overall core reactivity, power distributions, reactivity coefficients, CEA worth and Xenon reactivity. The results of the verification efforts include data for both CEPAK and DIT cross-sections.

The verification uses experimental data from the Fort Calhoun reactor and independent calculations performed by CE and Exxon Nuclear Company, (ENC). Experimental data is obtained from startup tests and core follow programs. Calculational data is obtained from startup predictions, special analysis of startup tests or design lifetime computations.

5.1 Core Reactivity

The analysis of predicted reactivity for Fort Calhoun Station utilizes studies of startup tests and plant data obtained during operation at power. The parameter used to measure reactivity is the critical boron concentration.

Comparisons between measured and calculated critical boron concentrations for the unrodded HZP core are presented in Table 5-1. The results using the DIT cross-sections are consistent with those reported in Reference 5-2.

5.0 VERIFICATION OF NEUTRONICS MODELS FOR FORT CALHOUN STATION (Continued)

5.1 Core Reactivity (Continued)

Operating plant data has been analyzed and evaluations of core reactivity predictions carried out. The measured and calculated full power and unrodded core critical boron concentrations for Cycles 4, 5, 6, 7 and 8 are shown in Figures 5-1 through 5-5. There is little difference between calculated curves utilizing either CEPAK or DIT cross-sections for Cycles 6, 7, and 8. Results for the operating plant data comparisons demonstrate the District's ability to calculate core reactivity.

5.2 Power Distributions

Extensive comparisons of power distributions have been performed for Fort Calhoun and other CE reactors. These comparisons are contained in References 5-2 and 5-3. The data given for Fort Calhoun in Reference 5-3 were supplied by the District.

5.2.1 Radial Power Distributions

The District has performed comprehensive core follow calculations since the start of Cycle 3 in 1976. Table 5-2 summarizes the results of comparisons between the axially integrated assembly power as calculated by ROCS and that measured by CECOR using the self-powered rhodium detector for Cycles 3, 4, 5, 6, 7 and 8. These comparisons are only performed for instrumented assemblies because CECOR calculates the power for non-instrumented assemblies using coupling coefficients derived from the physics codes. The instrumented assembly powers are calculated by a method independent of the predictive code. Sample comparisons for Cycle 8 are included in Appendix A of this document.

5.2 Power Distributions (Continued)

5.2.1 Radial Power Distributions (Continued)

The extensive comparison between the calculated and measured radial power distributions verifies the capability of the District to calculate these power distributions.

5.2.2 Axial Power Distributions

The District has benchmarked the ROCS code against CECOR measured axial power distributions. Appendix B contains comparisons of core average and selected assembly axial power distributions for Cycles 5 through 8.

The District has benchmarked the QUIX code against measured data by comparing the QUIX calculated ASI and the CECOR measured ASI during an axial oscillation test performed during Cycle 8 power ascension testing. The lead bank CEA's remained in the core during the entire test. The result of the comparison is shown in Figure 5-6.

The comparisons demonstrate the District's capability to calculate axial power distributions using both ROCS and QUIX.

5.3 Reactivity Coefficients

The capability of the District's ROCS model to predict the Isothermal Temperature Coefficient (ITC) and the Power Coefficient (PC) has been benchmarked against physics tests conducted at Fort Calhoun for all operating cycles. Table 5-3 shows the com-

5.3 Reactivity Coefficients (Continued)

parison between calculated and measured ITC's for zero power startup testing at the beginning of the cycle. Also included are calculations performed by ENC, using XTG. The comparison of measured and calculated ITC's for "at power" conditions is shown in Table 5-4. The comparison of measured and calculated Power Coefficients is shown in Table 5-5. In all cases, the ROCS code accurately predicts the behavior of the core and the results using the DIT cross-sections are consistent with results reported in Reference 5-2.

5.4 CEA Reactivity Worth

The District has extensively benchmarked the ROCS code against mesured and independently calculated values of CEA reactivity worth. Tables 5-6 through 5-13 show the results of this benchmarking effort. CE performed the PDQ calculations for Cycles 1, 2 and 4. ENC performed the XTG calculations for Cycles 6, 7 and 8. The District performed all 2-D and 3-D ROCS calculations and the Cycle 5 PDQ calculations. These results demonstrate the District's capability to calculate CEA worths and the results using DIT cross-sections are consistent with the results reported in Reference 5-2.

5.5 Comparisons to Critical CEA Positions Following a Reactor Trip

Another measure of the ability of the 3-D ROCS model to accurately predict reactivity changes is its ability to predict the critical boron concentration and CEA position following a reactor trip. A study of this type was done for criticalities during the recovery from a reactor trip for Cycle 2. This study showed that the maximum reactivity error between measured critical parameters and calculated parameters was [ ] $\Delta\rho$. This demonstrates the ability of the District's ROCS model to accurately model the power defect and xenon buildup and decay.

5.6 Comparison to Independent Radial Power Distribution Calculations

Comparisons between the District's ROCS model calculations and ENC XTG model calculations of the HFP radial power distributions have been performed. Figures 5-7 through 5-12 show comparisons between CEPAK-ROCS model and XTG model calculations for the beginning and end of Cycle 6, 7 and 8. Figures 5-13 through 5-18 show comparisons between DIT-ROCS model and XTG model calculations for the beginning and end of Cycle 6, 7 and 8. The comparisons show good agreement between the independent models.

5.7 The District's Ongoing Benchmarking Program

Much of the data reported in this section was drawn from the District's ongoing benchmarking program. This program includes startup physics testing predictions, reactor testing analysis and a core follow effort. This program will provide additional verification data in the future.

5.8 Summary

The District has an ongoing neutronics methodology verification program. The results of this verification program for previous cycles demonstrate the ability of the District to utilize the neutronics methods described in this document.

Table 5-1

Unrodded HZP Critical Boron Concentrations Calculations

Cycle	Measured ppm	3-D* ROCS (CEPAK)	2-D* ROCS (CEPAK)	3-D ROCS (DIT)	PDQ (CEPAK)	XTG
1	933	[	[	-	[	
2	1240			-		
3	1000		]	-	]	
4	1027		-	-	-	
5	1242		-	-	-	
6	1230		-	[	-	[
7	1241		-		-	
8	1240	]	-	]	-	]

* A 20 ppm bias has been applied to these calculations.

Table 5-2

Summary of Comparisons of Measured and Calculated
Integral Assembly Relative Power Densities

Cycle	Cycle Burnup (MWD/MTU)	CEPAK (%)	DIT (%)	Nominal Power % of Full Power
3	80	[	-	45
3	177.5		-	60
3	510		-	95
3	800		-	100
3	1000		-	100
3	1428		-	100
3	2510		-	100
3	3100		-	100
3	3500		-	100
3	4000		-	100
3	4500		-	100
3	5200		-	100
3	5800		-	100
3	6400		-	100
3	7200		-	90
3	7715		-	80
4	200		-	100
4	1000		-	100
4	2000		-	100
4	3000		-	100
4	4000		-	100
4	5000		-	100
4	6000	]	-	100

Cycle	Cycle Burnup (MWD/MTU)	CEPAK (%)	DIT (%)	Nominal Power % of Full Power
4	7000	[	-	100
4	8200		-	100
5	300		-	100
5	1000		-	100
5	2000		-	100
5	3000		-	100
5	4000		-	100
5	5000		-	100
5	6000		-	100
6	50		[ ]	66
6	500		-	100
6	1000		-	100
6	2000		[ ]	90
6	3000		-	65
6	4000		[ ]	75
6	5000		-	75
6	5800		[ ]	75
6	6500			100
6	7500		-	50
6	8500		[ ]	95
6	9500			95
6	10500			95
7	135			70
7	500		-	100
7	1000		-	100
7	2000		[ ]	100
7	3000	]	-	100

Cycle	Cycle Burnup (MWD/MTU)	CEPAK (%)	DIT (%)	Nominal Power % of Full Power
7	4000	[	[	100
7	5000		-	100
7	6000		[	100
7	7000		-	100
7	8000		[	100
7	9725			100
8	50	]		45
8	250	-		100
8	1000	[		100
8	2000	]	]	100

Table 5-3

Low Power Physics Isothermal Temperature Coefficients

Cycle	Boron Concentration (ppm)	Measured (Δρ/°F)	CEPAK* ROCS (Δρ/°F)	DIT ROCS (Δρ/°F)	XTG (Δρ/°F)
1	993	$0.26 * 10^{-4}$	[	-	-
1	854	$-0.11 * 10^{-4}$		-	-
2	1240	$0.41 * 10^{-4}$		-	-
2	1198	$0.32 * 10^{-4}$		-	-
2	1164	$0.09 * 10^{-4}$		-	-
3	1000	$-0.078 * 10^{-4}$		-	-
4	1020	$0.14 * 10^{-4}$		-	-
5	1228	$0.20 * 10^{-4}$		-	-
6	1213	$0.23 * 10^{-4}$		[	[
7	1213	$0.12 * 10^{-4}$			
8	1240	$0.16 * 10^{-4}$	]	]	]

* Calculated results were biased by $0.20 * 10^{-4}$ Δρ/°F

Table 5-4

Comparison of Calculated and Measured
Isothermal Temperature Coefficient

BOC

Cycle	Percent of Rated Power	Critical Boron Concentration (ppm)	Measured ITC (*$10^4 \Delta\rho/°F$)	Calculated* CEPAK-ROCS ITC (X$10^4 \Delta\rho/°F$)	Calculated DIT-ROCS ITC (X$10^4 \Delta\rho/°F$)
1				[	
2	69(1)	927	-0.28		-
3	46(1)	720	-0.41		-
4	92(1)	690	-0.42		-
5	93(1)	876	-0.19		-
6	95(1)	848	-0.46		[
7	96(2)	817	-0.52		
8	79(2)	817	-0.84	]	]

EOC

1	75(1)	239	-0.98	[	-
2	46(1)	104	-1.62		-
3	90(1)	62	-1.65		-
4	95(1)	44	-1.41		-
5	94(1)	296	-0.97		-
6	96(2)	307	-1.51		[
7	95(2)	192	-1.85	]	]

(1) Full Rated Power = 1420 MWt

(2) Full Rated Power = 1500 MWt

* BOC calculated results were biased by 0.20 * 10-4 $\Delta\rho/°F$ and EOC calculated results were biased by 0.40 * 10-4 $\Delta\rho/°F$.

Table 5-5

Comparison of Calculated and Measured Power Coefficients

Cycle	Burnup MWD/MTU	Percent of Rated Power	Critical Boron Conc.	Measured Power Coeff. ($\Delta\rho$/% Power)	CEPAK-ROCS Calculated Power Coeff. ($\Delta\rho$/% Power)	DIT-ROCS Calculated Power Coeff. ($\Delta\rho$/% Power)
2	10877	46(1)	104	-1.95×10^{-4}		-
3	157	46(1)	720	-1.47×10^{-4}		-
3	1513	90(1)	535	-1.12×10^{-4}		-
3	4183	90(1)	309	-1.31×10^{-4}		-
3	7208	90(1)	62	-1.48×10^{-4}		-
4	267	92(1)	690	-1.04×10^{-4}		-
4	4690	94(1)	288	-1.12×10^{-4}		-
4	8027	95(1)	44	-1.10×10^{-4}		-
5	426	93(1)	876	-1.05×10^{-4}		-
5	6815	94(1)	296	-1.25×10^{-4}		-
6	400	95(1)	848	-1.11×10^{-4}		
6	6467	96(2)	307	-1.45×10^{-4}		
7	450	96(2)	817	-0.98×10^{-4}		
7	6900	95(2)	283	-1.30×10^{-4}		
7	7800	95(2)	192	-1.57×10^{-4}		
8		79(2)	817	-1.18×10^{-4}		

(1) Full Rated Power = 1420 MWt

(2) Full Rated Power = 1500 MWt

Table 5-6

Cycle 1 CEA Worths

Group	Measured (%Δρ)	Calculated CEPAK-ROCS 3-D (%Δρ)	Calculated CEPAK-ROCS 2-D (%Δρ)	Calculated CEPAK-PDQ 2-D (%Δρ)
4	0.58	[		
3	0.57			
2	2.01			
A	3.06			
B	2.10			
Total (4+3+2+A+B)	8.32	]		]

Table 5-7

Cycle 2 CEA Worths

Group	Measured (%Δρ)	Calculated CEPAK-ROCS 3-D (%Δρ)	Calculated CEPAK-ROCS 2-D (%Δρ)	Calculated CEPAK-PDQ 2-D (%Δρ)
4	0.65	[	[	[
3	0.41			
2	1.67		]	
1	0.95		-	
Total (4+3+2+1)	3.68	]	-	]

Table 5-8

Cycle 3 CEA Worths

Group	Measured (%Δρ)	Calculated CEPAK-ROCS 3-D (%Δρ)	Calculated CEPAK-ROCS 2-D (%Δρ)
4	0.74	[ ]	[ ]
3	0.59		
2	1.96		
1	0.80		-
Total (4+3+2+1)	4.09		-

Table 5-9

Cycle 4 CEA Worths

Group	Measured (%Δρ)	Calculated CEPAK-ROCS 3-D (%Δρ)	Calculated CEPAK-ROCS 2-D (%Δρ)
4	0.63	[ ]	[ ]
3	0.63		
2	1.90		
1	0.92		-
Total (4+3+2+1)	4.05		-

Table 5-10

Cycle 5 CEA Worths

Group	Measured (%Δρ)	Calculated CEPAK-ROCS 3-D (%Δρ)	Calculated CEPAK-ROCS 2-D (%Δρ)	Calculated CEPAK-PDQ 2-D (%Δρ)
4	0.57	[ ]	[ ]	[ ]
3	0.67			
2	1.40			
1	0.99		-	-
Total (4+3+2+1)	3.63		-	-

Table 5-11

Cycle 6 CEA Worths

Group	Measured (%Δρ)	Calculated XTG (%Δρ)	Calculated CEPAK-ROCS 3-D (%Δρ)	Calculated DIT-ROCS 2-D (%Δρ)	Calculated DIT-ROCS 3-D (%Δρ)
4	0.52	[ ]	[ ]	[ ]	-
3	0.66				-
2	1.57				-
1	0.93				-
Total (4+3+2+1)	3.68				[ ]

Table 5-12

Cycle 7 CEA Worths

Group	Measured (%Δρ)	Calculated XTG (%Δρ)	Calculated CEPAK-ROCS 3-D (%Δρ)	Calculated DIT-ROCS 2-D (%Δρ)	Calculated DIT-ROCS 3-D (%Δρ)
4	0.49	[ ]	[ ]	[ ]	-
3	0.47				-
2	1.65				-
1	0.70				-
Total (4+3+2+1)	3.27				[ ]

Table 5-13

Cycle 8 CEA Worths

Group	Measured (%Δρ)	Calculated XTG (%Δρ)	Calculated CEPAK-ROCS 3-D (%Δρ)	Calculated DIT-ROCS 2-D (%Δρ)	Calculated DIT-ROCS 3-D (%Δρ)
4	0.58	[ ]	[ ]	[ ]	[ ]
3	0.63				
2	0.99				
1	1.00				
Total (4+3+2+1)	3.20				

CYCLE 4
CRITICAL BORON CONCENTRATION vs BURNUP

FIGURE 5-1

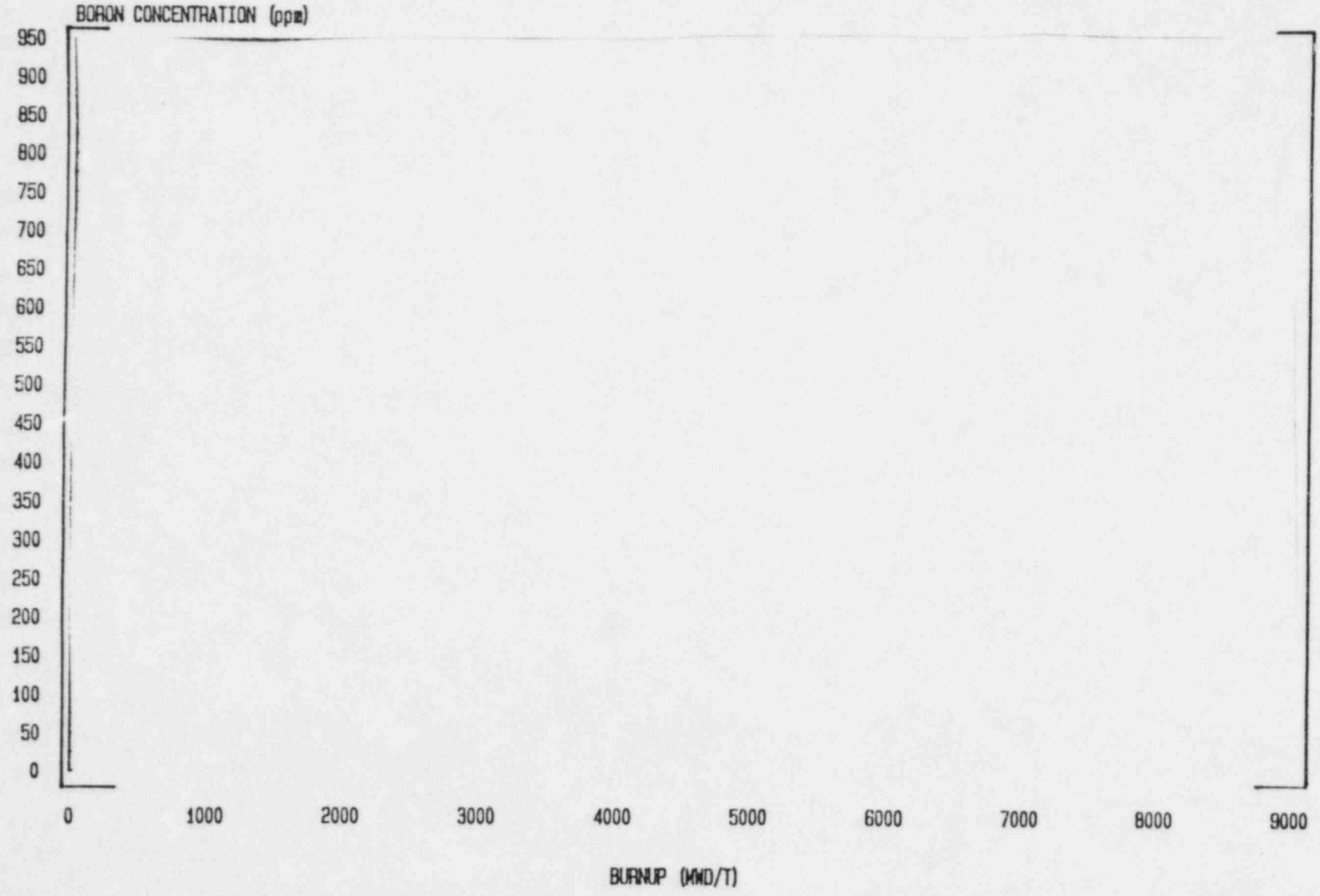

CYCLE 5
CRITICAL BORON CONCENTRATION vs BURNUP

FIGURE 5-2

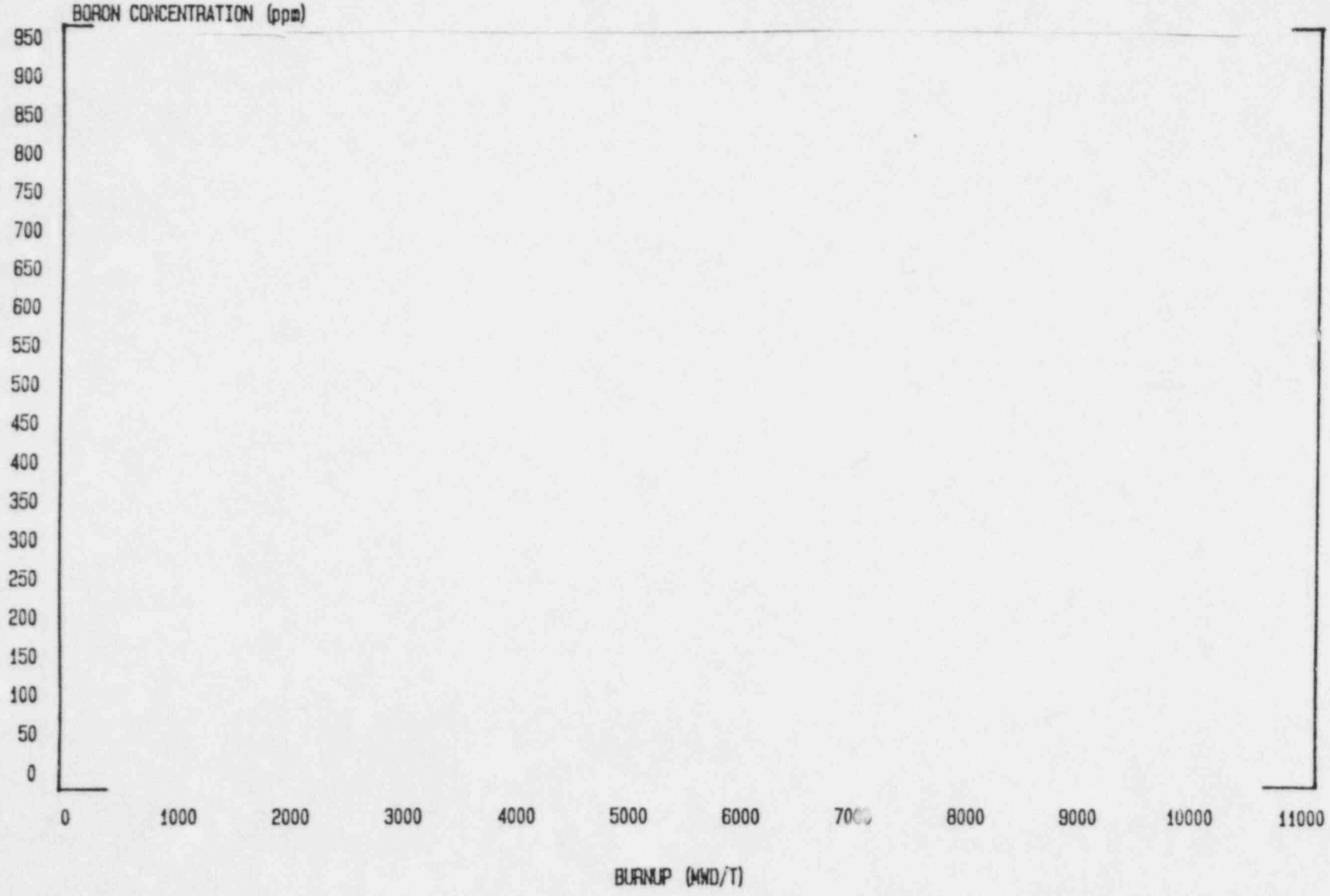

CYCLE 6
CRITICAL BORON CONCENTRATION vs BURNUP

FIGURE 5-3

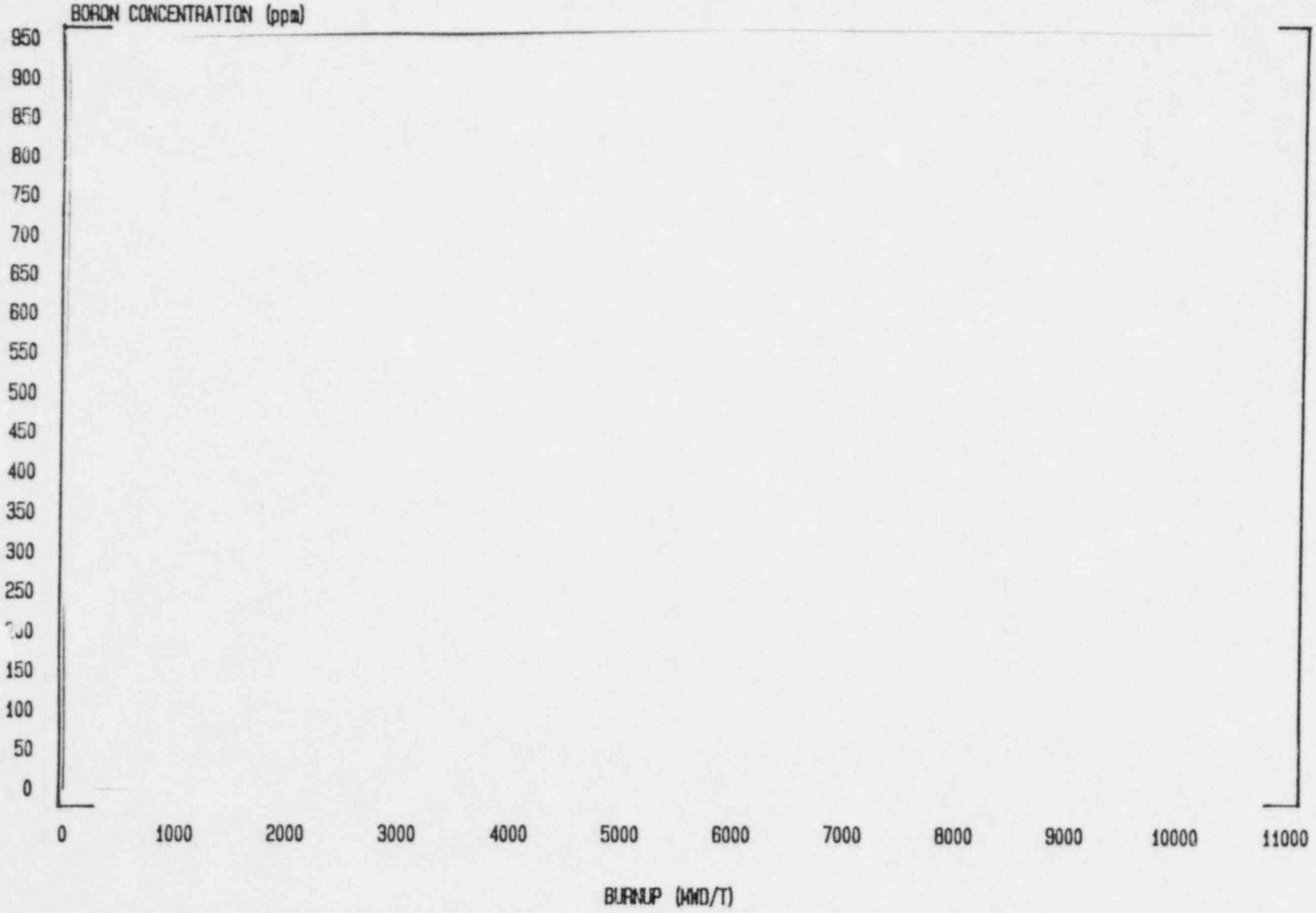

CYCLE 7
CRITICAL BORON CONCENTRATION vs BURNUP

FIGURE 5-4

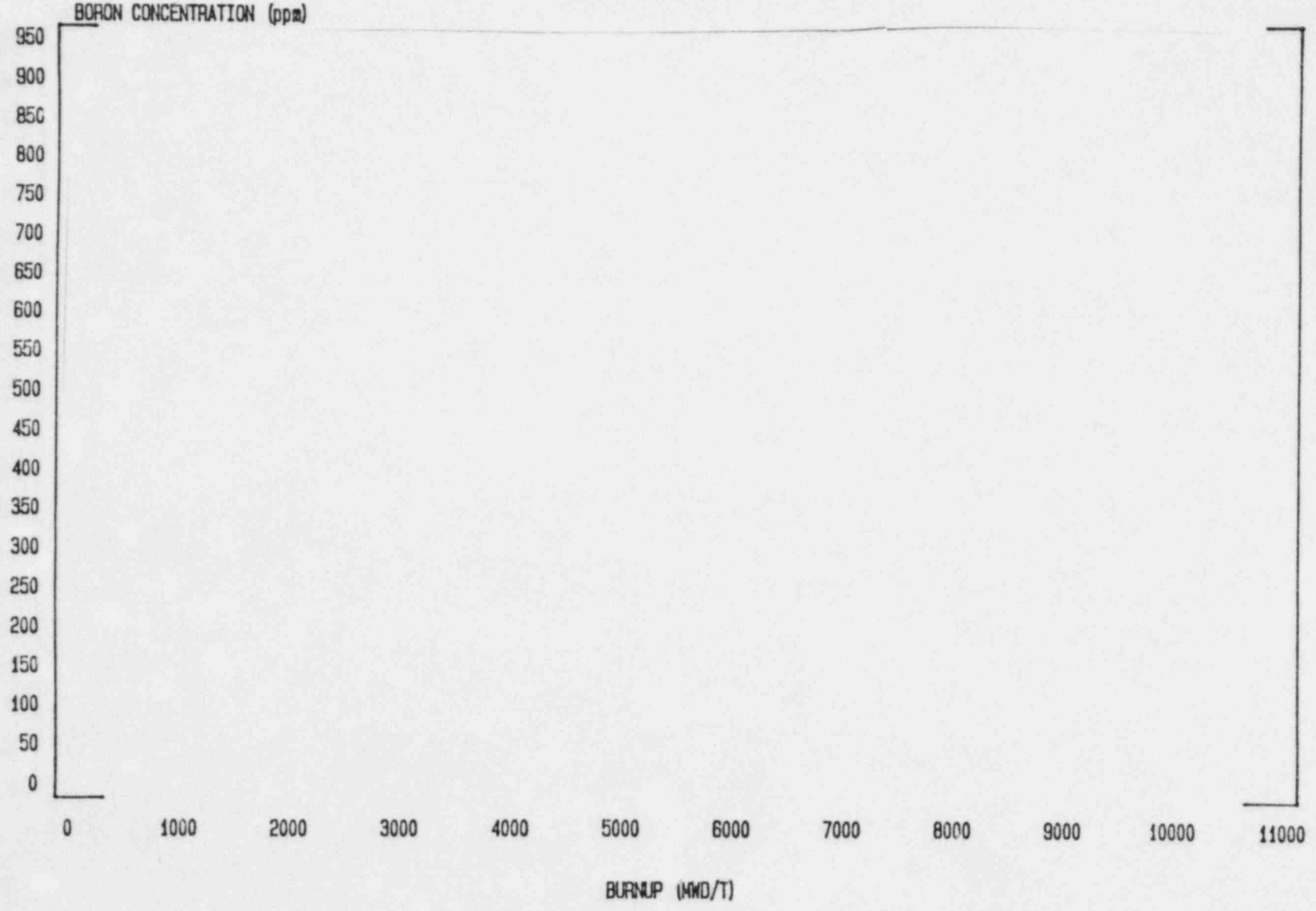

CYCLE 8
CRITICAL BORON CONCENTRATION vs BURNUP

FIGURE 5-5

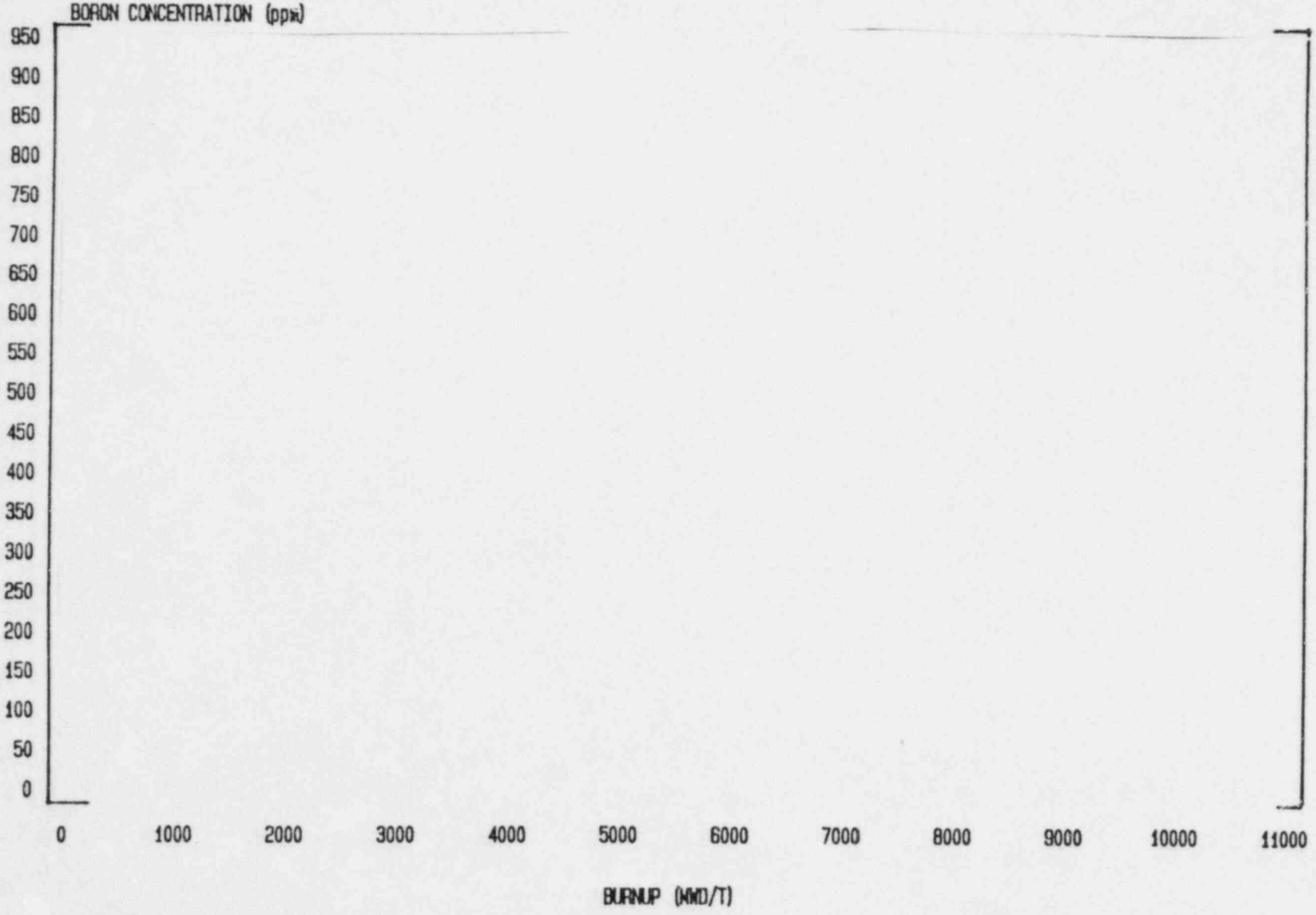

BENCHMARK OF QUIX ASI VS. CECOR ASI

Figure 5-6

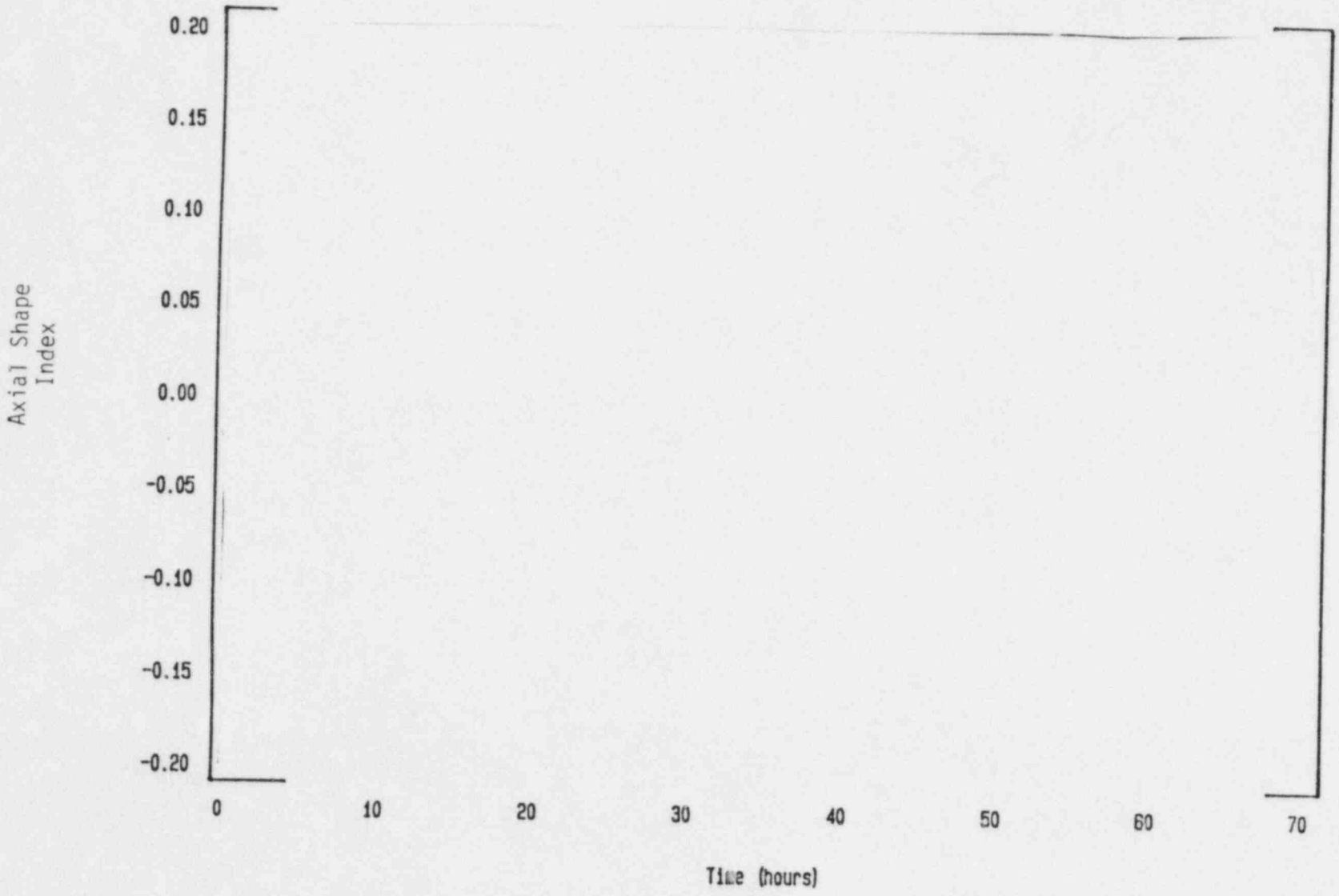

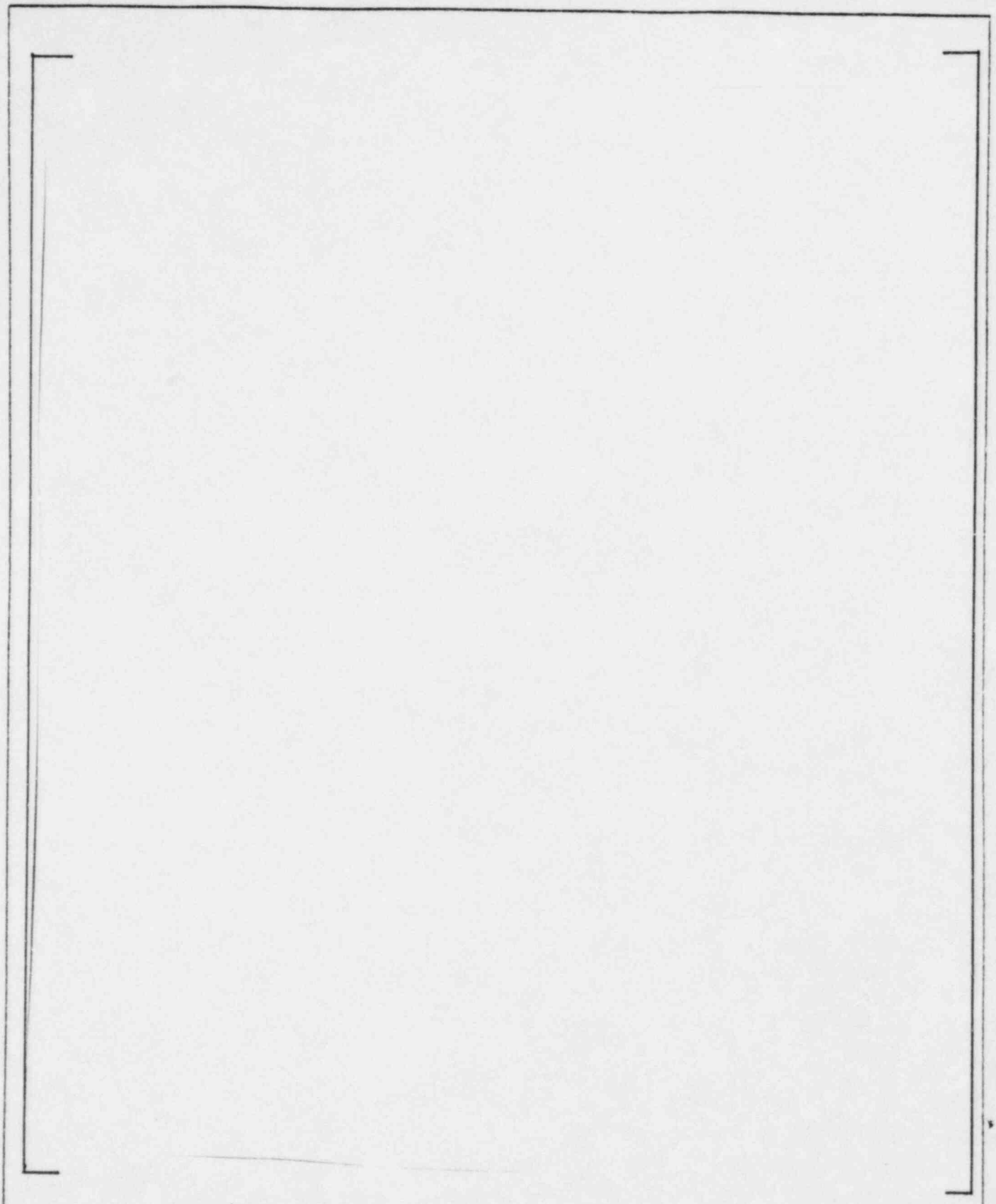

Assembly APD Comparison BOC & HFP ARO and ~ 870 ppm Boron	Omaha Public Power District Fort Calhoun Station-Unit No. 1	Figure 5-7

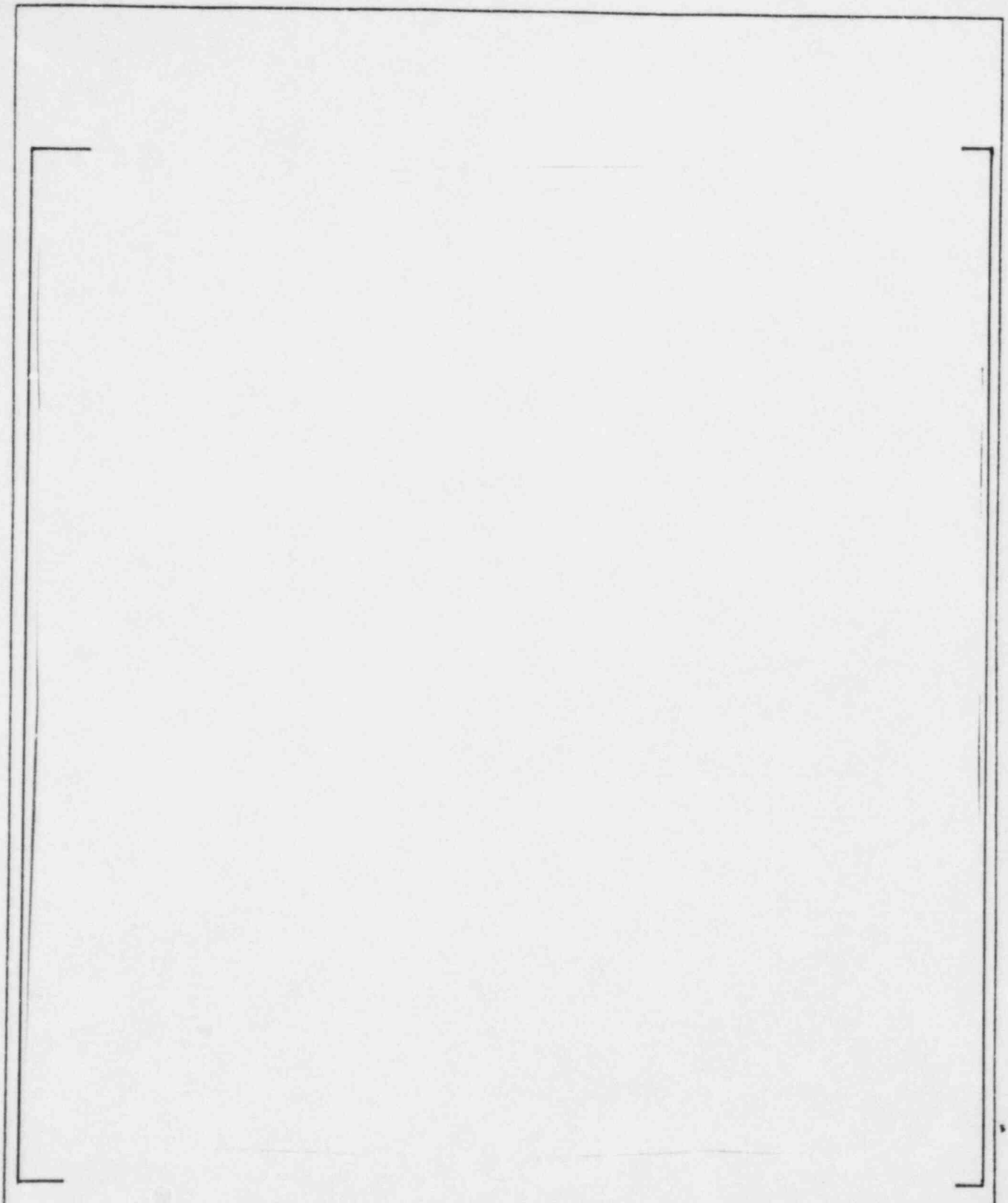

Assembly RPD Comparison EOC 6 10,000 MWD/MTU HFP ARO - 20 ppm Boron	Omaha Public Power District Fort Calhoun Station-Unit No. 1	Figure 5-8

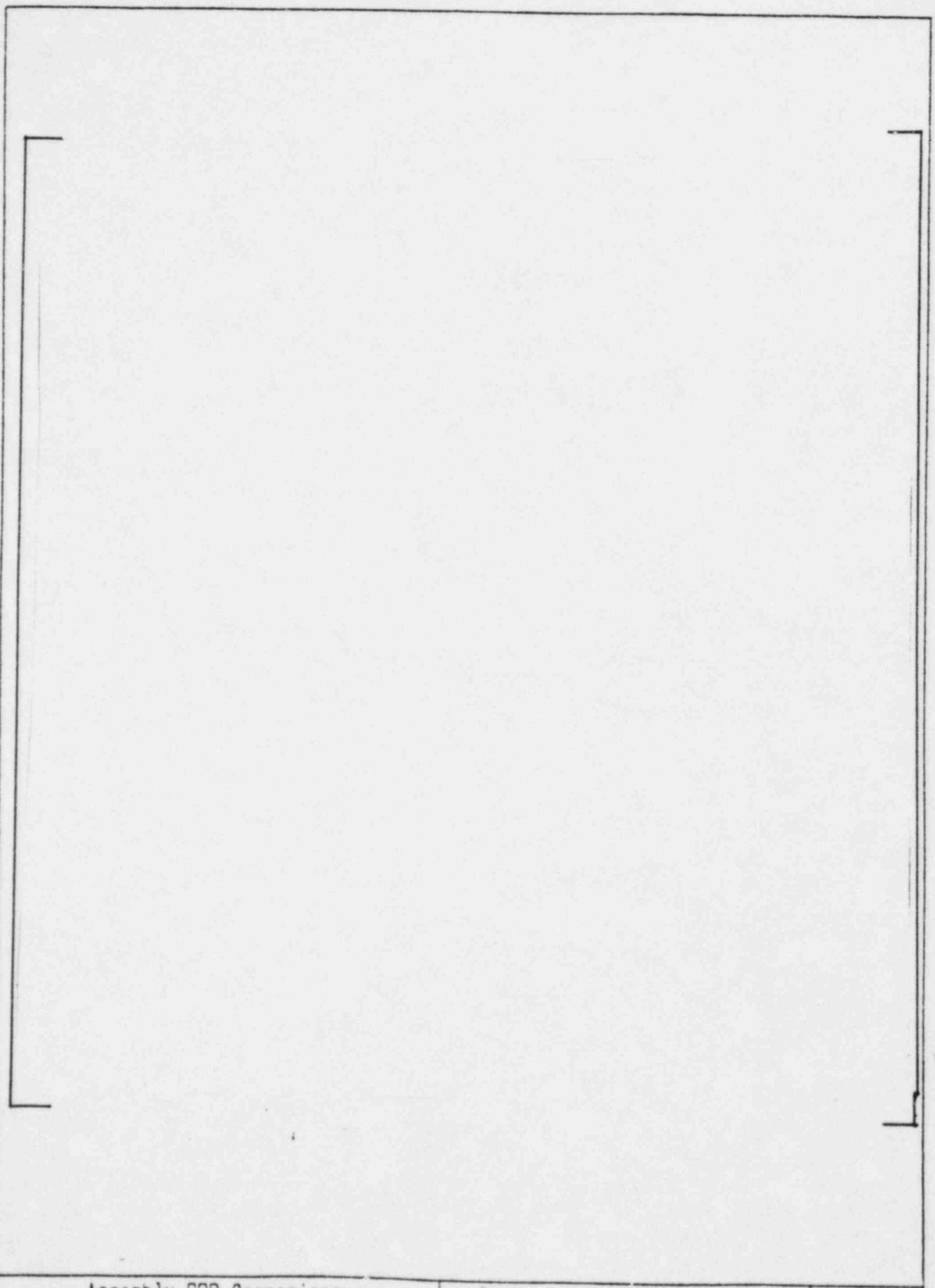

Assembly RPD Comparison BOC 7 HFP ARO and ~ 900 ppm Boron	Omaha Public Power District Fort Calhoun Station-Unit No. 1	Figure 5-9

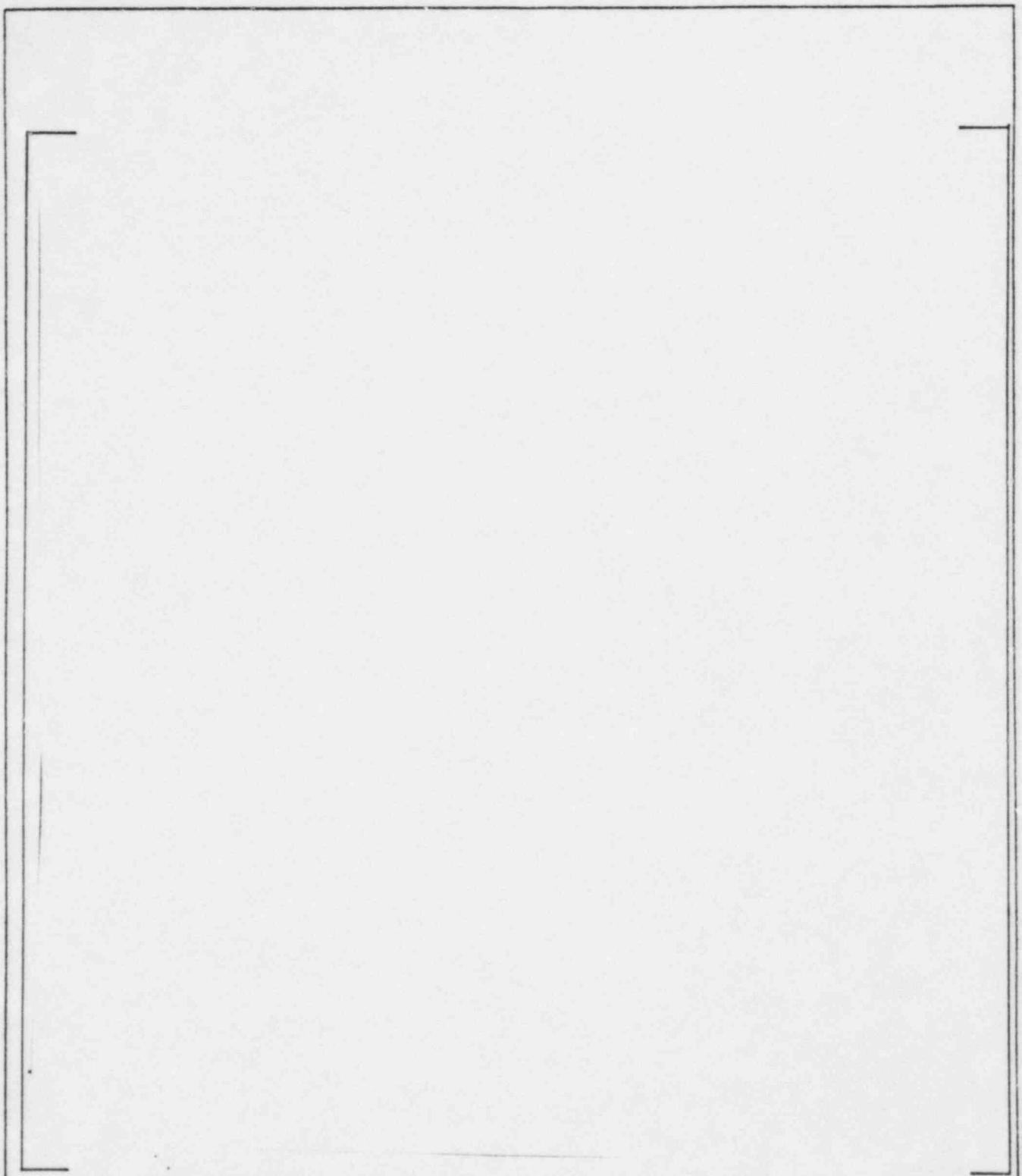

Assembly RPD Comparison EOC 7 10,000 MWD/MTU HFP ARO ~ 1 ppm Boron	Omaha Public Power District Fort Calhoun Station-Unit No. 1	Figure 5-10

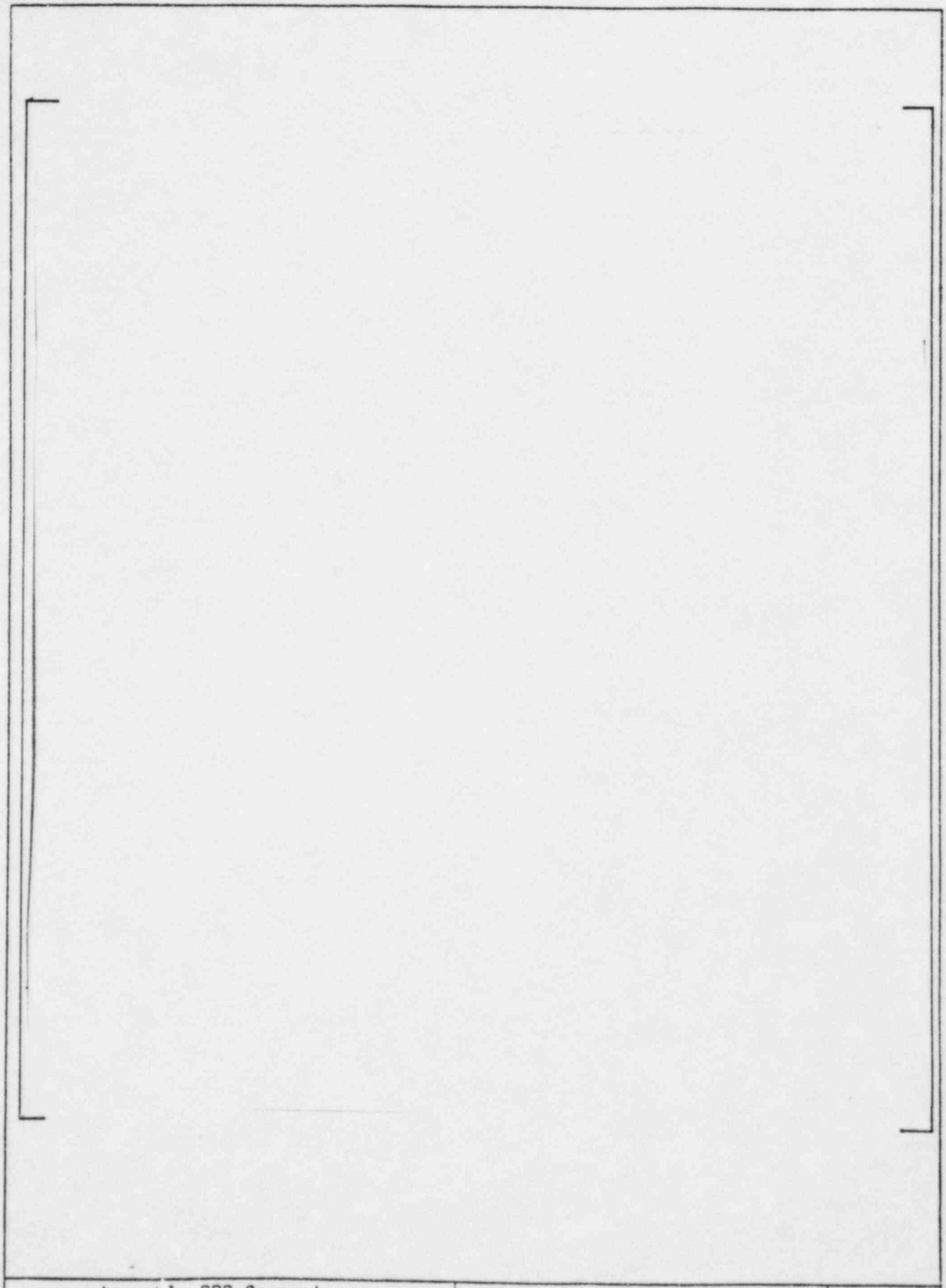

Assembly RPD Comparison BOC 8 HFP ARO and ~ 770 ppm Boron	Omaha Public Power District Fort Calhoun Station-Unit No. 1	Figure 5-11

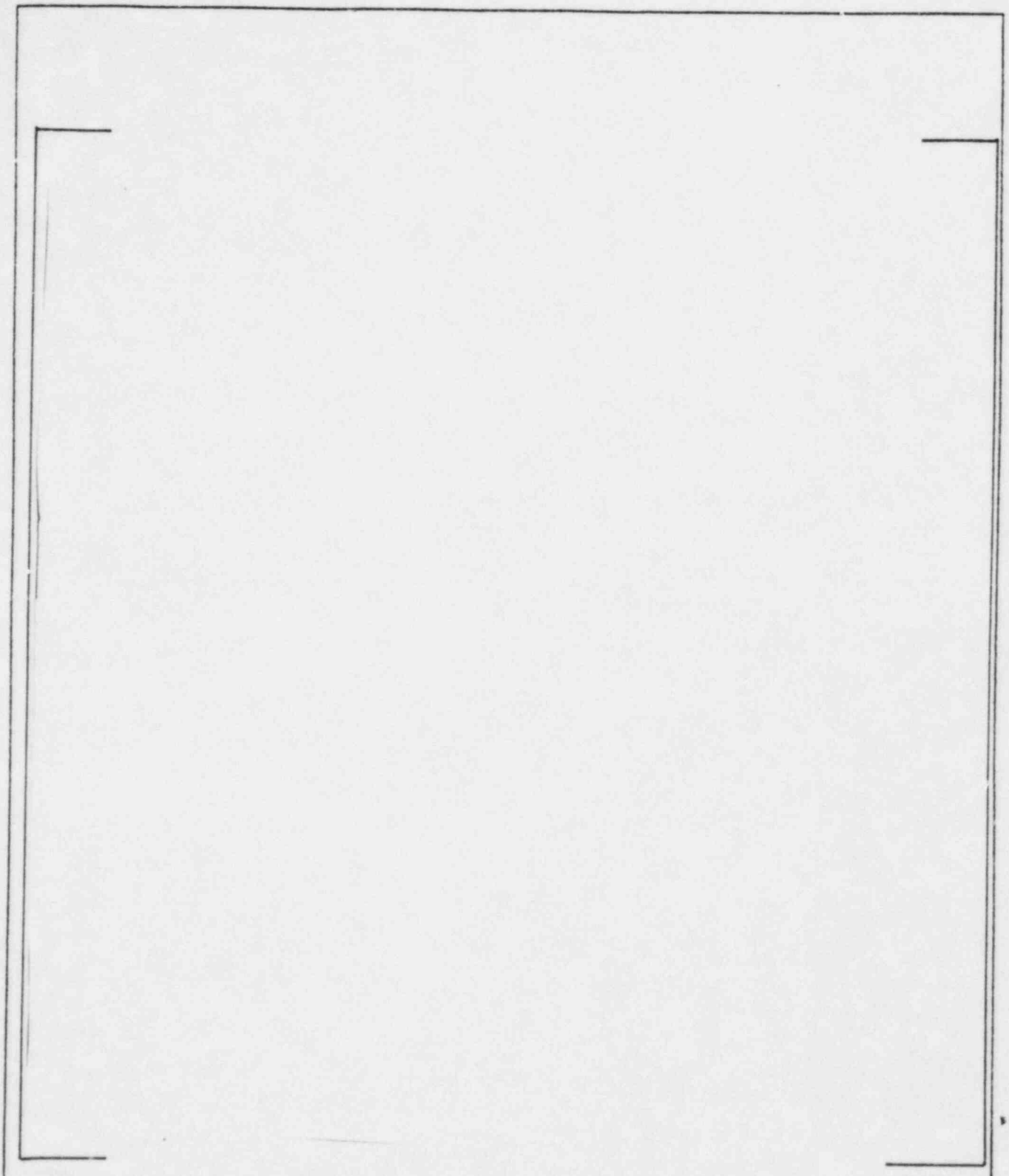

Assembly RPD Comparison EOC 8 9000 MWD/MTU HFP ARO ~ 1 ppm Boron	Omaha Public Power District Fort Calhoun Station-Unit No. 1	Figure 5-12

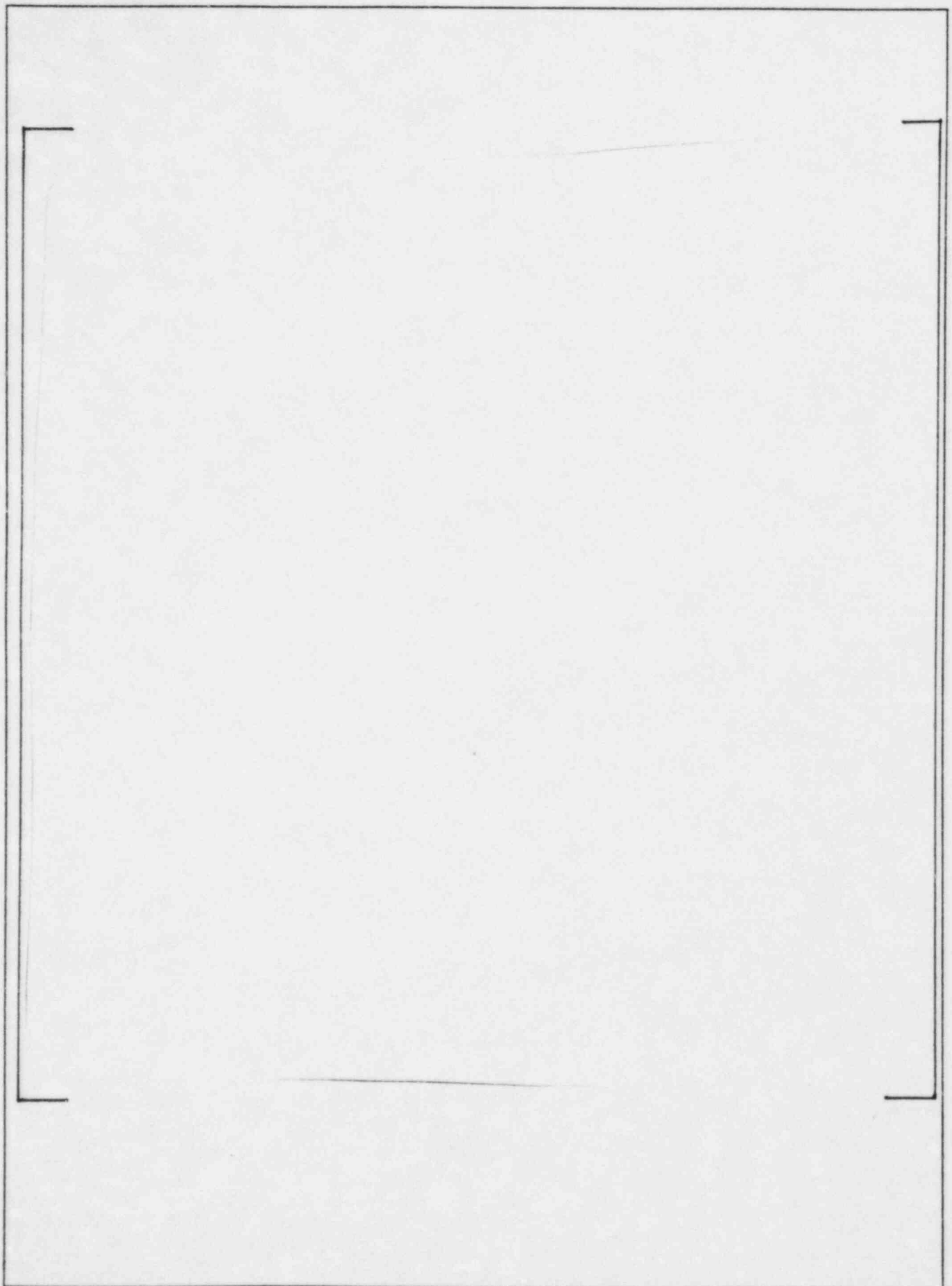

Assembly RPD Comparison BOC 6 HFP ARO and 870 ppm Boron	Omaha Public Power District Fort Calhoun Station-Unit No. 1	Figure 5-13

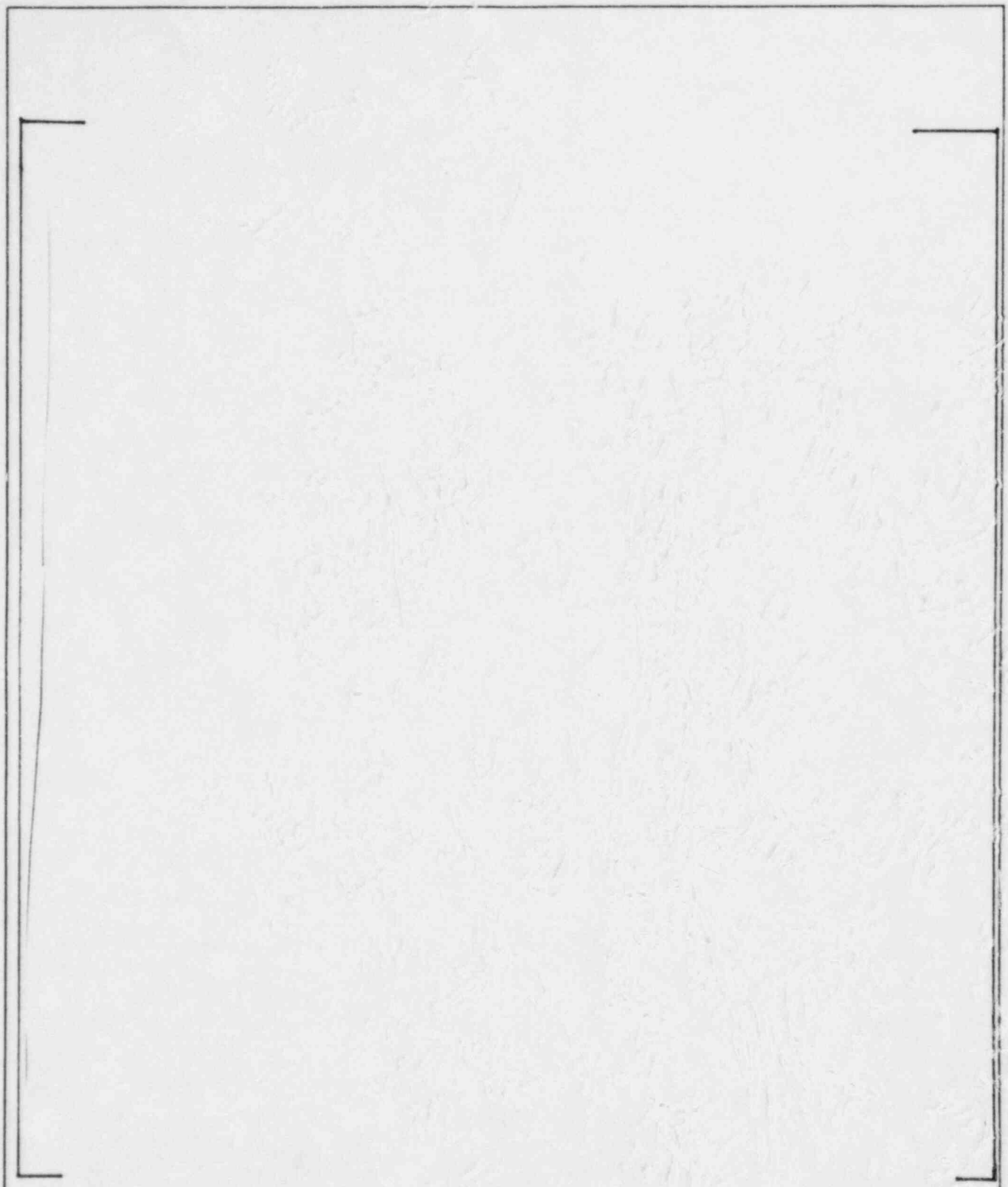

Assembly RPD Comparison EOC 6 10 000 MWD/MTU HFP ARO 20 ppm Boron	Omaha Public Power District Fort Calhoun Station-Unit No. 1	Figure 5-14

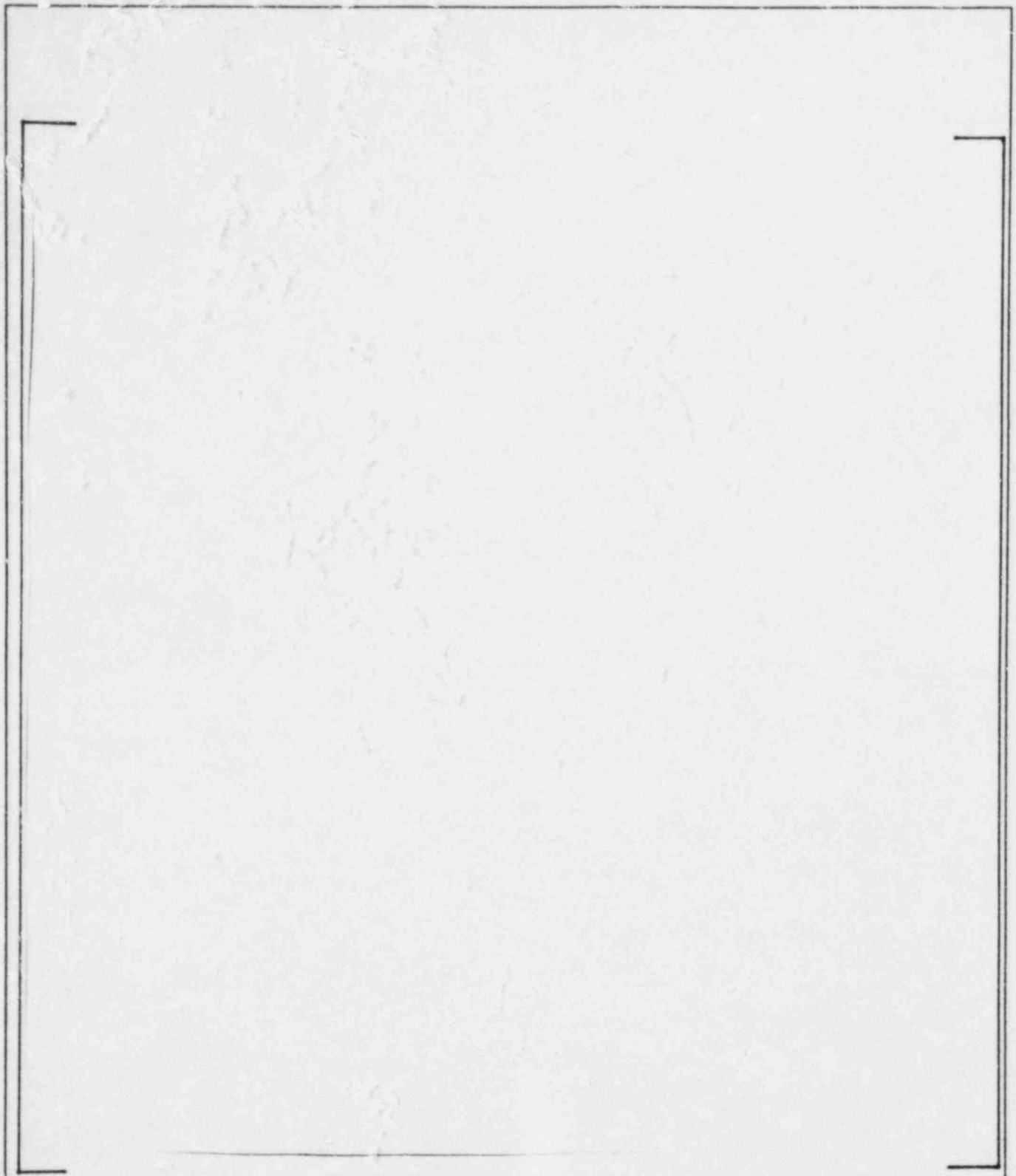

Assembly RPD Comparison BOC 7 HFP ARO and 900 ppm Boron	Omaha Public Power District Fort Calhoun Station-Unit No. 1	Figure 5-15

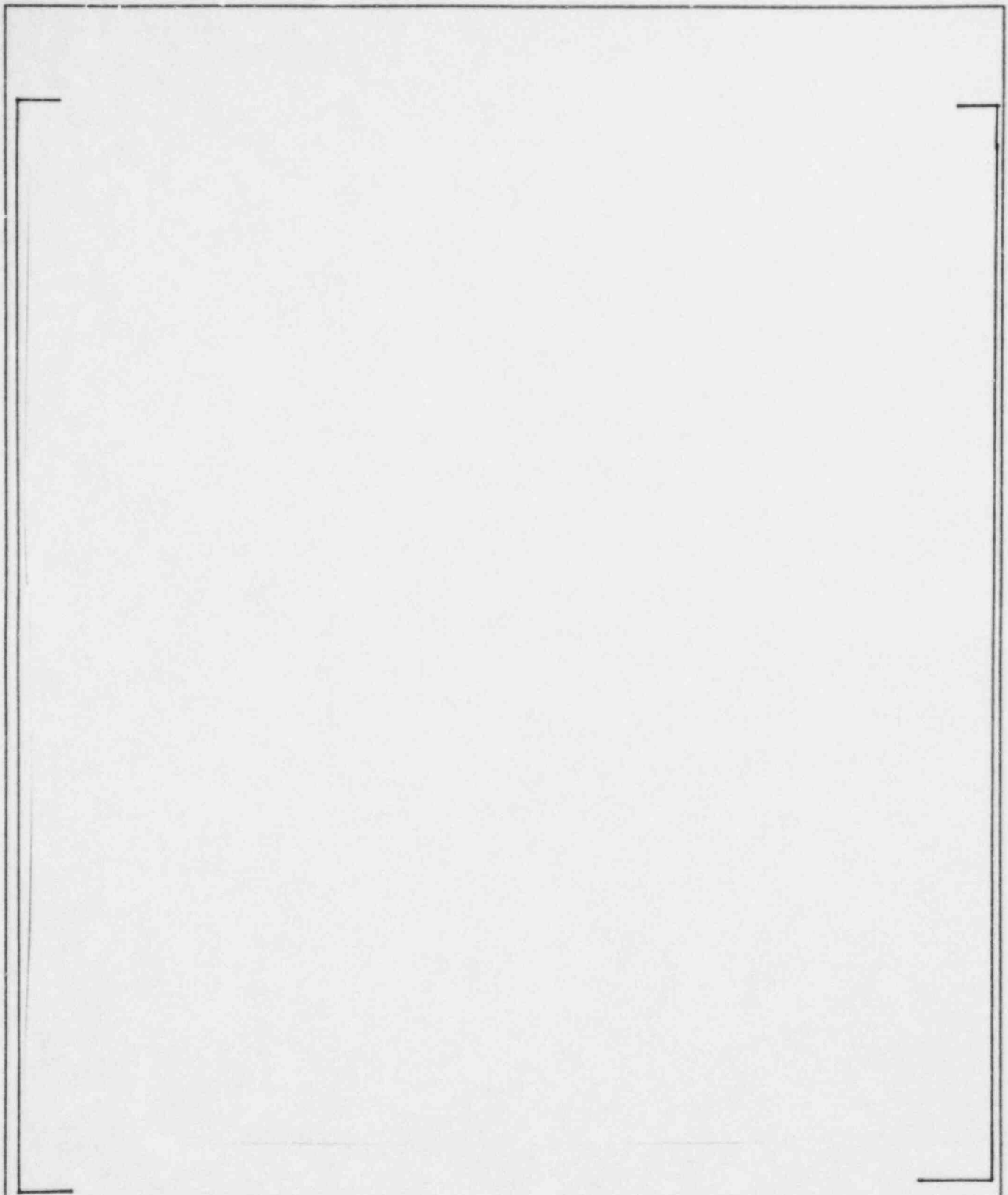

Assembly RPD Comparison EOC 7 10 000 MWD/MTU HFP ARO 1 ppm Boron	Omaha Public Power District Fort Calhoun Station-Unit No. 1	Figure 5-16

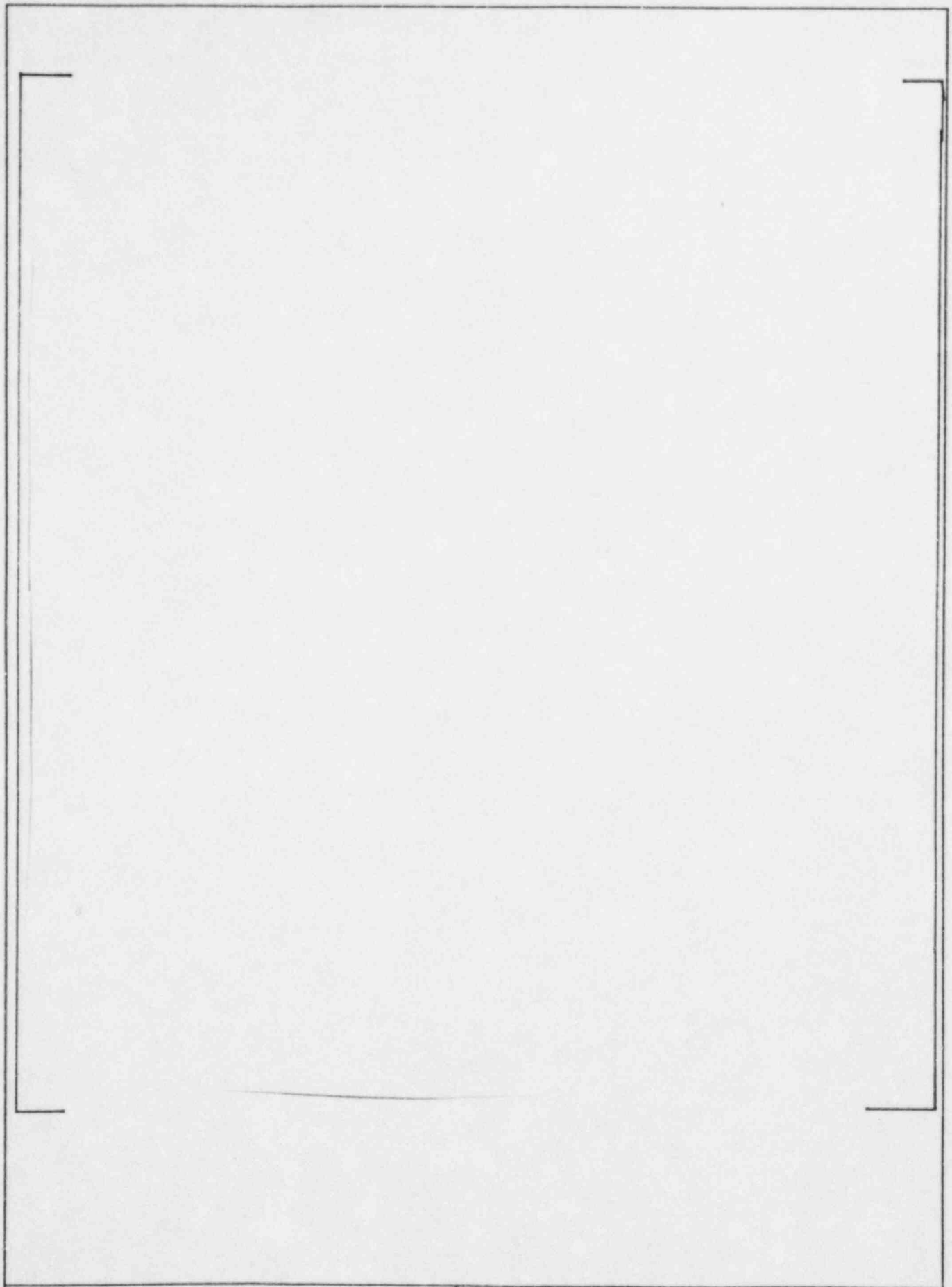

Assembly RPD Comparison BOC 8 HFP ARO and 770 ppm Boron	Omaha Public Power District Fort Calhoun Station-Unit No. 1	Figure 5-17

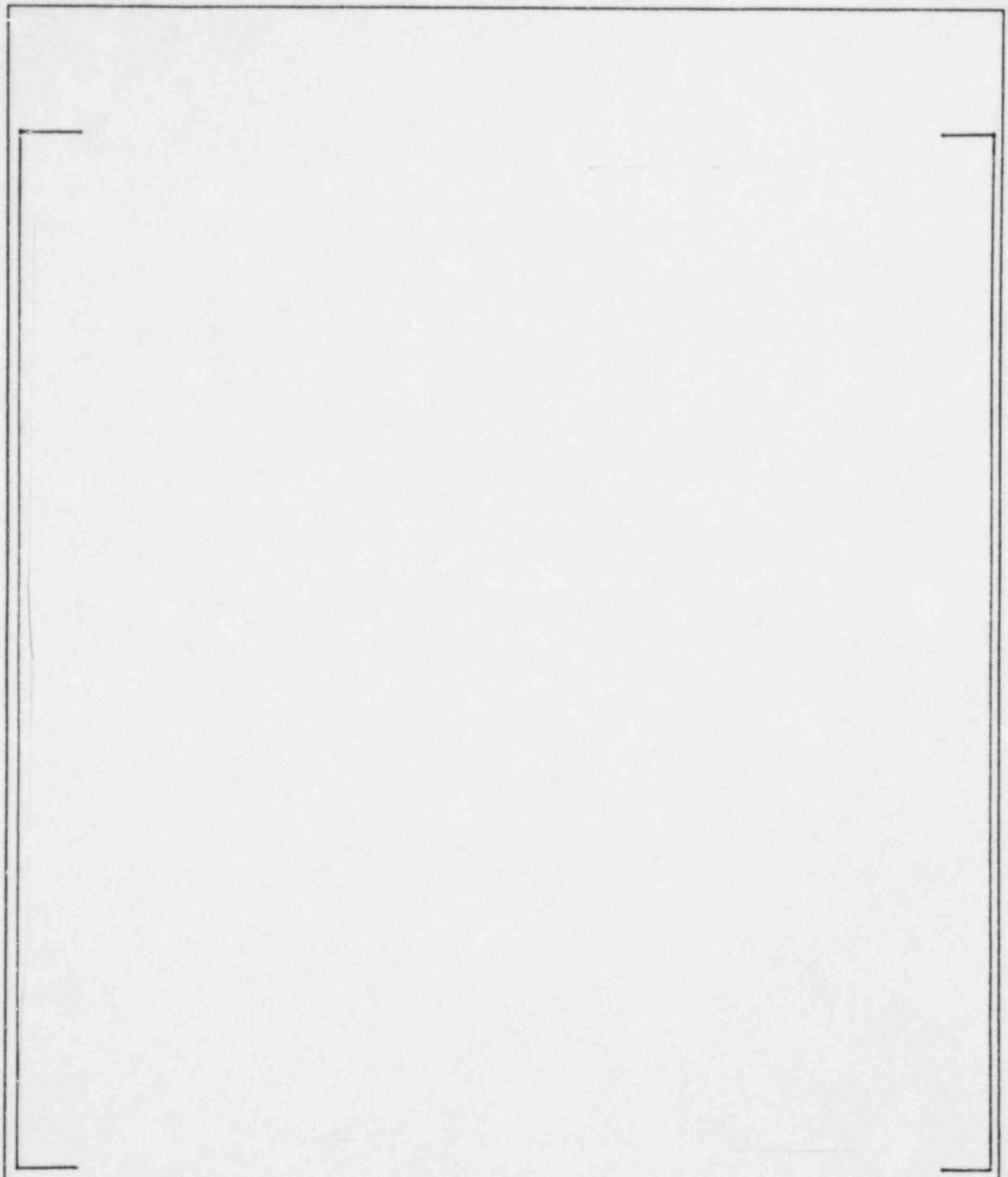

Assembly RPD Comparison EDC 8 9000 MWD/MTU HFP ARO 1 ppm Boron	Omaha Public Power District Fort Calhoun Station-Unit No. 1	Figure 5-18

6.0 REFERENCES

Section 2.0 References

2-1 ENDF-313, "Benchmark Testing of ENDF/B Data for Thermal Reactors, Archival Volume," July, 1981.

2-2 A. Jonsson, J. R. Rec and U. N. Singh, "Verification of a Fuel Assembly Spectrum Code Based on Integral Transport Theory," Trans. Am. Nucl. Soc., 28, 778 (1978).

2-3 CENPD-226-P, "The ROCS and DIT Computer Codes for Nuclear Design," December, 1981.

2-4 System 80 PSAR, CESSAR, Vol. 1, Chapter 4.3.3, Amendment No. 3, June 3, 1974.

2-5 W. R. Cadwell, "PDQ-7 Reference Manual," WAPD-TM-678, January, 1968.

2-6 T. G. Ober, J. C. Stark, I. C. Richard and J. K. Gasper "Theory, Capabilities, and Use of the Three Dimensional Reactor Operation and Control Simulator (ROCS)," Nucl. Sci. Eng., 64, 605, (1977).

2-7 System 80 PSAR, CESSAR, Vol. 1, Appendix 4A, Amendment No. 3, June 3, 1974.

2-8 CENPD-199-P, Revision 1-P, "CE Setpoint Methodology," April 1982.

Section 3.0 References

3-1 CENPD-199-P, Revision 1-P, "CE Setpoint Methodology," April 1982.

3-2 CENPD-226-P, "The ROCS and DIT Computer Codes for Nuclear Design," December, 1981.

Section 4.0 References

4-1 CENPD-153, Revision 1-P-A, "Evaluation of Uncertainties in the Nuclear Power Peaking Measured by the Self-Powered Fixed In-Core Detector System," May, 1980.

4-2 "Development and Verification of a Fuel Temperature Correlation for Power Feedback and Reactivity Coefficient Application," P. H. Gavin and P. C. Rohr, Trans. Am. Nucl. Soc. 30, p. 765, 1978.

4-3 A. F. Henry, "Computation of Parameters Appearing in the Reactor Kinetic Equations," WAPD-142, December 1955.

4-4 R. W. Hardie, W. W. Litke, Jr., "PERT-V, A Two Dimensional Perturbation Code for Fast Reactor Analysis," BNWL-1162.

6.0 REFERENCES

Section 4.0 References (Continued)

4-5 CENPD-226-P, "The ROCS and DIT Computer Codes for Nuclear Design," December, 1981.

4-6 CENPD-199-P, Revision 1-P, "CE Setpoint Methodology," April 1982.

Section 5.0 References

5-1 CEN-242-(0)-P, OPPD Responses to NRC Questions on Fort Calhoun Cycle 8, February 18, 1983.

5-2 CENPD-226-P, "The ROCS and DIT Computer Codes for Nuclear Design," December, 1981.

5-3 CENPD-153-P, "INCA/CECOR Power Peaking Uncertainty," May, 1980.

APPENDIX A

CYCLE 8 RADIAL POWER DISTRIBUTION COMPARISONS

CEPAK

OMAHA CY8 45 PERCENT
INST ONLY ROCS-CECOR COMPARISON
LEVEL 1 BOC 8

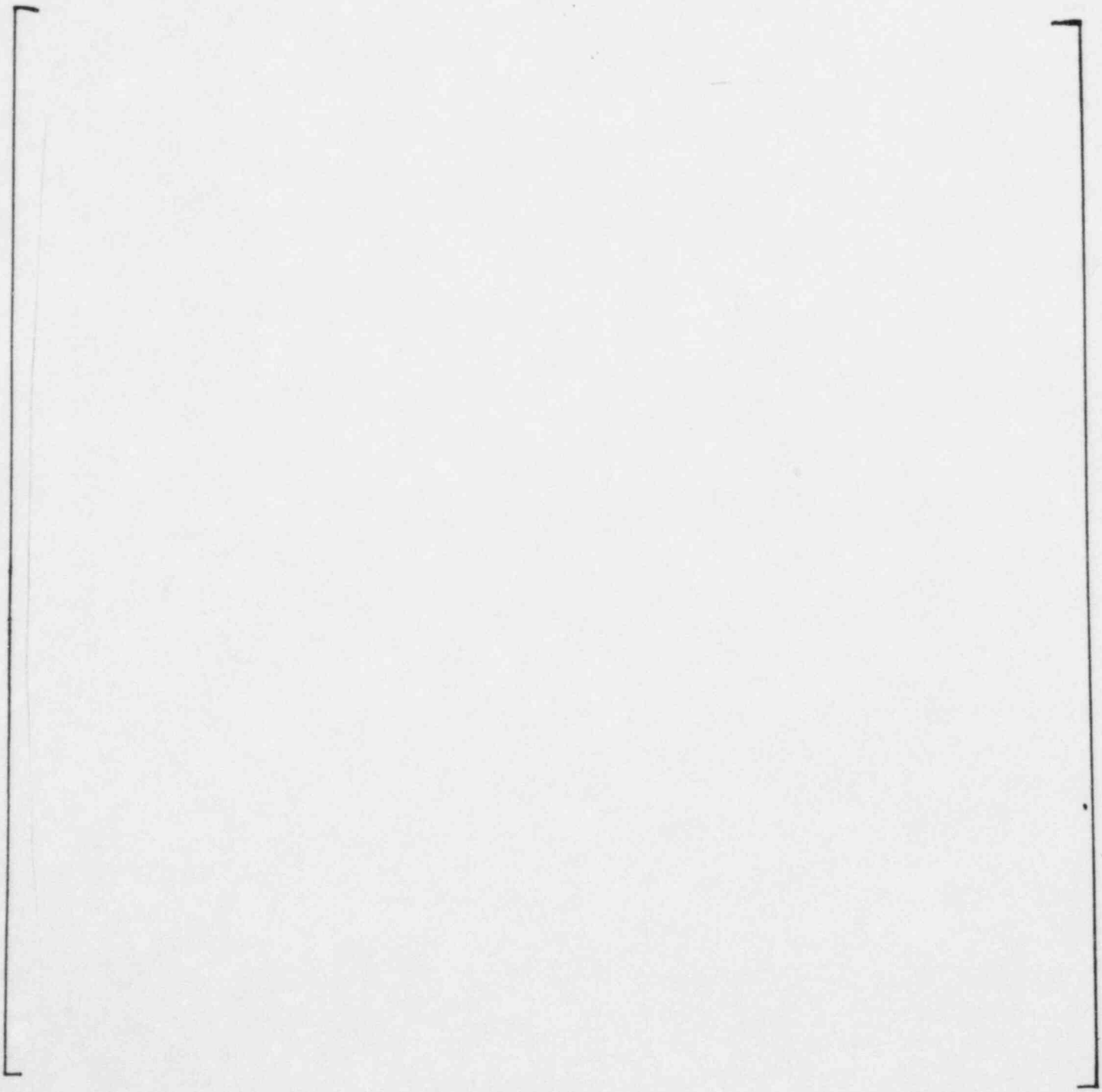

CEPAK

OMAHA CY8 45 PERCENT
INST ONLY ROCS-CECOR COMPARISON
LEVEL 2 BOC 8

CEPAK

OMAHA CY8 45 PERCENT
INST CNLY ROCS-CECOR COMPARISON
LEVEL 3 BOC 8

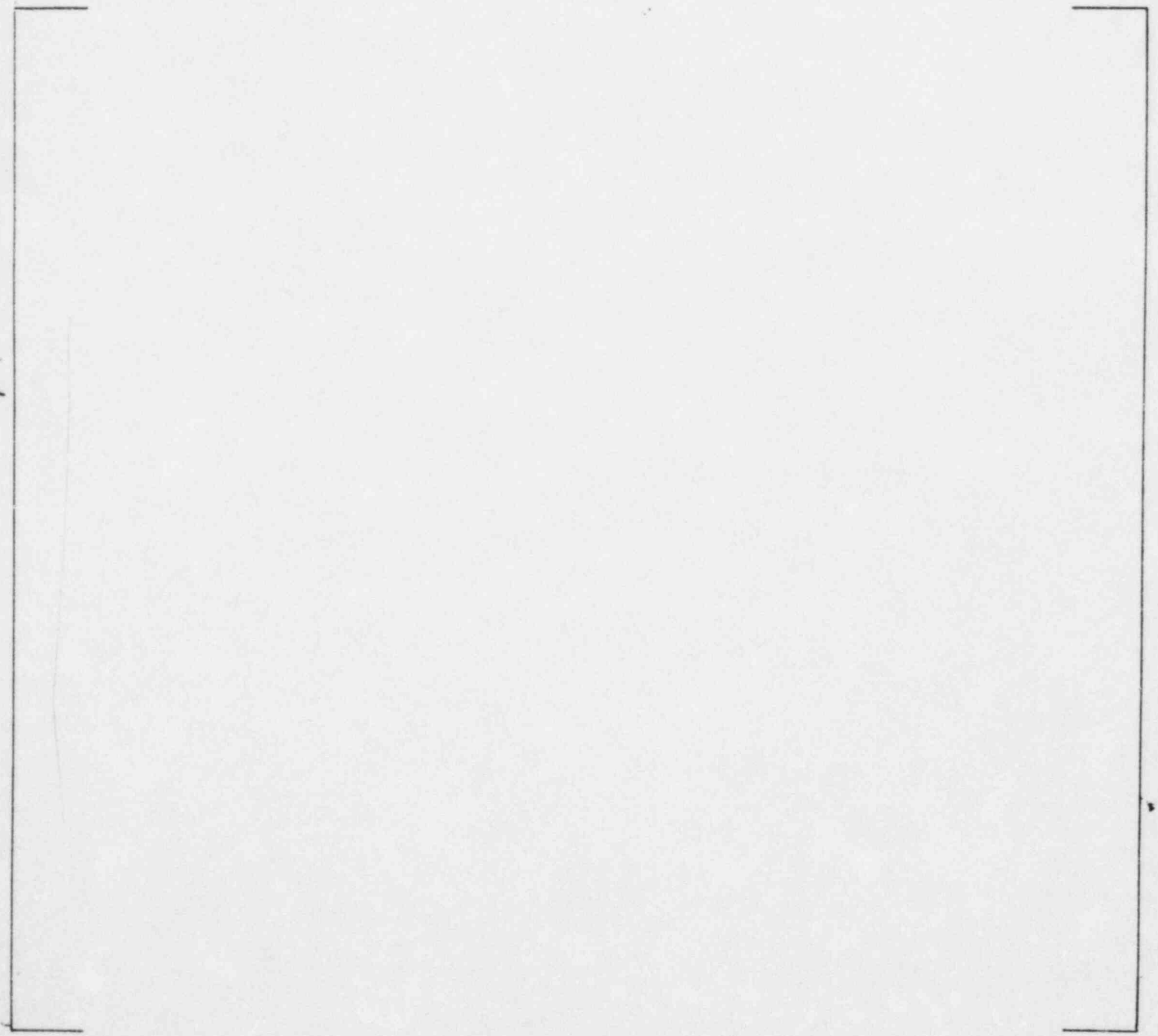

CEPAK

OMAHA CY8 45 PERCENT
INST ONLY ROCS-CECOR COMPARISON
LEVEL 4 BOC 8

CEPAK

OMAHA CY8 45 PERCENT
INST ONLY ROCS-CECOR COMPARISON
AXIALLY INTEGRATED BOC 8

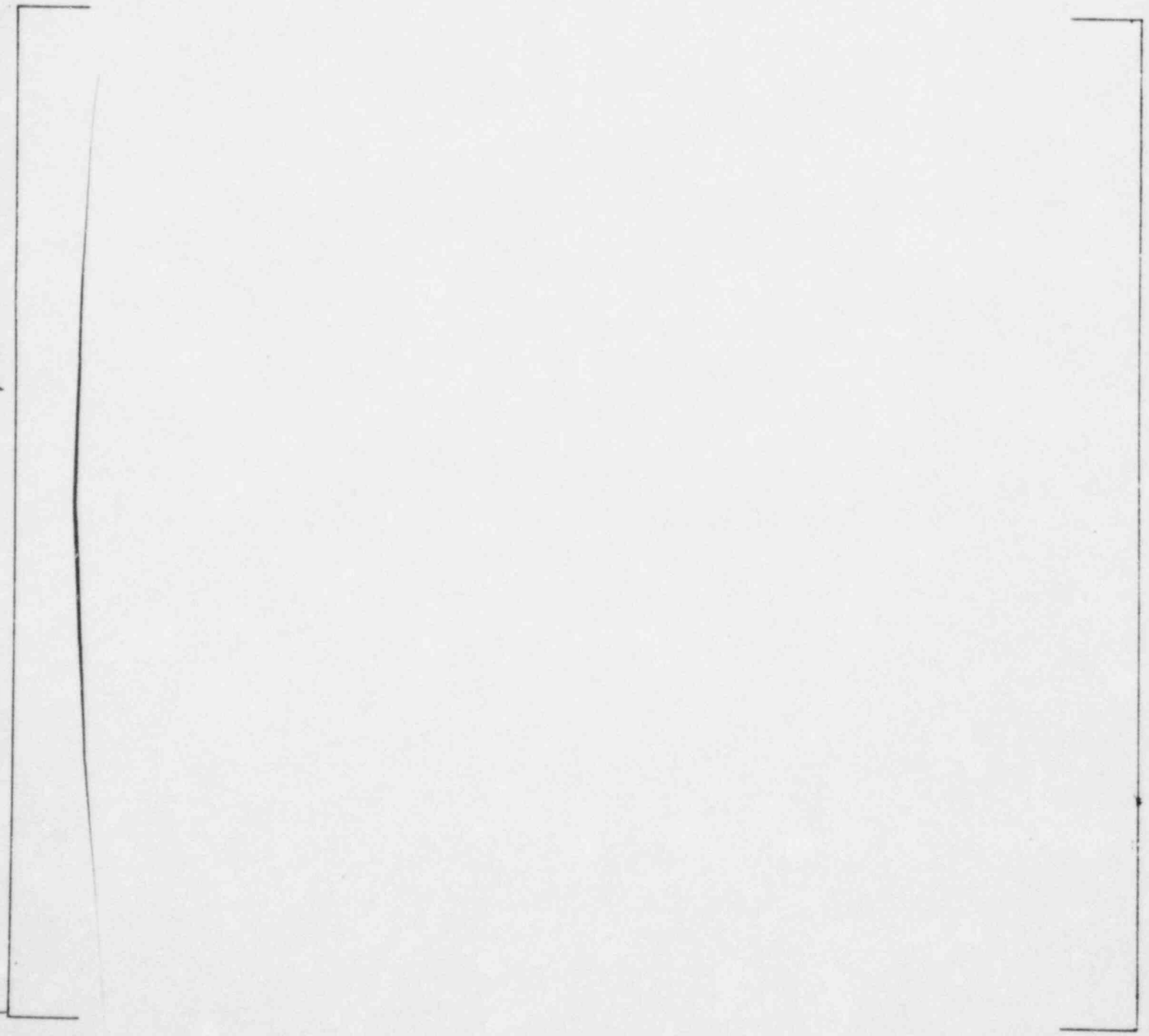

CEPAK

OMAHA CY8 99 PERCENT
INST ONLY ROCS-CECOR COMPARISO
N LEVEL 1 1000 MWD/T

CEPAK

OMAHA CY8 99 PERCENT
INST ONLY ROCS-CECOR COMPARISO
N LEVEL 2 1000 MWD/T

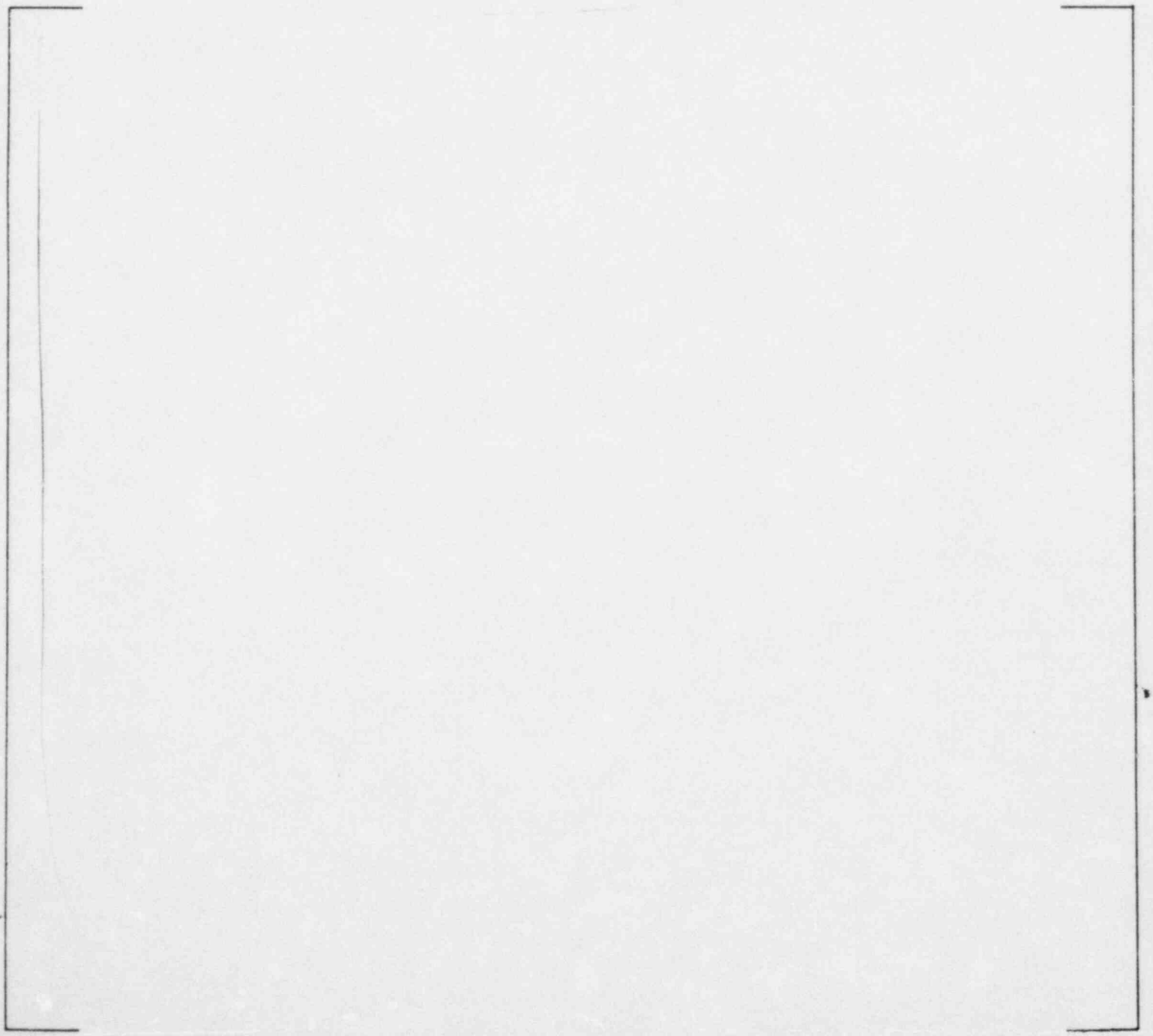

CEPAK

OMAHA CY8 45 PERCENT
INST ONLY ROCS-CECOR COMPARISON
LEVEL 3 BOC 8

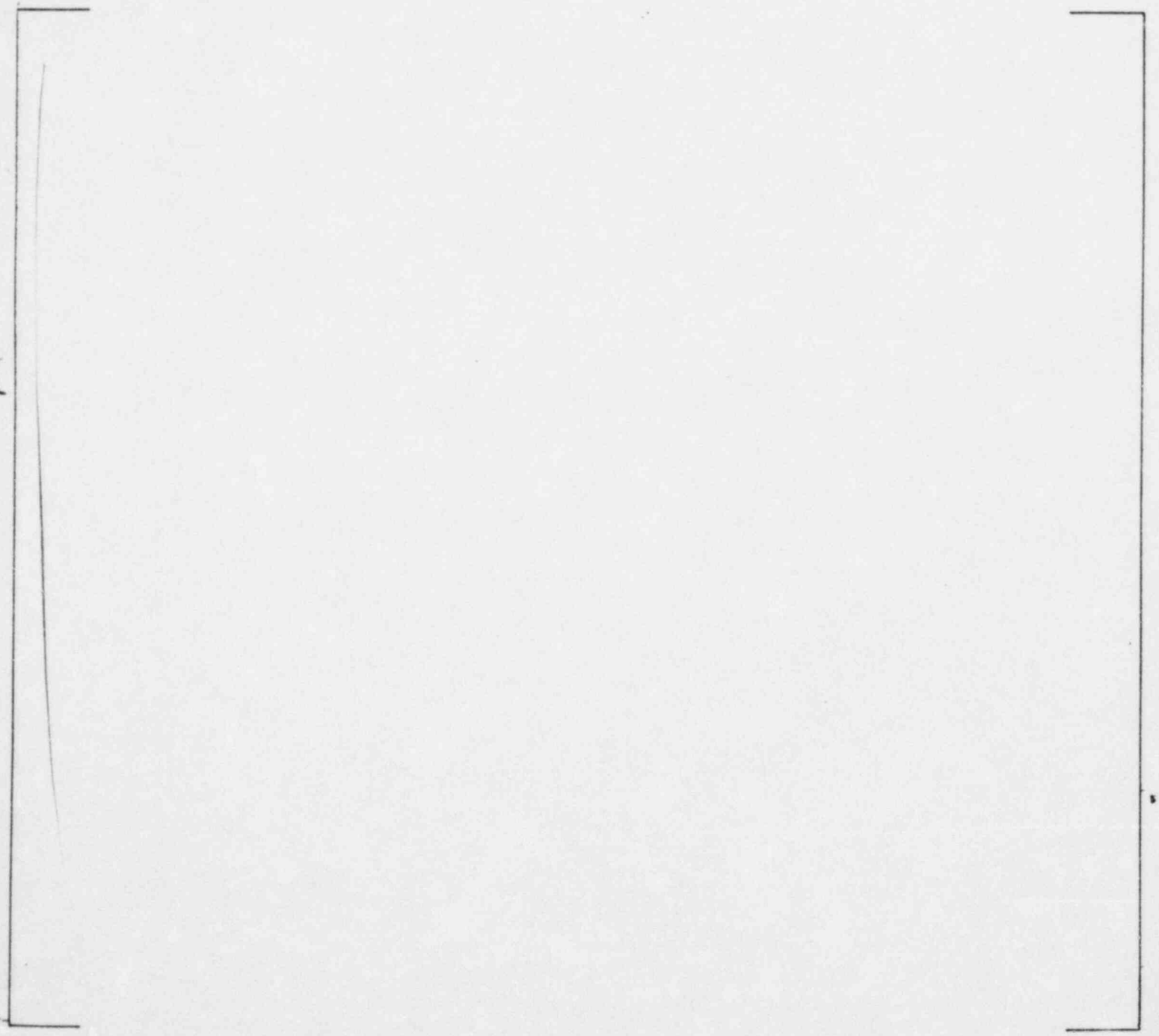

CEPAK

OMAHA CY8 99 PERCENT
INST ONLY ROCS-CECOR COMPARISO
N LEVEL 4 1000 MWD/T

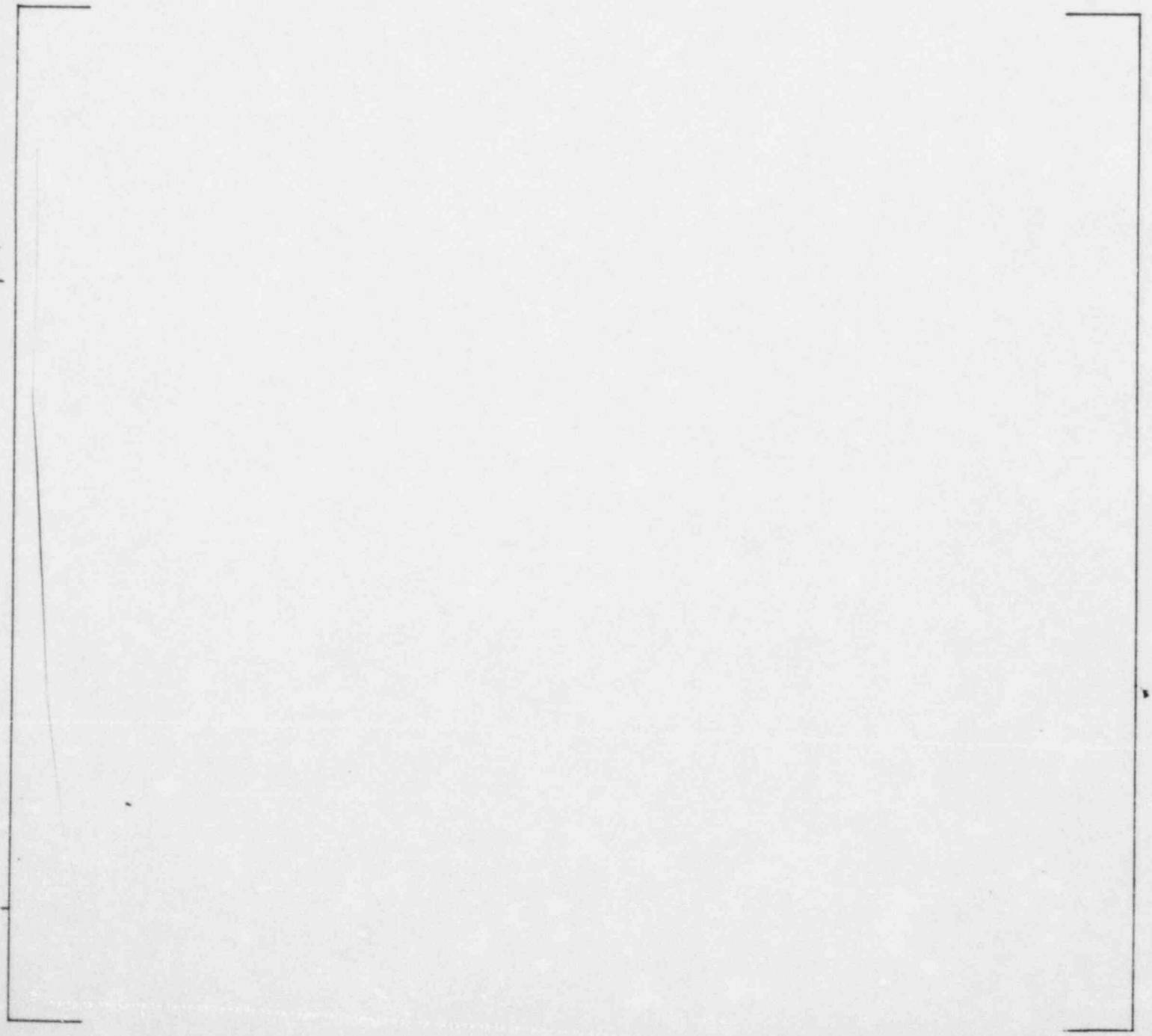

CEPAK

OMAHA CY8 99 PERCENT
INST ONLY RODS-CECOR COMPARISO
N AXIALLY INTEGRATED 1000 MWD/T

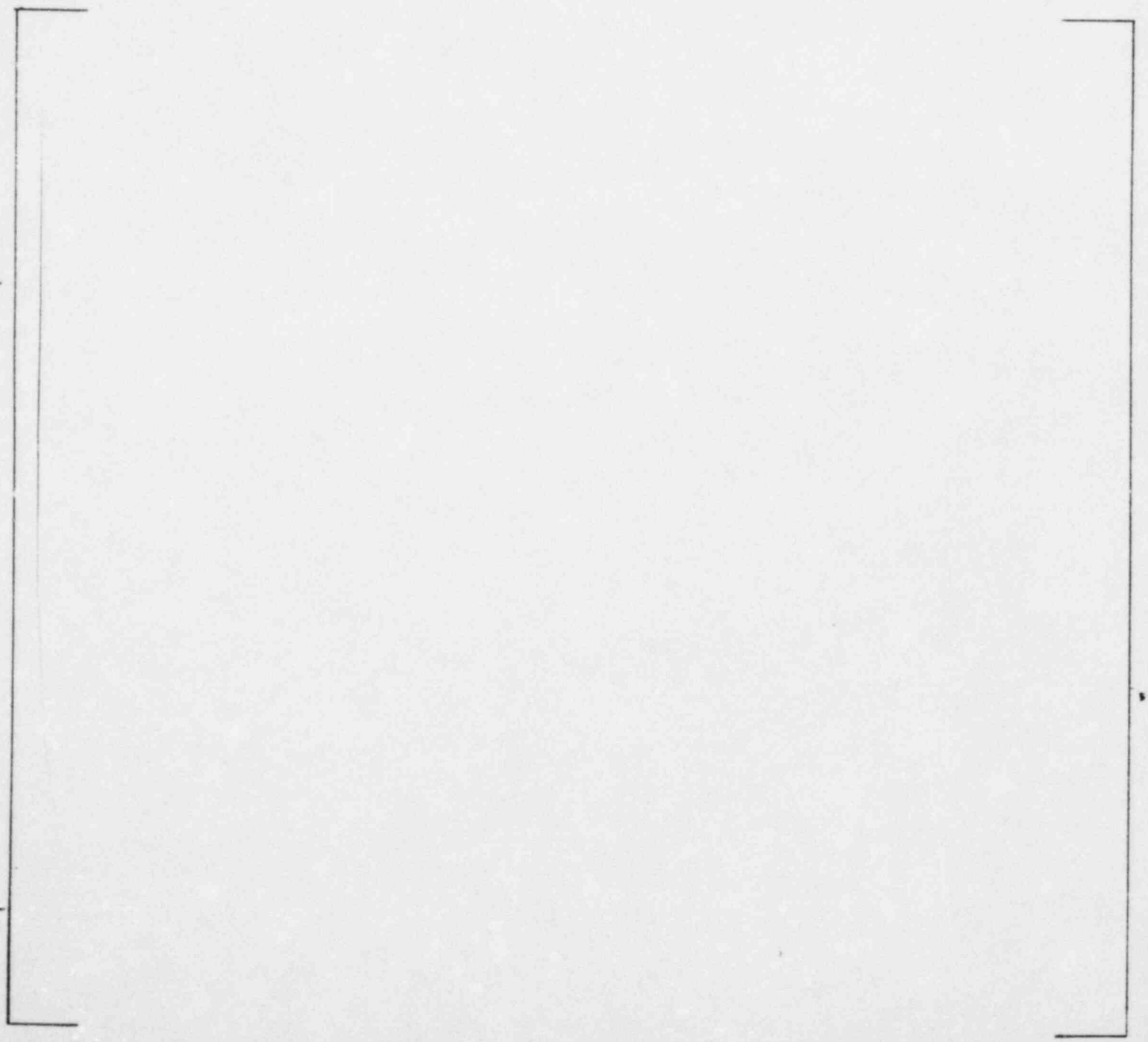

CEPAK

OMAHA CY8 99 PERCENT
INST ONLY ROCS-CECOR COMPARISO
N LEVEL 1 2000 MWD/T

CEPAK

OMAHA CY8 99 PERCENT
INST ONLY ROCS-CECOR COMPARISO
N LEVEL 2 2000 MWD/T

CEPAK

OMAHA CY8 99 PERCENT
INST ONLY ROCS-CECOR COMPARISO
N LEVEL 3 2000 MWD/T

CEPAK

OMAHA CY8 99 PERCENT
INST ONLY ROCS-CECOR COMPARISON
N LEVEL 4 2000 MWD/T

CEPAK

OMAHA CY8 99 PERCENT
INST ONLY ROCS-CECOR COMPARISO
N AXIALLY INTEGRATED 2000 MWD/T

DIT

OMAHA CY8 45 PERCENT
INST ONLY ROCS-CECOR COMPARISON
LEVEL 1 45 MWD/T

DIT

OMAHA CY8 45 PERCENT
INST ONLY ROCS-CECOR COMPARISON
LEVEL 2 45 MWD/T

DIT

OMAHA CY8 45 PERCENT
INST ONLY ROCS-CECOR COMPARISON
LEVEL 3 45 MWD/T

DIT

OMAHA CY8 45 PERCENT
INST ONLY ROCS-CECOR COMPARISON
LEVEL 4 45 MWD/T

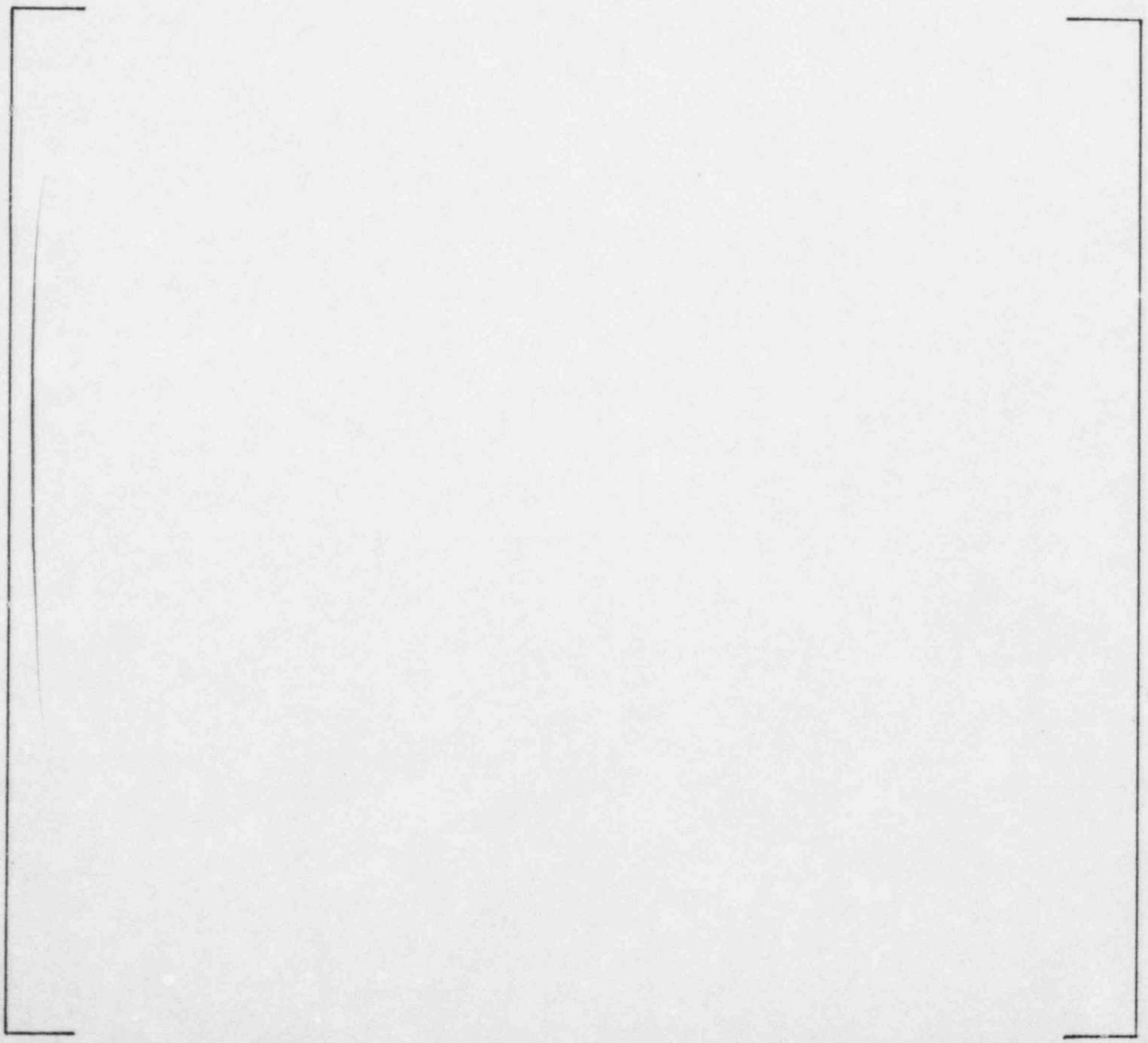

DIT

OMAHA CY8 45 PERCENT
INST ONLY ROCS-CECOR COMPARISON
AXIALLY INTEGRATED 45 mwD/T

DIT

OMAHA CY8 79 PERCENT
INST ONLY ROCS-CECOR COMPARISON
LEVEL 1 230 mwD/T

DIT

OMAHA CY8 79 PERCENT
INST ONLY ROCS-CECOR COMPARISON
LEVEL 2 230 MWD/T

DIT

OMAHA CY8 79 PERCENT
INST ONLY ROCS-CECOR COMPARISON
LEVEL 3 230 MWD/T

DIT

OMAHA CY8 79 PERCENT
INST ONLY ROCS-CECOR COMPARISON
LEVEL 4 230 MWD/T

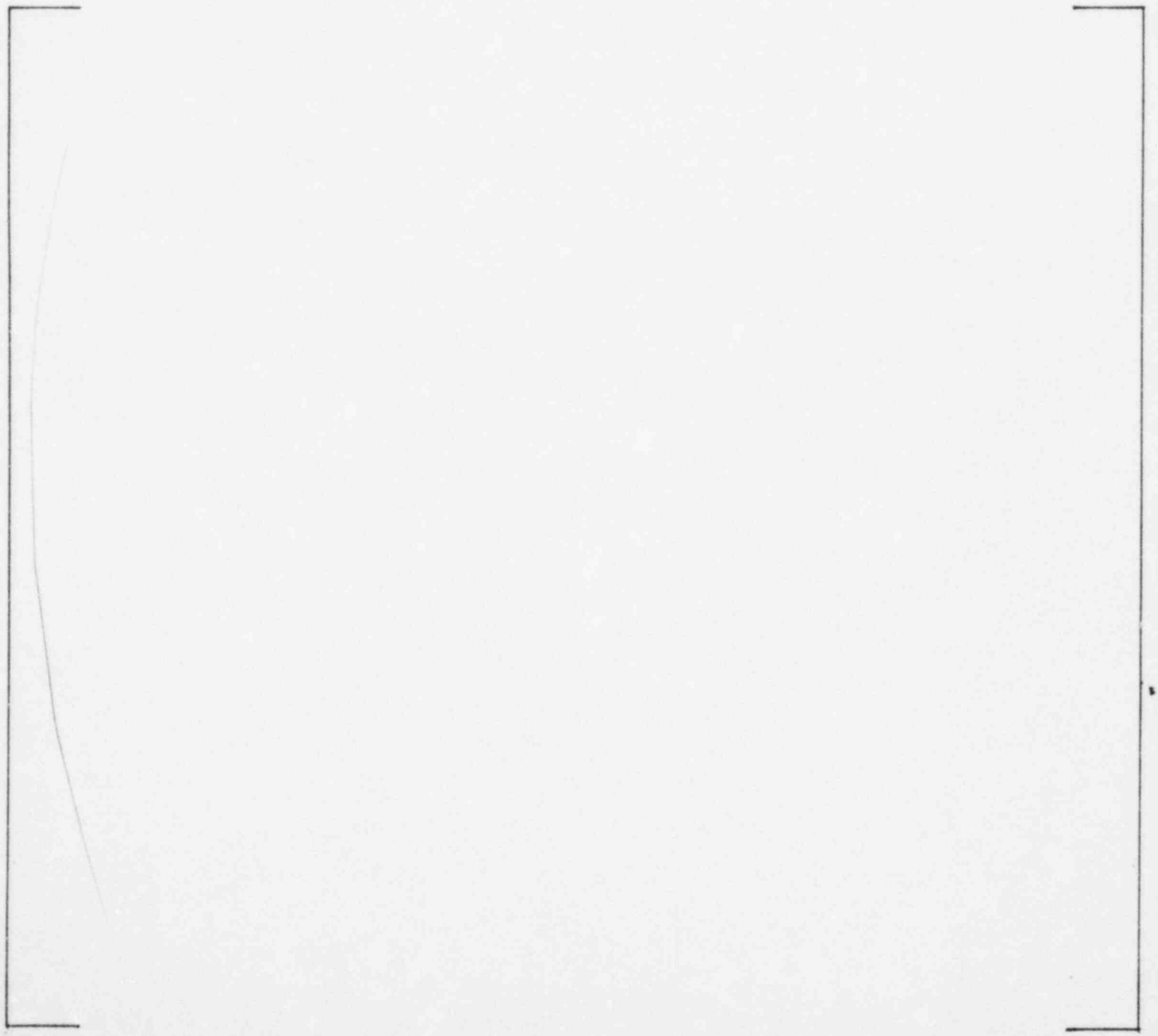

DIT

OMAHA CY8 79 PERCENT
INST ONLY ROCS-CECOR COMPARISON
AXIALLY INTEGRATED 230 MWD/T

DIT

OMAHA CY8 99 PERCENT
INST ONLY ROCS-CECOR COMPARISON
LEVEL 1 1000 mwD/T

DIT

OMAHA CY8 99 PERCENT
INST ONLY ROCS-CECOR COMPARISON
LEVEL 2 1000 MWD/T

DIT

OMAHA CY8 99 PERCENT
INST ONLY ROCS-CECOR COMPARISON
LEVEL 3 ~~1000~~ MWD/T

DIT

OMAHA CY8 99 PERCENT
INST ONLY ROCS-CECOR COMPARISON
LEVEL 4 1000 MWD/T

DIT

OMAHA CY8 99 PERCENT
INST ONLY ROCS-CECOR COMPARISON
AXIALLY INTEGRATED 1000 MWD/T

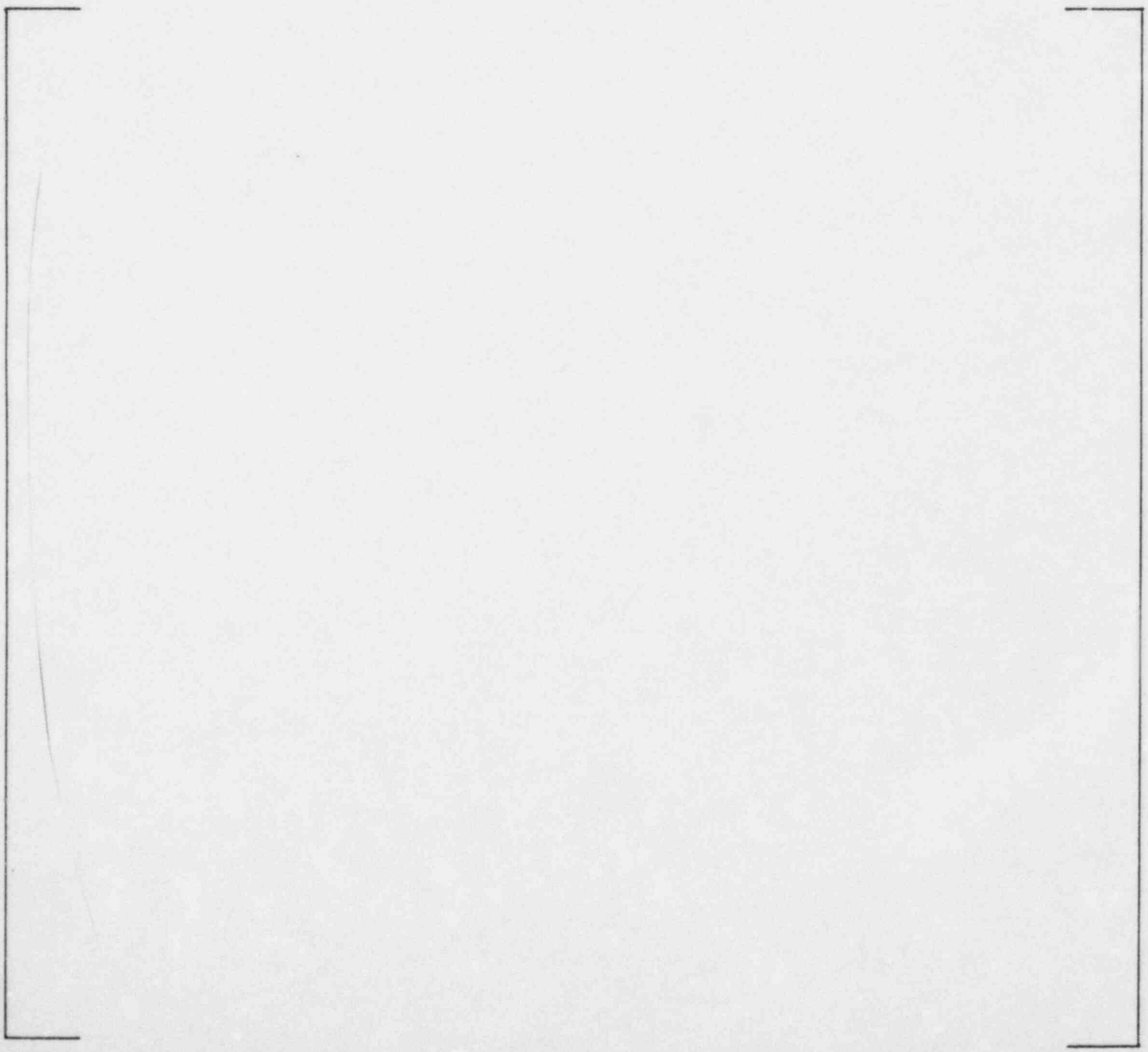

DIT

OMAHA CY8 99 PERCENT
INST ONLY ROCS-CECOR COMPARISON
LEVEL 1 2000 MWD/T

DIT

OMAHA CY8 99 PERCENT
INST ONLY ROCS-CECOR COMPARISON
LEVEL 2 2000 mwD/T

DIT

OMAHA CY8 99 PERCENT
INST ONLY ROCS-CECOR COMPARISON
LEVEL 3 2000 MWD/T

DIT

OMAHA CY8 99 PERCENT
INST ONLY ROCS-CECOR COMPARISON
LEVEL 4 2000 MWD/T

DIT

OMAHA CY8 99 PERCENT
INST ONLY ROCS-CECOR COMPARISON
AXIALLY INTEGRATED 2000 MWD/T

APPENDIX B

AXIAL POWER
DISTRIBUTION COMPARISONS

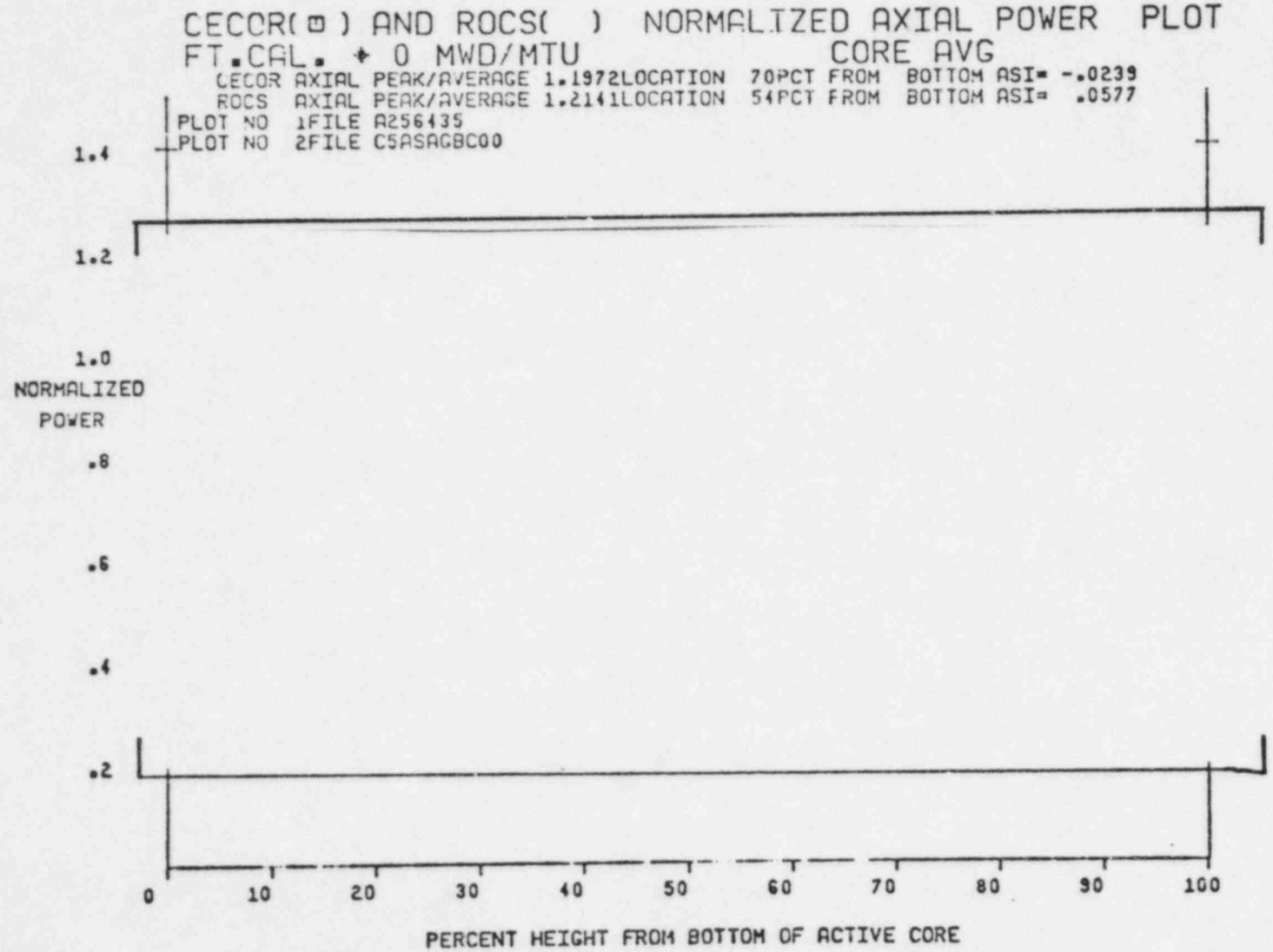
CECOR( ) AND ROCS( ) NORMALIZED AXIAL POWER PLOT
FT.CAL. + 0 MWD/MTU
CORE AVG
CECOR AXIAL PEAK/AVERAGE 1.1972LOCATION 70PCT FROM BOTTOM ASI= -.0239
ROCS AXIAL PEAK/AVERAGE 1.2141LOCATION 54PCT FROM BOTTOM ASI= .0577
PLOT NO 1FILE A256435
PLOT NO 2FILE C5ASAGBC00
1.4
1.2
1.0
NORMALIZED
POWER
.8
.6
.4
.2
0
10
20
30
40
50
60
70
80
90
100
PERCENT HEIGHT FROM BOTTOM OF ACTIVE CORE

Cycle 5

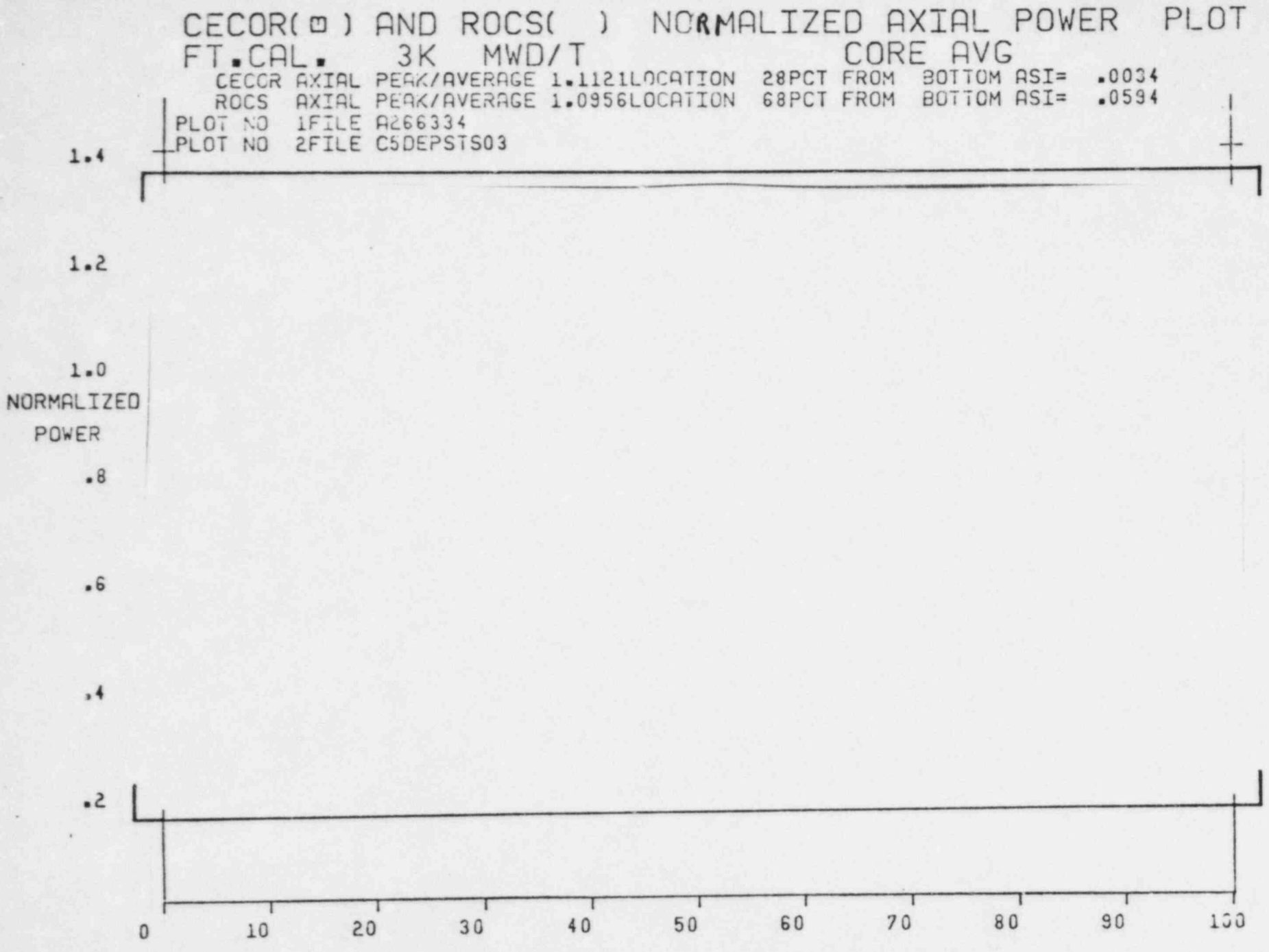
CECOR( ) AND ROCS( ) NORMALIZED AXIAL POWER PLOT
FT.CAL. 3K MWD/T CORE AVG
CECOR AXIAL PEAK/AVERAGE 1.1121LOCATION 28PCT FROM BOTTOM ASI= .0034
ROCS AXIAL PEAK/AVERAGE 1.0956LOCATION 68PCT FROM BOTTOM ASI= .0594
PLOT NO 1FILE A266334
PLOT NO 2FILE C5DEPSTS03
1.4
1.2
1.0
NORMALIZED
POWER
.8
.6
.4
.2
0
10
20
30
40
50
60
70
80
90
100
PERCENT HEIGHT FROM BOTTOM OF ACTIVE CORE

Cycle 5

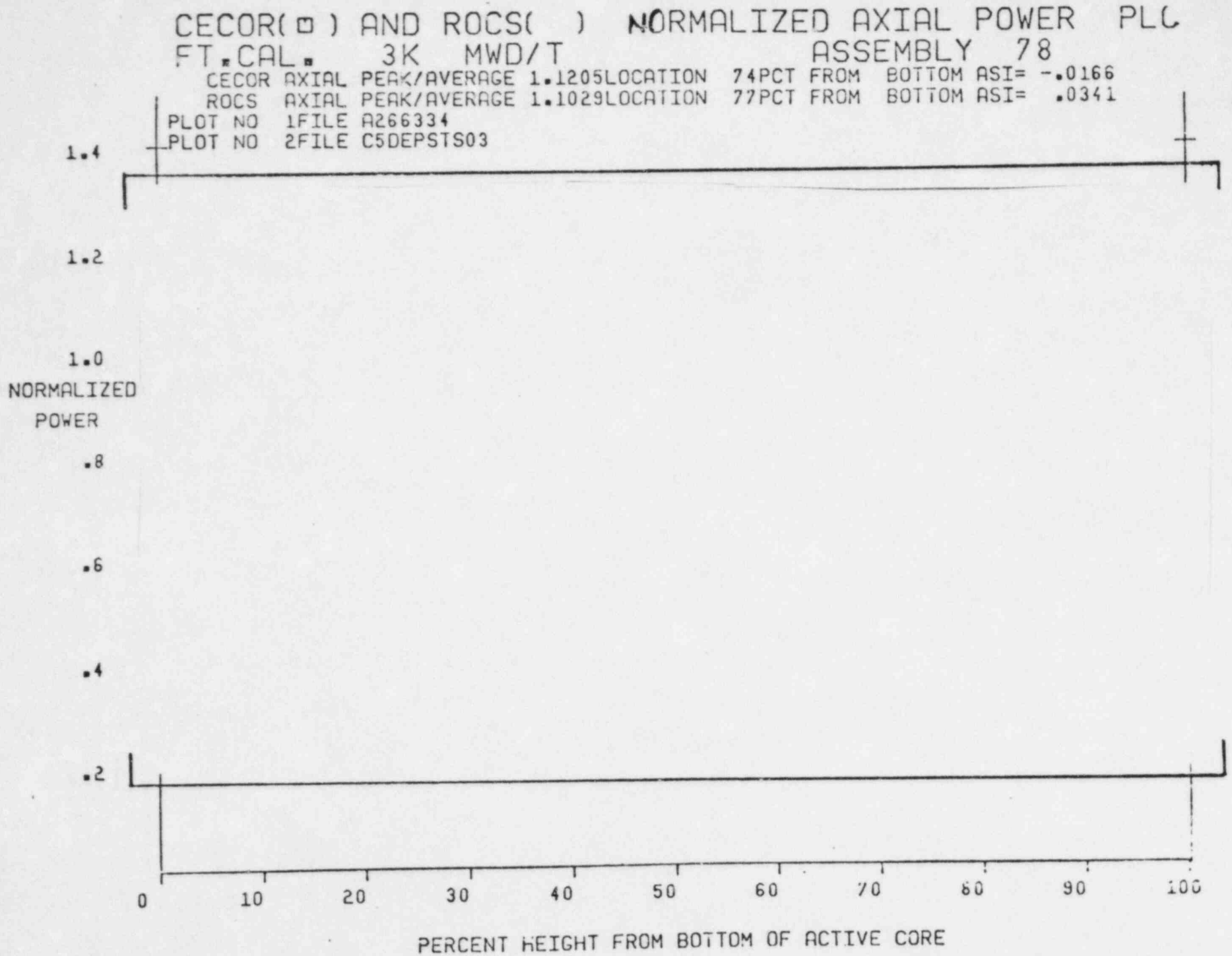
CECOR(□) AND ROCS( ) NORMALIZED AXIAL POWER PLO
FT.CAL. 3K MWD/T ASSEMBLY 78
CECOR AXIAL PEAK/AVERAGE 1.1205LOCATION 74PCT FROM BOTTOM ASI= -.0166
ROCS AXIAL PEAK/AVERAGE 1.1029LOCATION 77PCT FROM BOTTOM ASI= .0341
PLOT NO 1FILE A266334
PLOT NO 2FILE C5DEPSTS03
1.4
1.2
1.0
NORMALIZED
POWER
.8
.6
.4
.2
0
10
20
30
40
50
60
70
80
90
100
PERCENT HEIGHT FROM BOTTOM OF ACTIVE CORE

Cycle 5

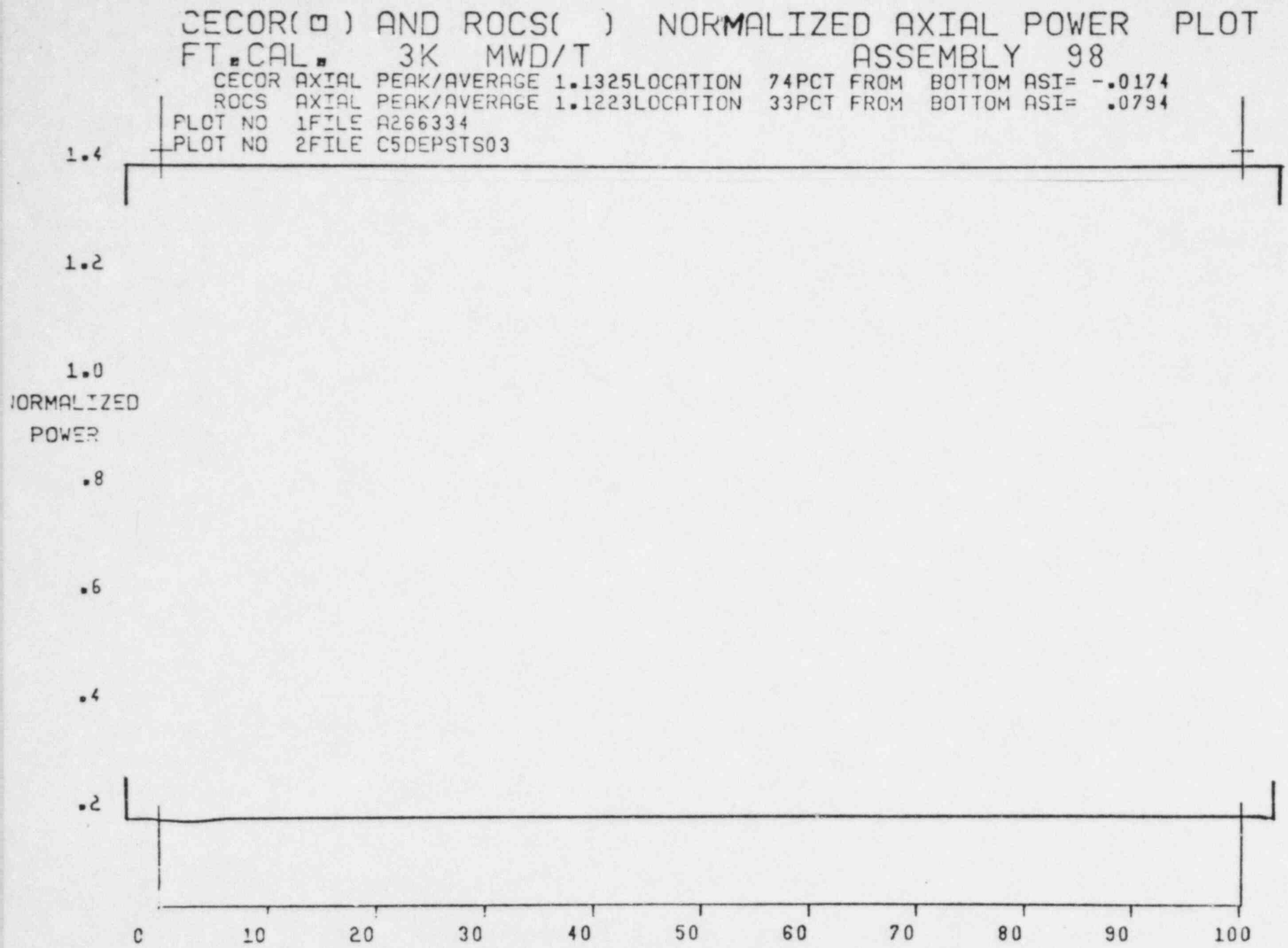
CECOR(□) AND ROCS( ) NORMALIZED AXIAL POWER PLOT
FT.CAL. 3K MWD/T ASSEMBLY 98
CECOR AXIAL PEAK/AVERAGE 1.1325LOCATION 74PCT FROM BOTTOM ASI= -.0174
ROCS AXIAL PEAK/AVERAGE 1.1223LOCATION 33PCT FROM BOTTOM ASI= .0794
PLOT NO 1FILE A266334
PLOT NO 2FILE C5DEPSTS03
1.4
1.2
1.0
NORMALIZED
POWER
.8
.6
.4
.2
0
10
20
30
40
50
60
70
80
90
100
PERCENT HEIGHT FROM BOTTOM OF ACTIVE CORE

Cycle 5

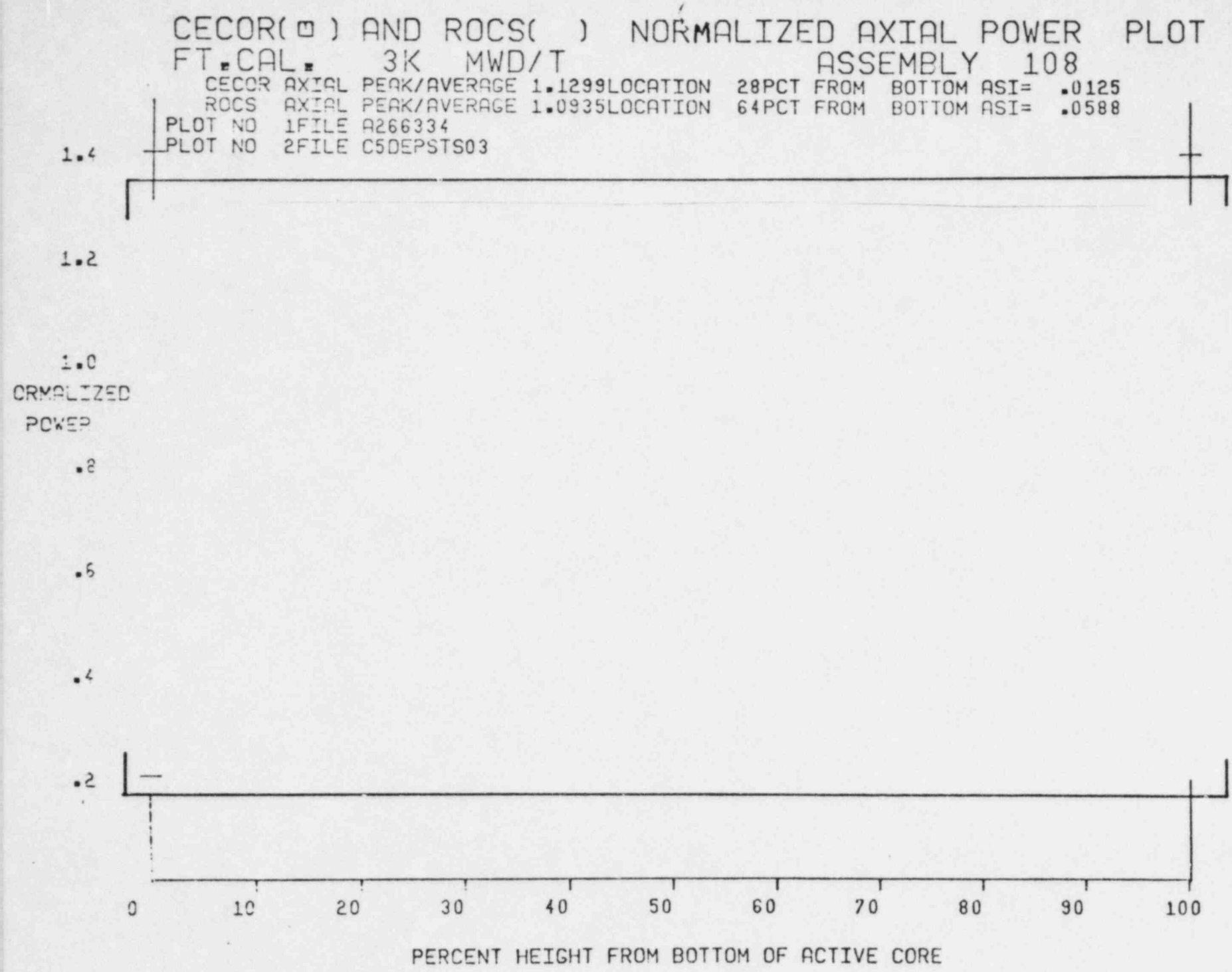
CECOR( ) AND ROCS( ) NORMALIZED AXIAL POWER PLOT
FT.CAL. 3K MWD/T ASSEMBLY 108
CECOR AXIAL PEAK/AVERAGE 1.1299LOCATION 28PCT FROM BOTTOM ASI= .0125
ROCS AXIAL PEAK/AVERAGE 1.0935LOCATION 64PCT FROM BOTTOM ASI= .0588
PLOT NO 1FILE A266334
PLOT NO 2FILE C5DEPSTS03
1.4
1.2
1.0
CRMALIZED
POWER
.8
.6
.4
.2
0
10
20
30
40
50
60
70
80
90
100
PERCENT HEIGHT FROM BOTTOM OF ACTIVE CORE

Cycle 5

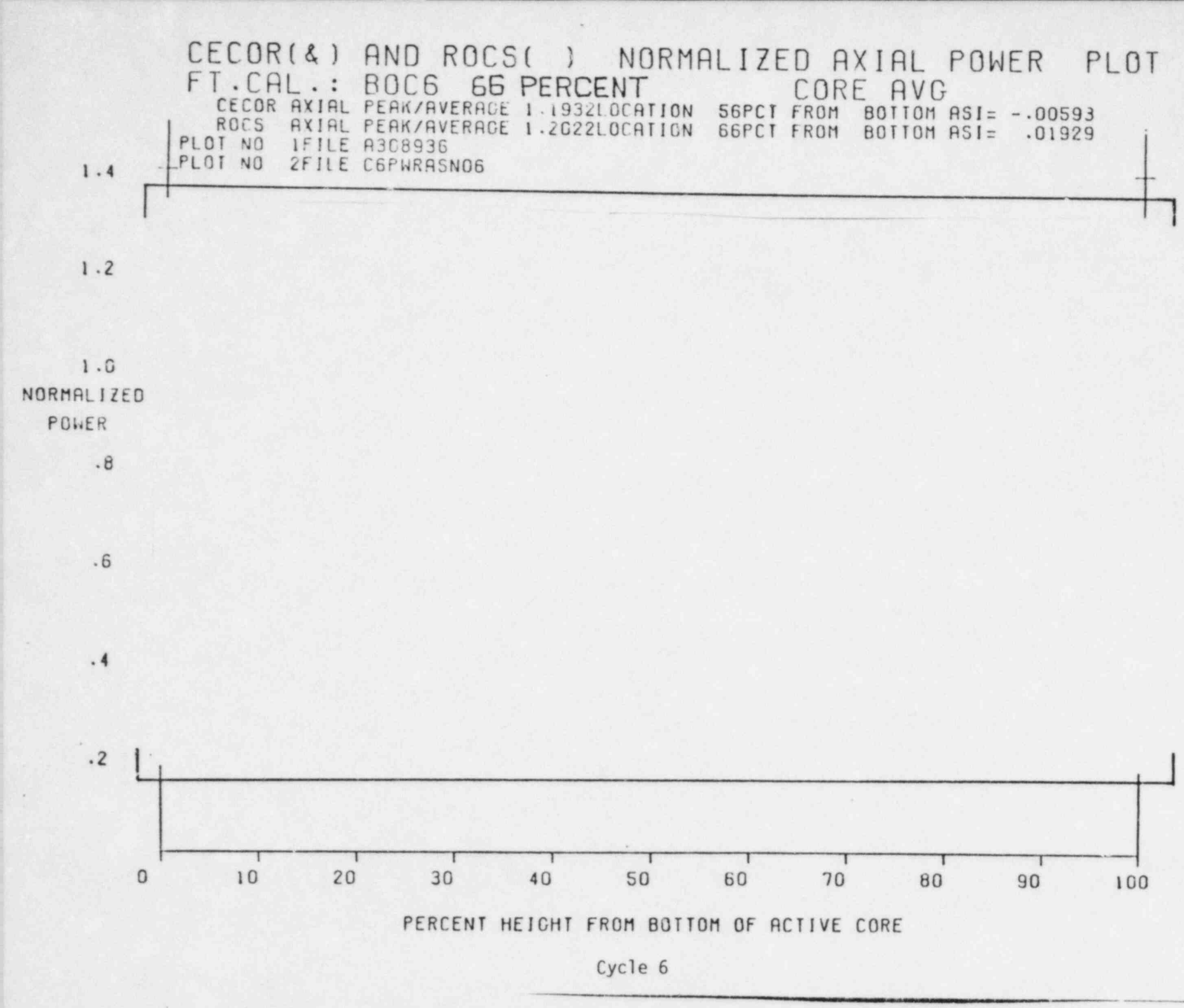
CECOR(&) AND ROCS( ) NORMALIZED AXIAL POWER PLOT
FT.CAL.: BOC6 66 PERCENT CORE AVG
CECOR AXIAL PEAK/AVERAGE 1.1932LOCATION 56PCT FROM BOTTOM ASI= -.00593
ROCS AXIAL PEAK/AVERAGE 1.2022LOCATION 66PCT FROM BOTTOM ASI= .01929
PLOT NO 1FILE A3O8936
PLOT NO 2FILE C6PWRASNO6
1.4
1.2
1.0
NORMALIZED
POWER
.8
.6
.4
.2
0
10
20
30
40
50
60
70
80
90
100
PERCENT HEIGHT FROM BOTTOM OF ACTIVE CORE

Cycle 6

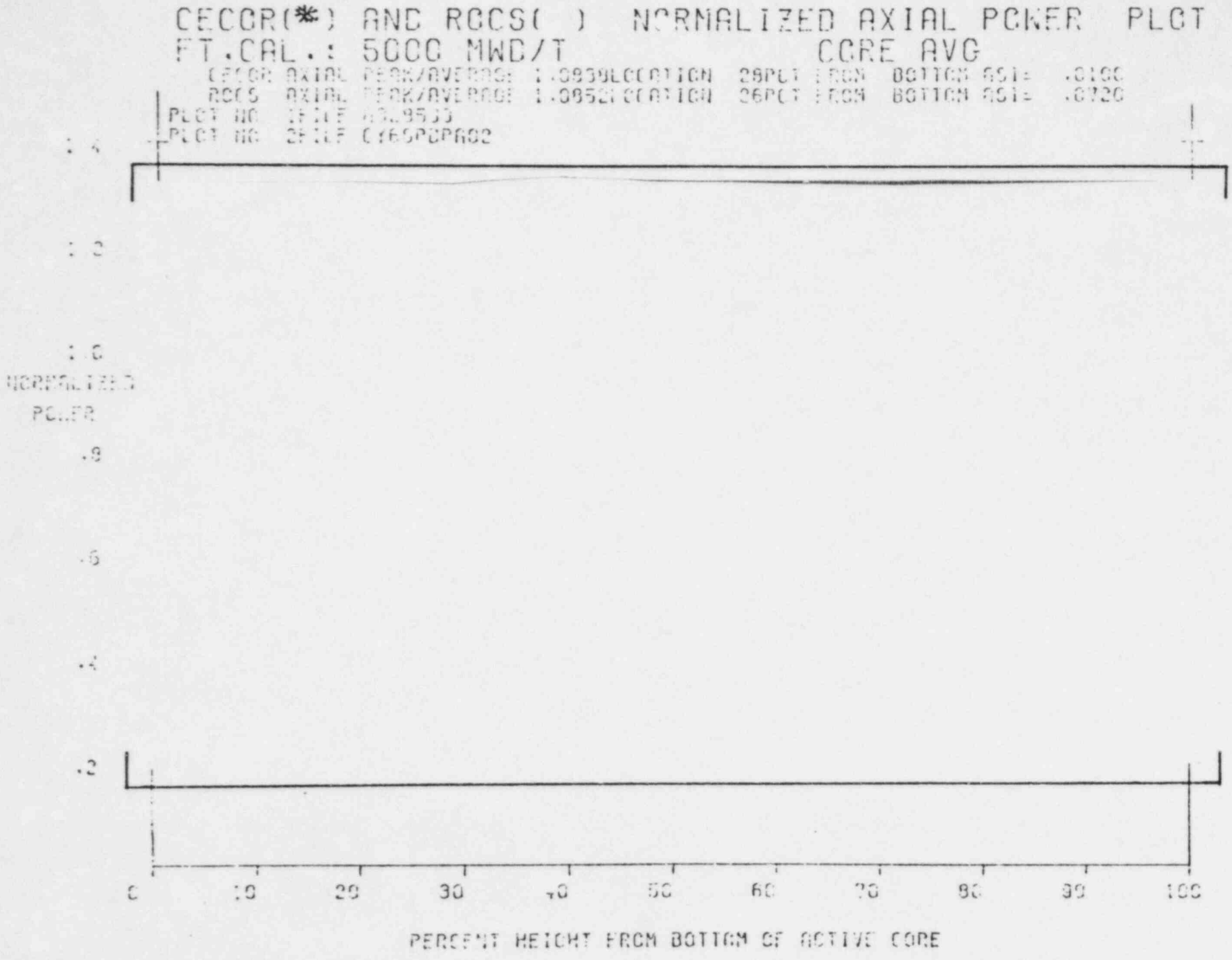
CECOR(*) AND RCCS( ) NORMALIZED AXIAL POWER PLOT
FT.CAL.: 5000 MWD/T CORE AVG
CECOR AXIAL PEAK/AVERAGE: 1.0830LOCATION 28PCT FROM BOTTOM AST= .0100
RCCS AXIAL PEAK/AVERAGE: 1.0852LOCATION 26PCT FROM BOTTOM AST= .0120
PLOT NO. 1FILE 03L953J
PLOT NO. 2FILE C16SPCPR02
1.4
1.2
1.0
NORMALIZED
POWER
.8
.6
.4
.2
0
10
20
30
40
50
60
70
80
90
100
PERCENT HEIGHT FROM BOTTOM OF ACTIVE CORE

Cycle 6

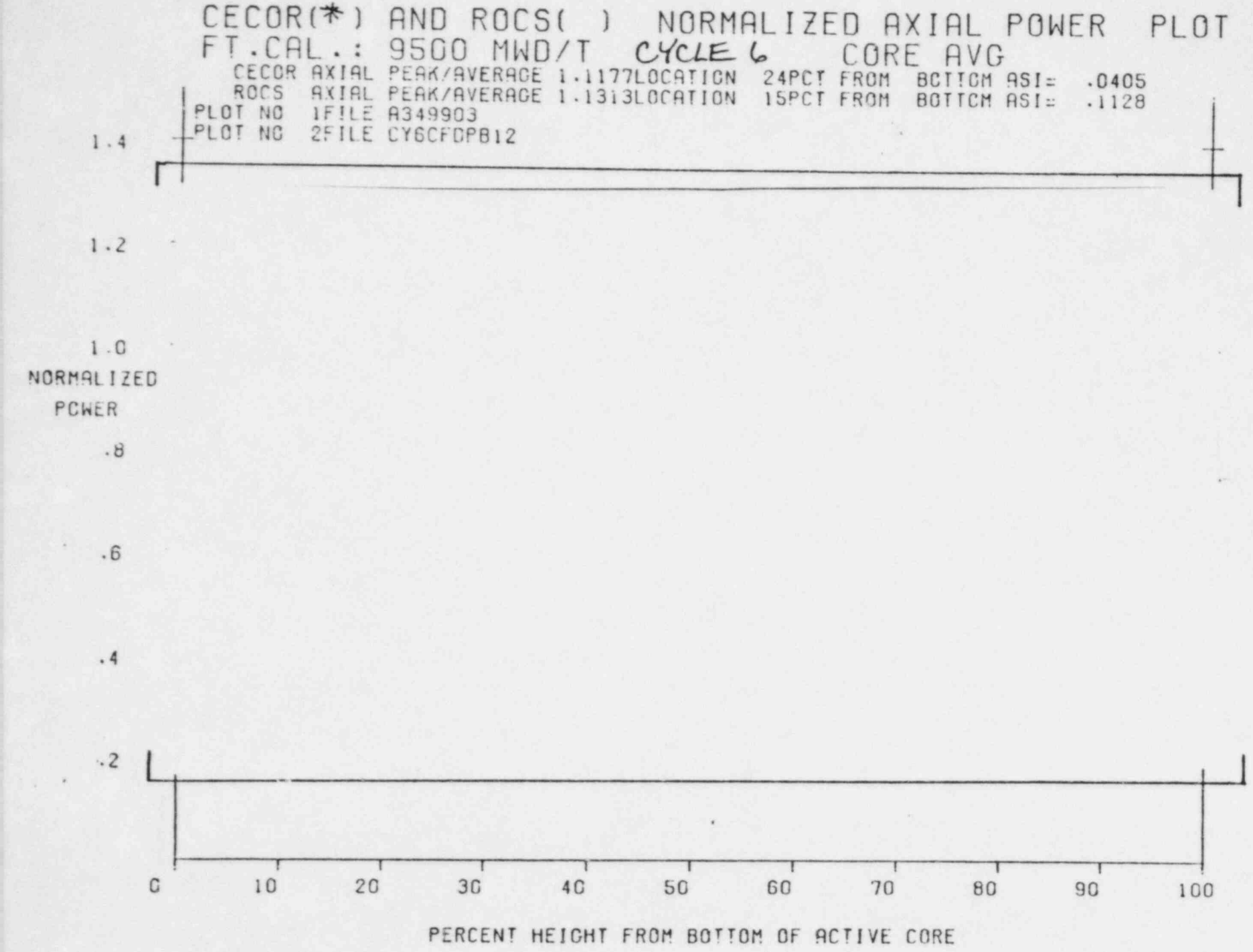
CECOR(*) AND ROCS( ) NORMALIZED AXIAL POWER PLOT
FT.CAL.: 9500 MWD/T CYCLE 6 CORE AVG
CECOR AXIAL PEAK/AVERAGE 1.1177LOCATION 24PCT FROM BOTTOM ASI= .0405
ROCS AXIAL PEAK/AVERAGE 1.1313LOCATION 15PCT FROM BOTTOM ASI= .1128
PLOT NO 1FILE A349903
PLOT NO 2FILE CY6CFDPB12
1.4
1.2
1.0
NORMALIZED
POWER
.8
.6
.4
.2
0
10
20
30
40
50
60
70
80
90
100
PERCENT HEIGHT FROM BOTTOM OF ACTIVE CORE

Cycle 6

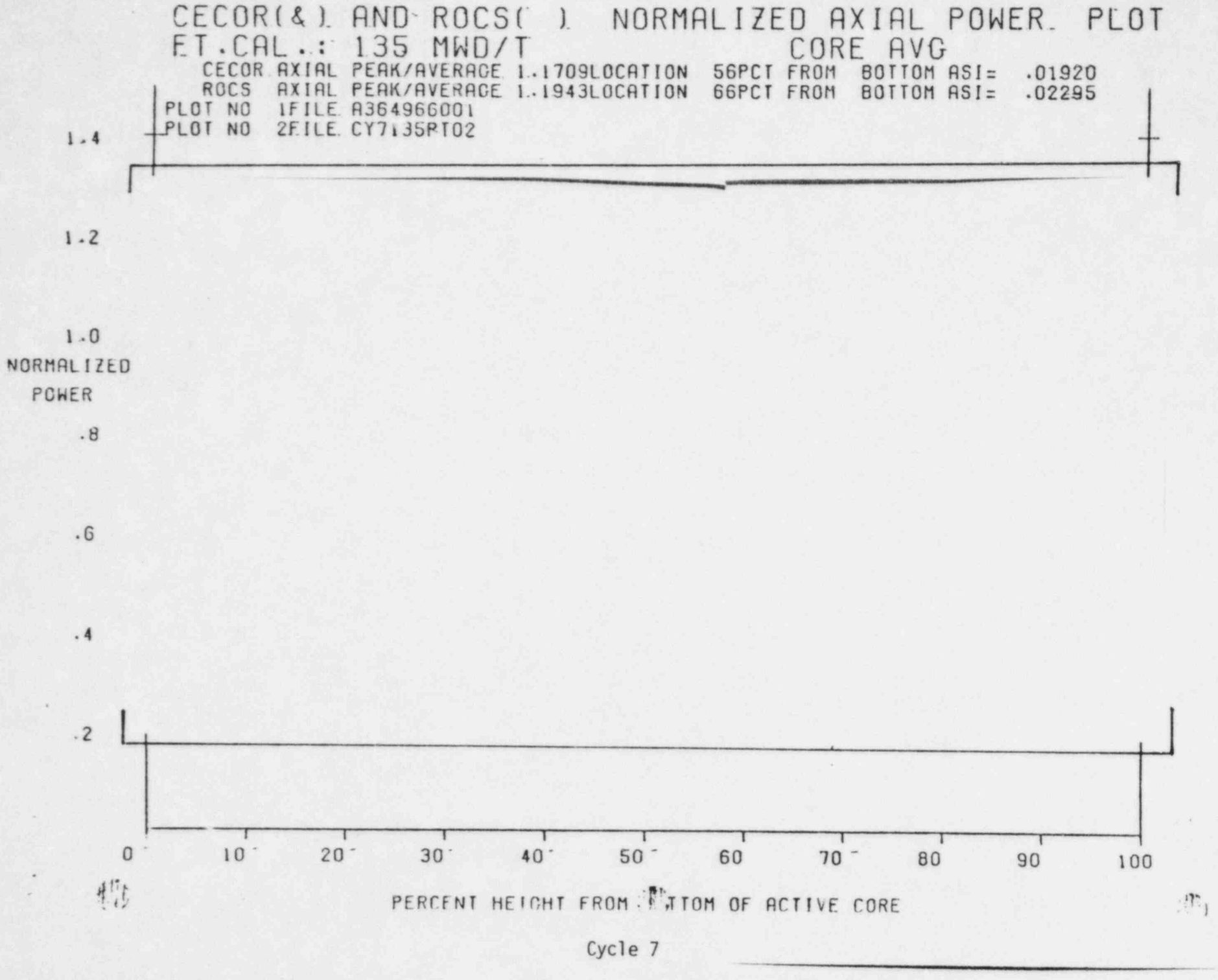
CECOR(&) AND ROCS( ) NORMALIZED AXIAL POWER PLOT
ET.CAL.: 135 MWD/T CORE AVG
CECOR AXIAL PEAK/AVERAGE 1.1709LOCATION 56PCT FROM BOTTOM ASI= .01920
ROCS AXIAL PEAK/AVERAGE 1.1943LOCATION 66PCT FROM BOTTOM ASI= .02295
PLOT NO 1FILE A364966001
PLOT NO 2FILE CY7135RT02
1.4
1.2
1.0
NORMALIZED
POWER
.8
.6
.4
.2
0
10
20
30
40
50
60
70
80
90
100
PERCENT HEIGHT FROM BOTTOM OF ACTIVE CORE

Cycle 7

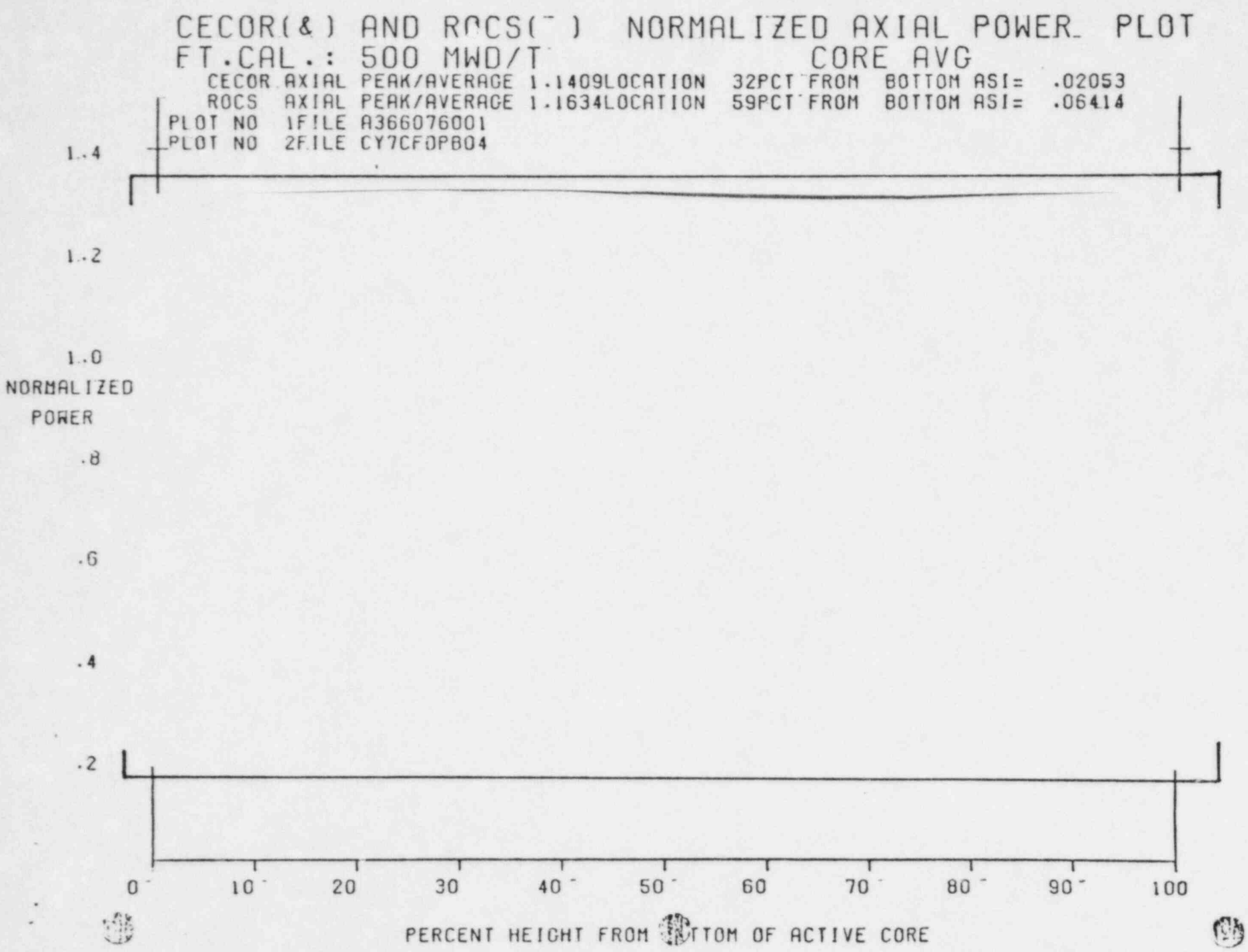
CECOR(&) AND ROCS(¯) NORMALIZED AXIAL POWER PLOT
FT.CAL.: 500 MWD/T CORE AVG
CECOR AXIAL PEAK/AVERAGE 1.1409LOCATION 32PCT FROM BOTTOM ASI= .02053
ROCS AXIAL PEAK/AVERAGE 1.1634LOCATION 59PCT FROM BOTTOM ASI= .06414
PLOT NO 1FILE A366076001
PLOT NO 2FILE CY7CFOPB04
1.4
1.2
1.0
NORMALIZED
POWER
.8
.6
.4
.2
0
10
20
30
40
50
60
70
80
90
100
PERCENT HEIGHT FROM BOTTOM OF ACTIVE CORE

Cycle 7

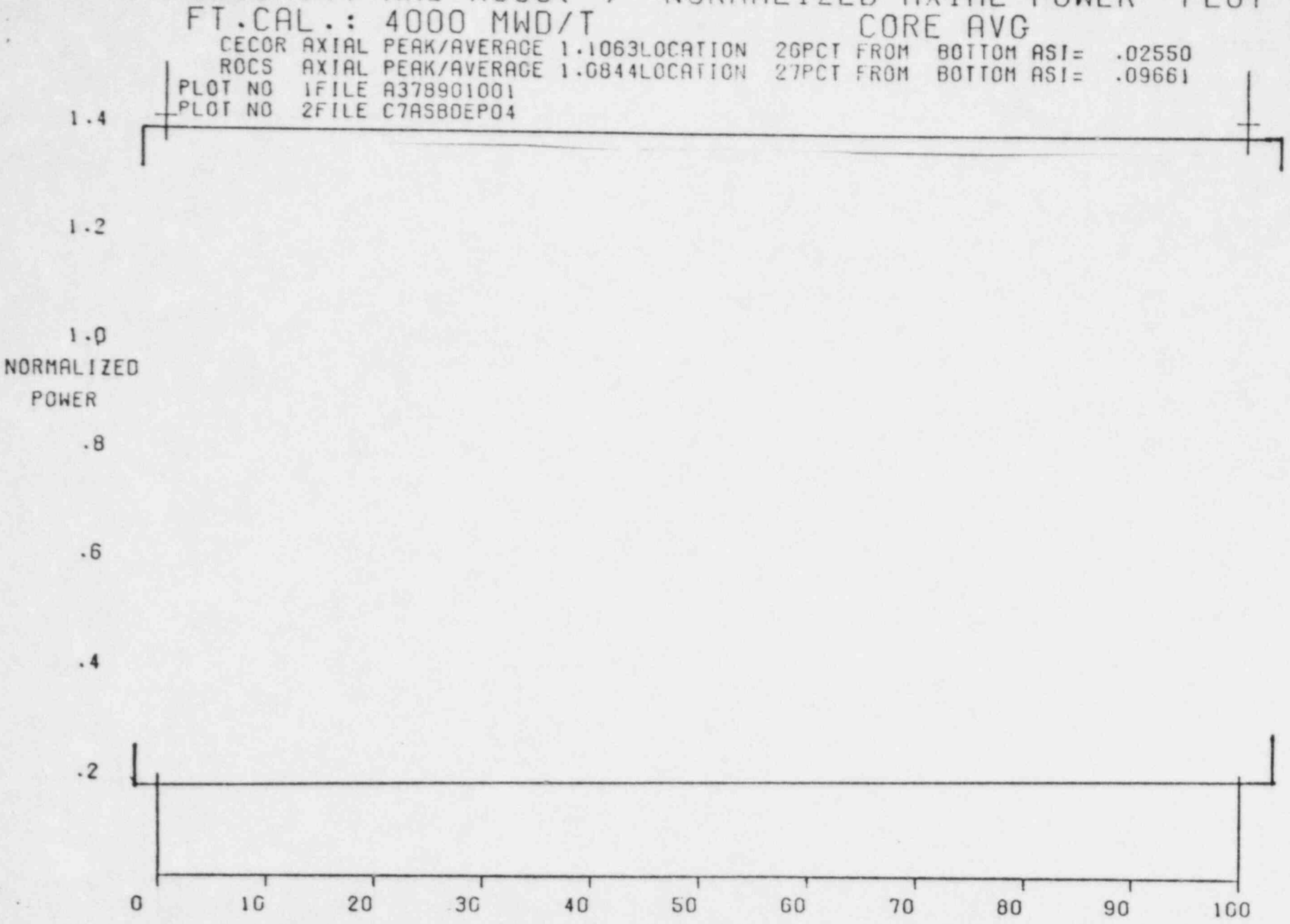
CECOR(&) AND ROCS( ) NORMALIZED AXIAL POWER PLOT
FT.CAL.: 4000 MWD/T
CORE AVG
CECOR AXIAL PEAK/AVERAGE 1.1063LOCATION 26PCT FROM BOTTOM ASI= .02550
ROCS AXIAL PEAK/AVERAGE 1.0844LOCATION 27PCT FROM BOTTOM ASI= .09661
PLOT NO 1FILE A37890100 1
PLOT NO 2FILE C7ASBOEP04
1.4
1.2
1.0
NORMALIZED
POWER
.8
.6
.4
.2
0
10
20
30
40
50
60
70
80
90
100
PERCENT HEIGHT FROM BOTTOM OF ACTIVE CORE

Cycle 7

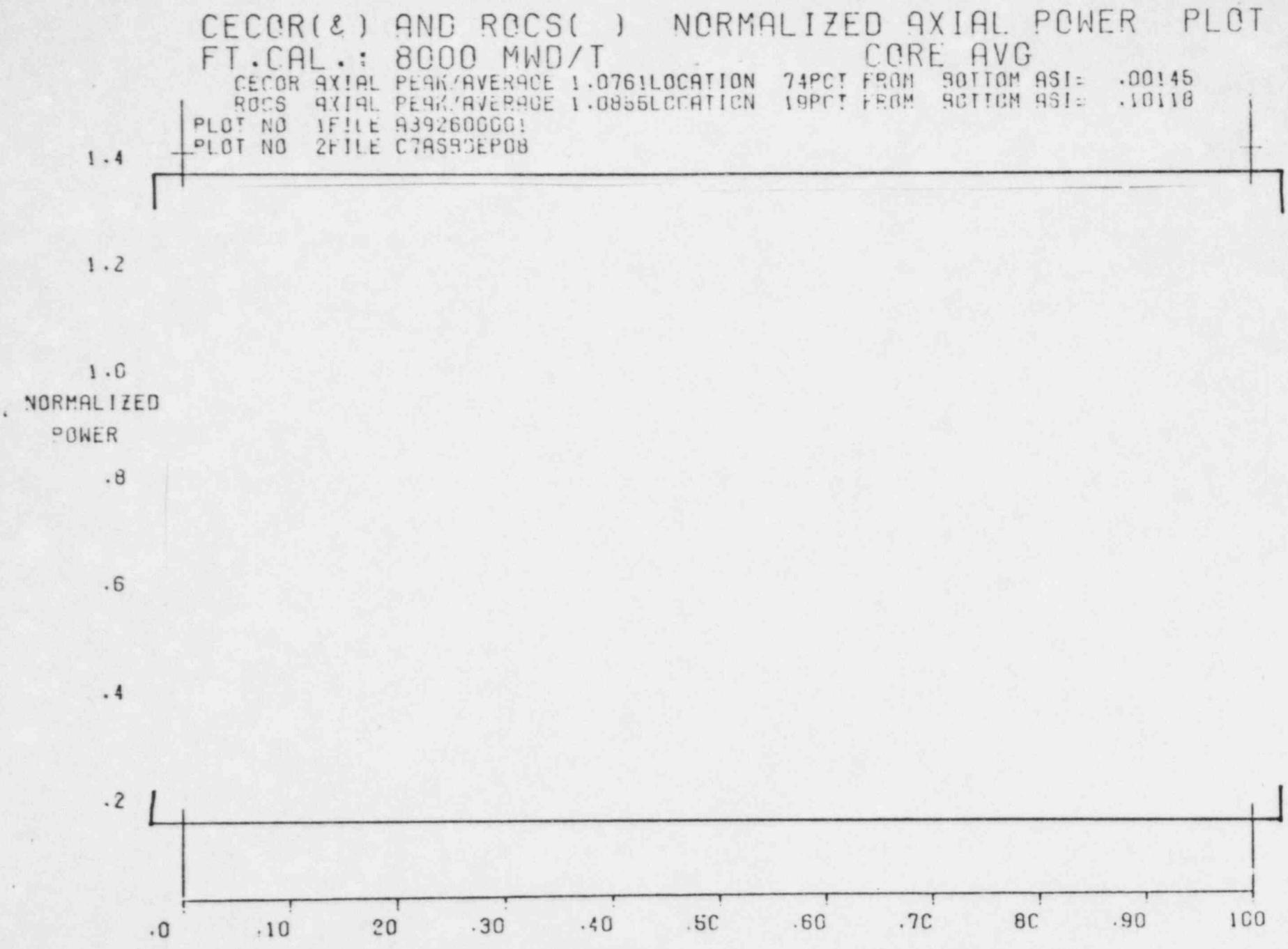
CECOR(&) AND ROCS( ) NORMALIZED AXIAL POWER PLOT
FT.CAL.: 8000 MWD/T CORE AVG
CECOR AXIAL PEAK/AVERAGE 1.0761LOCATION 74PCT FROM BOTTOM ASI= .00145
ROCS AXIAL PEAK/AVERAGE 1.0855LOCATION 19PCT FROM BOTTOM ASI= .10118
PLOT NO 1FILE A39260000
PLOT NO 2FILE C7AS90EP08
1.4
1.2
1.0
NORMALIZED
POWER
.8
.6
.4
.2
.0
.10
20
.30
.40
.5C
.60
.7C
8C
.90
100
PERCENT HEIGHT FROM BOTTOM OF ACTIVE CORE

Cycle 7

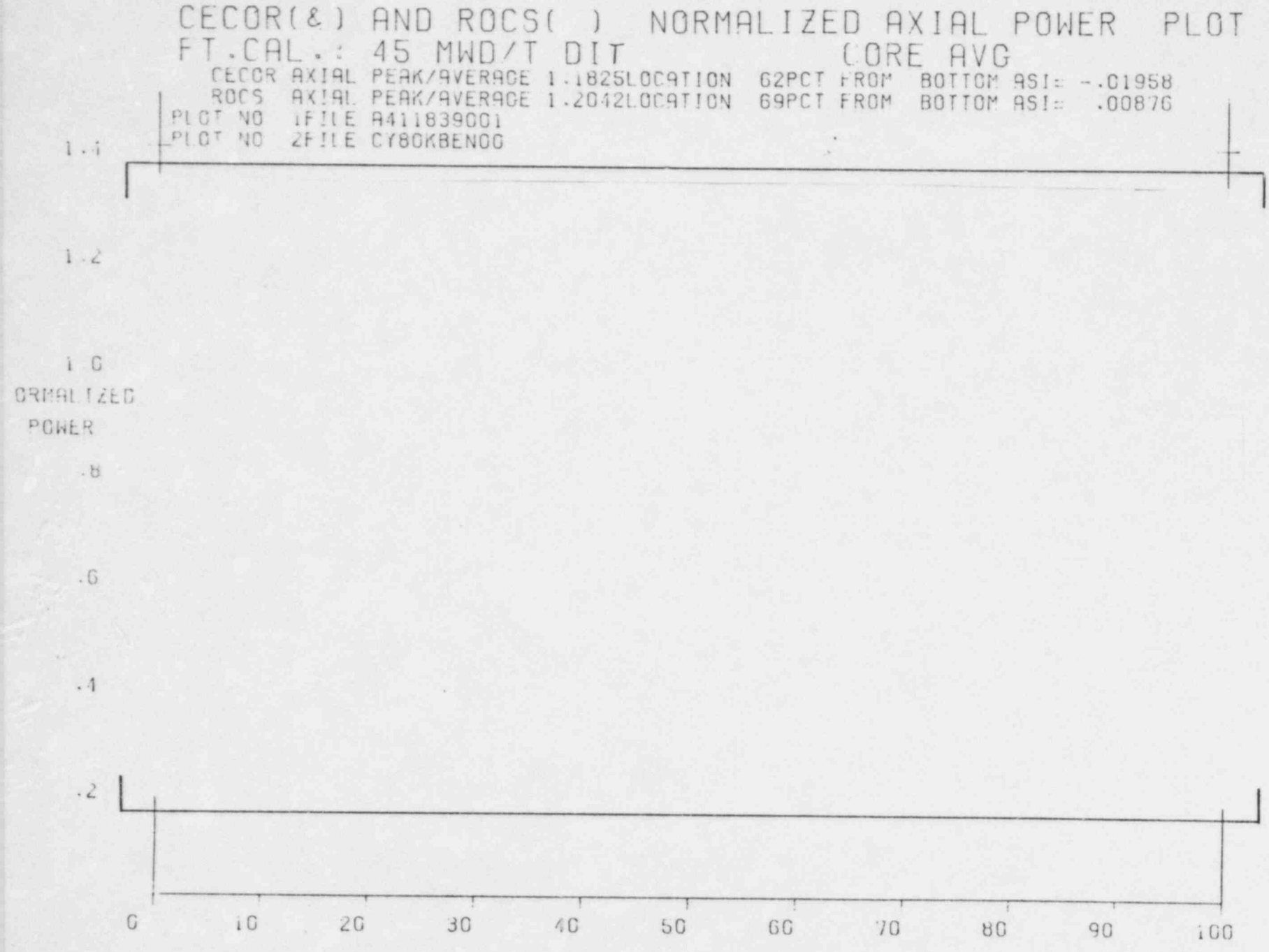
CECOR(&) AND ROCS( ) NORMALIZED AXIAL POWER PLOT
FT.CAL.: 45 MWD/T DIT CORE AVG
CECOR AXIAL PEAK/AVERAGE 1.1825LOCATION 62PCT FROM BOTTOM ASI= -.01958
ROCS AXIAL PEAK/AVERAGE 1.2042LOCATION 69PCT FROM BOTTOM ASI= .00876
PLOT NO 1FILE A411839001
PLOT NO 2FILE CY80KBEN00
1.4
1.2
1.0
ORMALIZED
POWER
.8
.6
.4
.2
0
10
20
30
40
50
60
70
80
90
100
PERCENT HEIGHT FROM BOTTOM OF ACTIVE CORE

Cycle 8

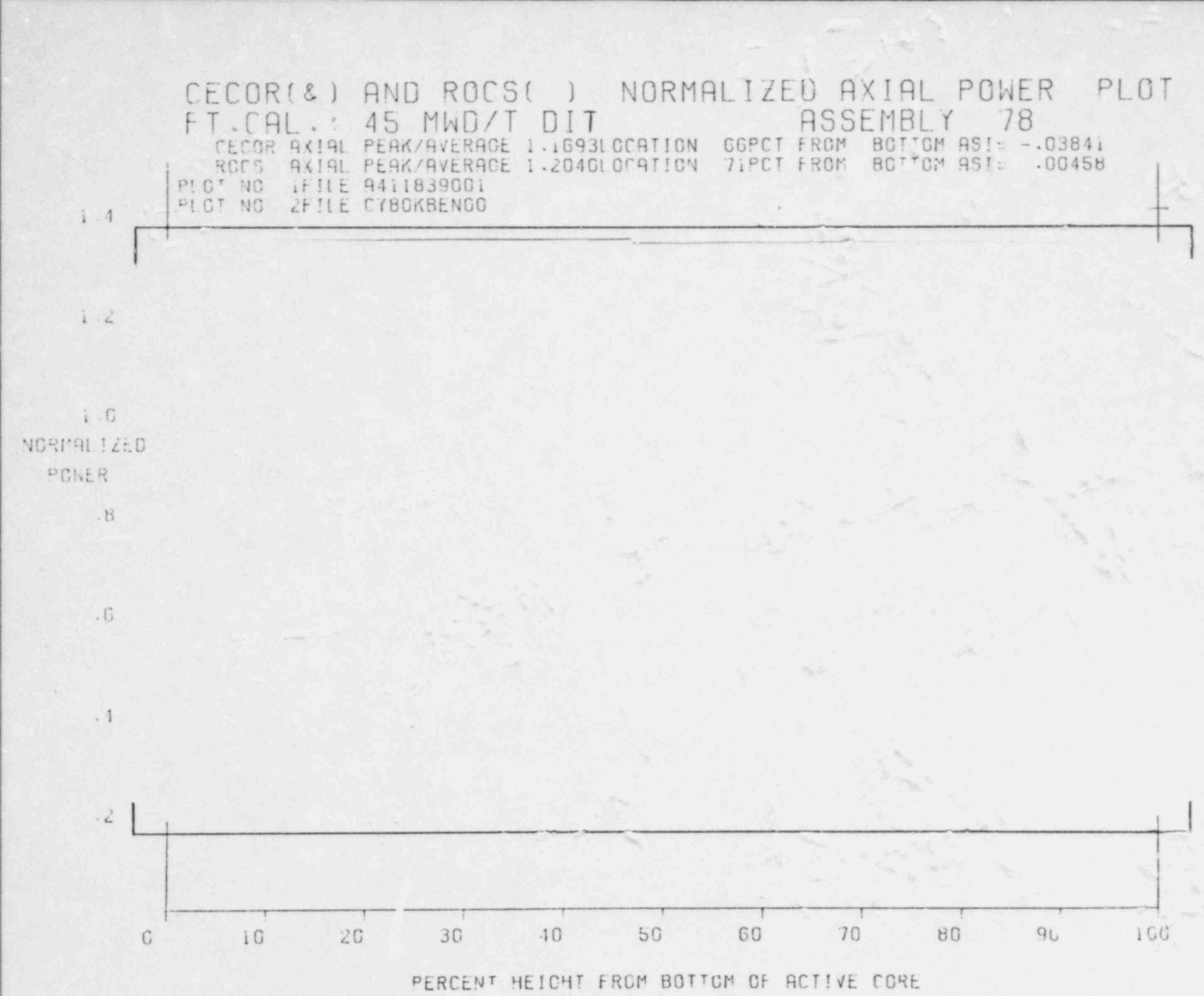
CECOR(&) AND ROCS( ) NORMALIZED AXIAL POWER PLOT
FT.CAL.: 45 MWD/T DIT ASSEMBLY 78
CECOR AXIAL PEAK/AVERAGE 1.1693LOCATION 66PCT FROM BOTTOM ASI= -.03841
ROCS AXIAL PEAK/AVERAGE 1.2040LOCATION 71PCT FROM BOTTOM ASI= .00458
PLOT NO 1FILE 9411839001
PLOT NO 2FILE C780KBENGO
1.4
1.2
1.0
NORMALIZED
POWER
.8
.6
.1
.2
0
10
20
30
40
50
60
70
80
90
100
PERCENT HEIGHT FROM BOTTOM OF ACTIVE CORE

Cycle 8

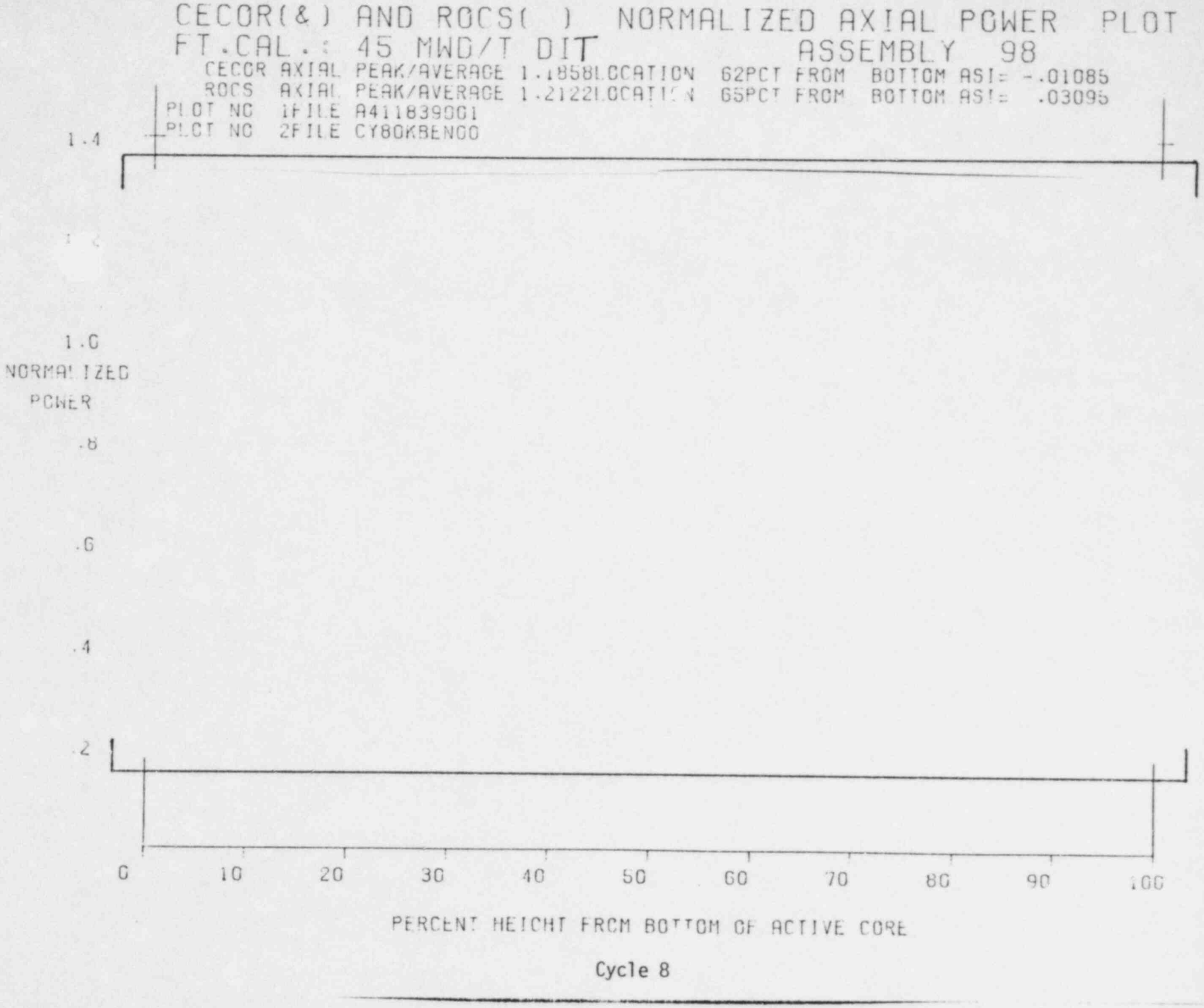
CECOR(&) AND ROCS( ) NORMALIZED AXIAL POWER PLOT
FT.CAL.: 45 MWD/T DIT ASSEMBLY 98
CECOR AXIAL PEAK/AVERAGE 1.1858LOCATION 62PCT FROM BOTTOM ASI= -.01085
ROCS AXIAL PEAK/AVERAGE 1.2122LOCATION 65PCT FROM BOTTOM ASI= .03095
PLOT NO 1FILE A41183900I
PLOT NO 2FILE CY80KBEN00
1.4
1.6
NORMALIZED
POWER
.8
.6
.4
.2
0
10
20
30
40
50
60
70
80
90
100
PERCENT HEIGHT FROM BOTTOM OF ACTIVE CORE

Cycle 8

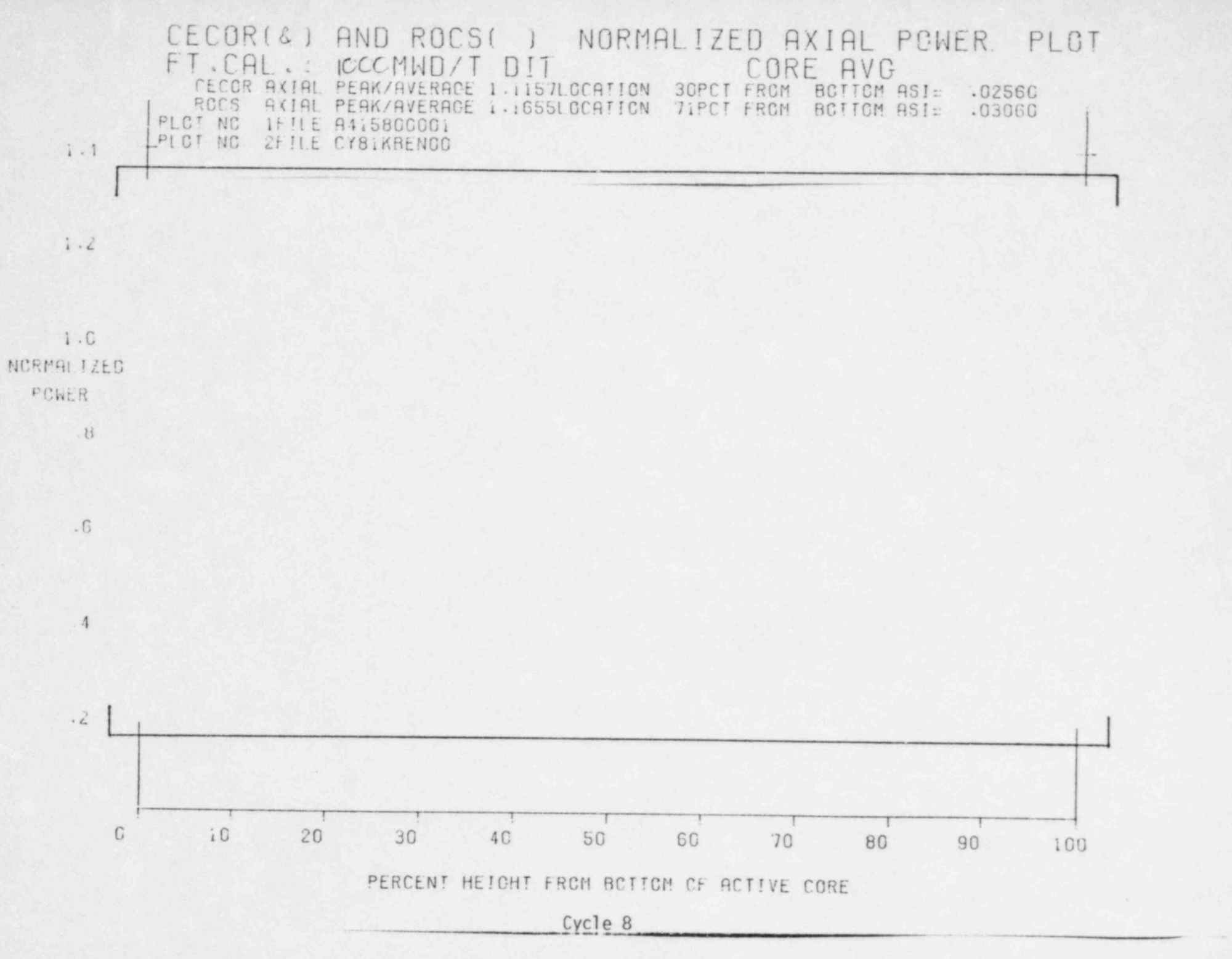
CECOR(&) AND ROCS( ) NORMALIZED AXIAL POWER PLOT
FT.CAL.: 10000MWD/T DIT CORE AVG
CECOR AXIAL PEAK/AVERAGE 1.1157LOCATION 30PCT FROM BOTTOM ASI= .02560
ROCS AXIAL PEAK/AVERAGE 1.1655LOCATION 71PCT FROM BOTTOM ASI= .03060
PLOT NO 1FILE A4158000G1
PLOT NO 2FILE CY81KRENOO
1.1
1.2
1.0
NORMALIZED
POWER
.8
.6
.4
.2
0
10
20
30
40
50
60
70
80
90
100
PERCENT HEIGHT FROM BOTTOM OF ACTIVE CORE

Cycle 8

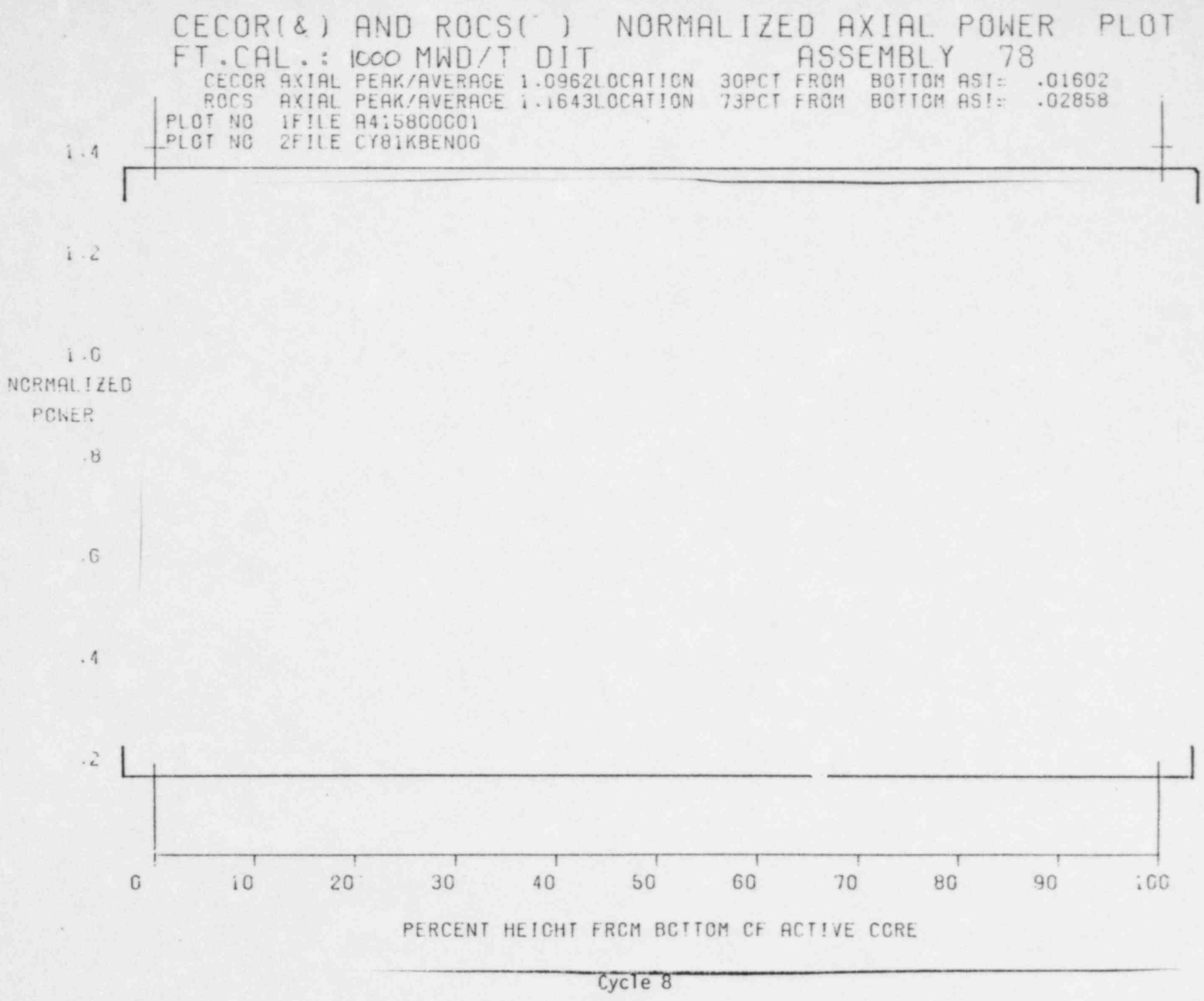
CECOR(&) AND ROCS( ) NORMALIZED AXIAL POWER PLOT
FT.CAL.: 1000 MWD/T DIT ASSEMBLY 78
CECOR AXIAL PEAK/AVERAGE 1.0962LOCATION 30PCT FROM BOTTOM ASI= .01602
ROCS AXIAL PEAK/AVERAGE 1.1643LOCATION 73PCT FROM BOTTOM ASI= .02858
PLOT NO 1FILE A4158OOCO1
PLOT NO 2FILE CY81KBENOO
1.4
1.2
1.0
NORMALIZED
POWER
.8
.6
.4
.2
0
10
20
30
40
50
60
70
80
90
100
PERCENT HEIGHT FROM BOTTOM OF ACTIVE CORE

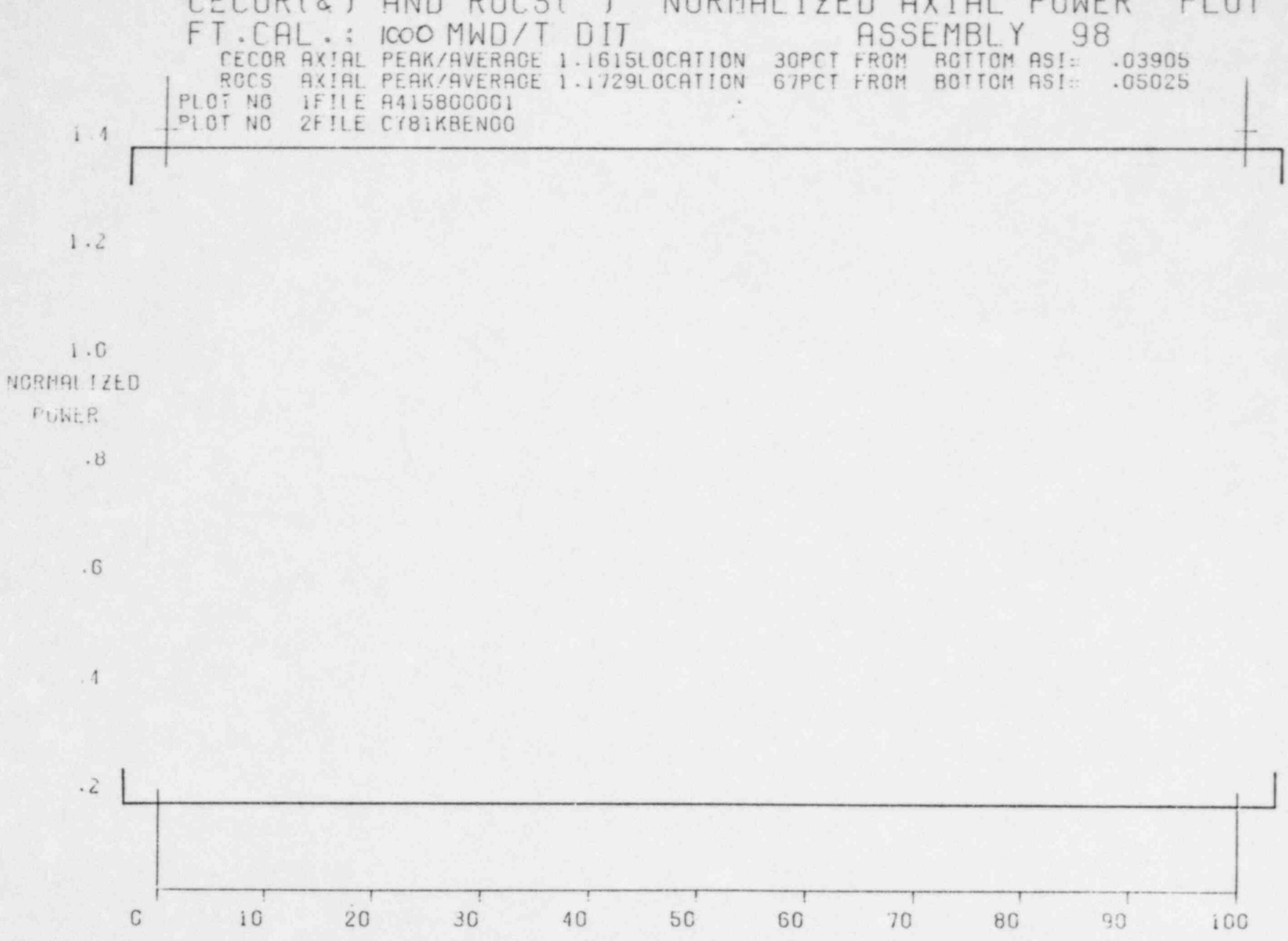
CECOR(&) AND ROCS( ) NORMALIZED AXIAL POWER PLOT
FT.CAL.: 1000 MWD/T DIT ASSEMBLY 98
CECOR AXIAL PEAK/AVERAGE 1.1615LOCATION 30PCT FROM BOTTOM ASI= .03905
ROCS AXIAL PEAK/AVERAGE 1.1729LOCATION 67PCT FROM BOTTOM ASI= .05025
PLOT NO 1FILE A41580C001
PLOT NO 2FILE C781KBEN00
1.4
1.2
1.0
NORMALIZED
POWER
.8
.6
.4
.2
0
10
20
30
40
50
60
70
80
90
100
PERCENT HEIGHT FROM BOTTOM OF ACTIVE CORE

Cycle 8

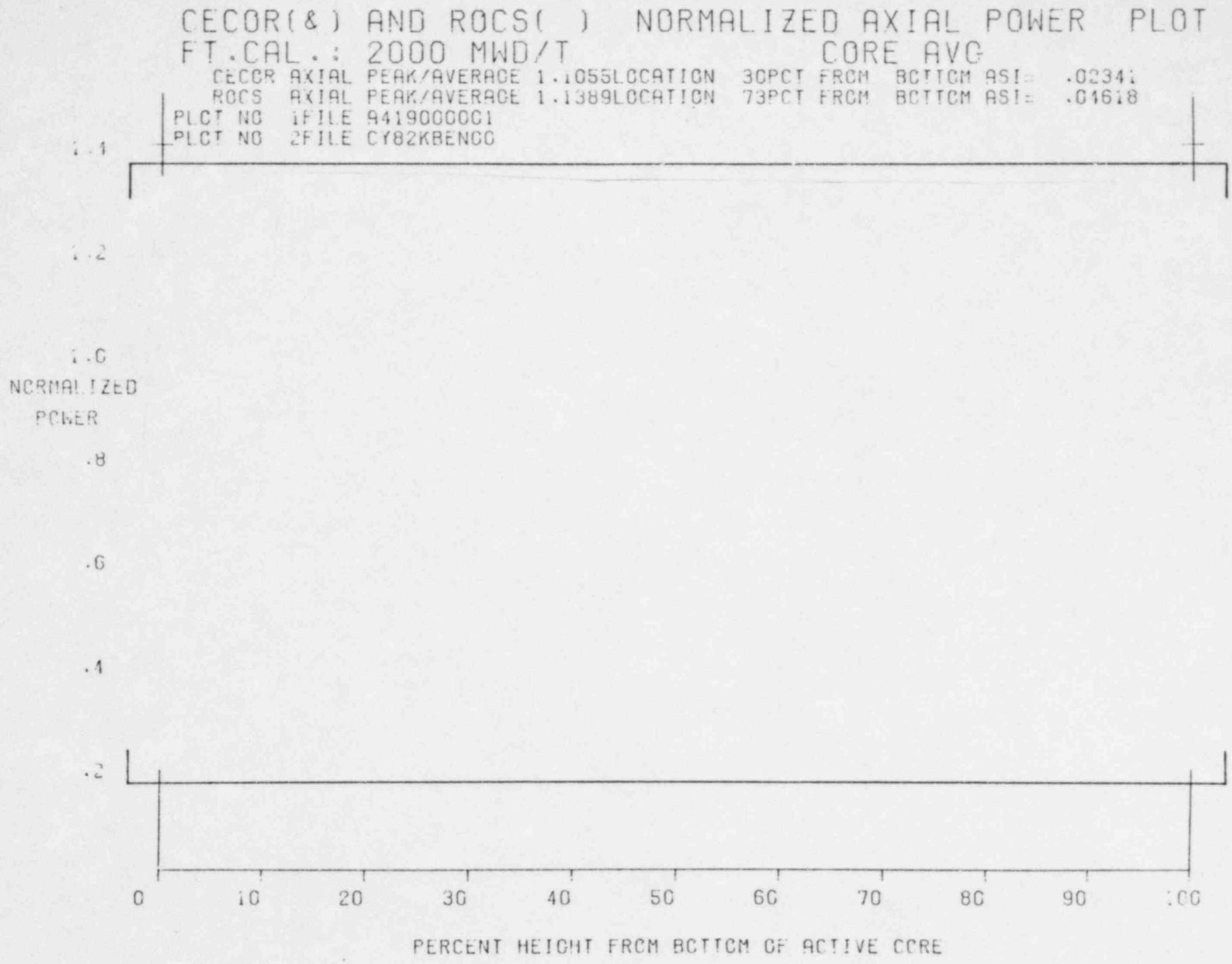
CECOR(&) AND ROCS( ) NORMALIZED AXIAL POWER PLOT
FT.CAL.: 2000 MWD/T CORE AVG
CECOR AXIAL PEAK/AVERAGE 1.1055LOCATION 30PCT FROM BOTTOM ASI= .02341
ROCS AXIAL PEAK/AVERAGE 1.1389LOCATION 73PCT FROM BOTTOM ASI= .01618
PLOT NO 1FILE 941900000C1
PLOT NO 2FILE CY82KBENCO
1.1
1.2
1.0
NORMALIZED
POWER
.8
.6
.4
.2
0
10
20
30
40
50
60
70
80
90
100
PERCENT HEIGHT FROM BOTTOM OF ACTIVE CORE

Cycle 8